GEORGIA INSTITUTE OF TECHNOLOGY
ENGINEERING EXPERIMENT STATION
ATLANTA, GEORGIA 30332

Commander
Rome Air Development Center (EMKC)
Griffiss Air Force Base
New York 13440

Attention: EMCVI-2

Subject: Quarterly Status Report 1, Project A-987
"Interference Reduction Techniques Employing Active Devices"
Contract No. AF30602-67-C-0066
Covering the period from 1 December 1966 to 28 February 1967

Dear Sir:

Objective:

To develop interference rejection networks employing a combination of active and passive techniques to obtain improved rejection of co-channel and adjacent channel interference.

Technical Program:

During the past quarter the technical effort of this project has been concentrated in three areas. These areas are:(1) the application of RF cancellation techniques at UHF, (2) the evaluation of quartz resonators as interference filter elements at VHF, and (3) an investigation of UHF Q multiplication techniques. The activities and results obtained in these areas are discussed in the following paragraphs.

Since this report covers the initial phase of the study program, a brief analysis of the adjacent channel interference reduction problem in the UHF region will aid in the establishment of desirable goals.

The rapidly expanding demand for communications between military units in a tactical situation has resulted in severe crowding of the rf spectrum. Any techniques which permit closer interference-free spacing of channels directly contributes to the expansion of communications capabilities.

The frequency spacing required between channels for interference-free operation is determined by a number of factors. An insight into the nature of the adjacent channel interference problem can be gained by the consideration of a typical operational situation. In the UHF region of 200 to 400 MHz, transmitters capable of producing output powers of 200 watts (+ 53 dbm) or more are quite common and typical receivers in this frequency range have sensitivities of -100 dbm. An operational setup might be that as illustrated in Figure 1, where a receiver is tuned to a relatively weak (-90 dbm) signal at 201 MHz while the strong undesired signal is at 200 MHz. Operational conditions often require that transmitters and receivers share the same antenna. In that case, if a 10 db signal to noise ratio is required in the receiver's rf stage to prevent excessive information loss, then the interfering signal must be attenuated 153 db to -100 dbm. The receiver preselector will provide approximately 50 db of attenuation to the undesired signal and an additional 20 db of attenuation will be supplied by antenna multicouplers. The remaining 83 db of attenuation necessary to reduce the +33 dbm signal out of the multicoupler to the -50 dbm permitted at the receiver's antenna terminals requires a filter technique exhibiting an attenuation slope of 16,600 db per octave.

Even with the use of high Q antenna multicouplers, a typical frequency separation of 2 MHz between the transmitter and receiver frequencies is commonly required for interference free operation in the region of 200 to 400 MHz. The reduction of the 2 MHz spacing to 0.1 MHz is a desired goal. A number of techniques which are applicable toward meeting this goal were investigated during the first

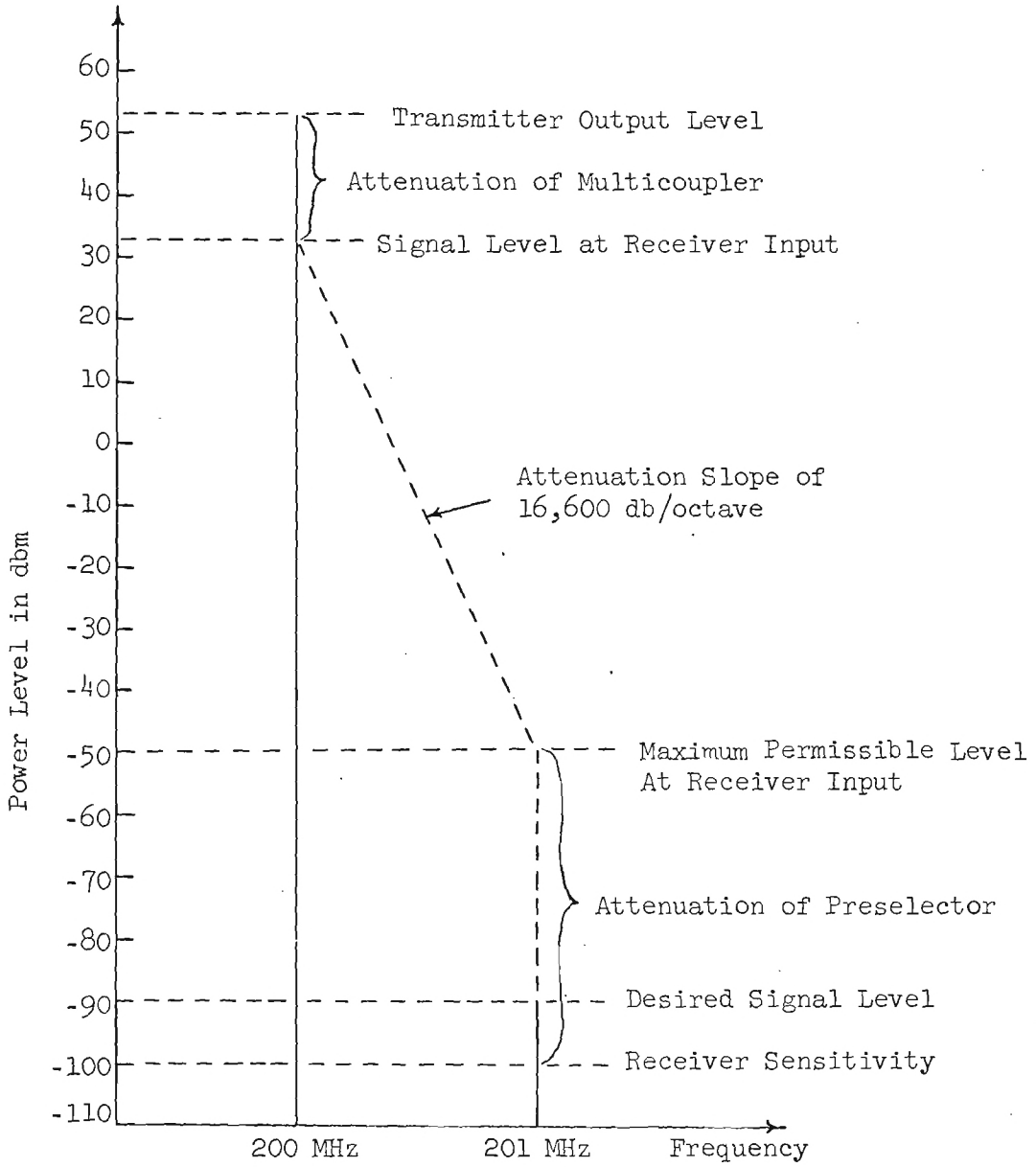

Figure 1. Illustration of Typical Adjacent Channel Interference Situation.

quarter of the project. The following is a discussion of these techniques.

RF Cancellation Techniques:

During the first quarter, a study was made of three possible techniques for the cancellation of an undesired signal. The characteristics of the operational situation will determine which approach is more appropriate for a specific interference problem. A typical interference situation can be conveniently represented by the vector diagram of Figure 2. The low level desired signal is represented by the short vector and the high level undesired signal is represented by the longer vector. Since the desired and undesired signals are not at the same frequency, the angular velocity of rotation of the two vectors will not be equal. If an auxiliary signal, represented by the dotted vector, is combined with the original two, cancellation of the undesired is obtained. This requires that the auxiliary signal identically match the undesirable signal in amplitude and frequency and that the phase angle between the two be π radians.

If the interfering transmitter or antenna is physically located nearby, a sample of the interference signal may be obtained and directed to the receiver in the manner shown in Figure 3. Referring to the vector diagram of Figure 2, the solid vector, S_1, represents the interference signal that reaches the receiver through the antenna lead, and the dotted vector, S_3, represents the signal on the auxiliary path.

Appropriate phase and amplitude corrections must be performed on the signal sample for cancellation of the undesired signal before entering the receiver front end. The angular frequencies, ω_1 and ω_3, of S_1 and S_3 are identical but the phase shift through the two paths will not necessarily be the same. For cancellation, a net difference of 180 degrees must exist in the phase shift through the two paths.

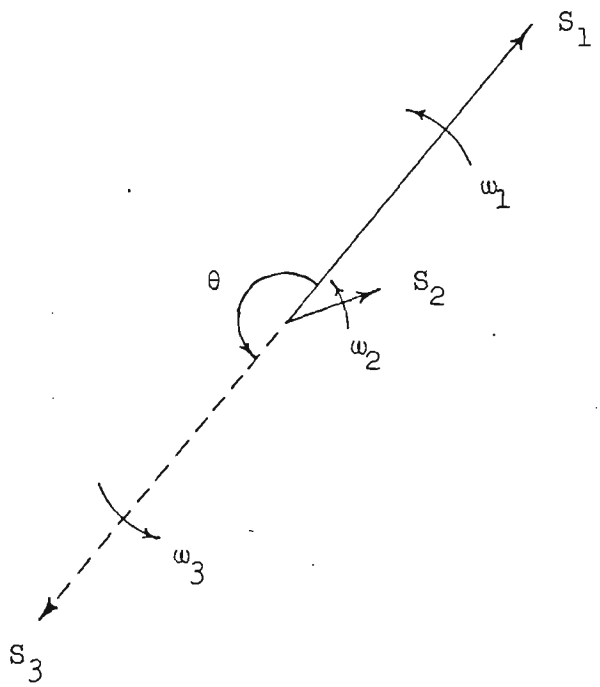

Figure 2. Vector Diagram Illustrating the Principles of the RF Cancellation Technique.

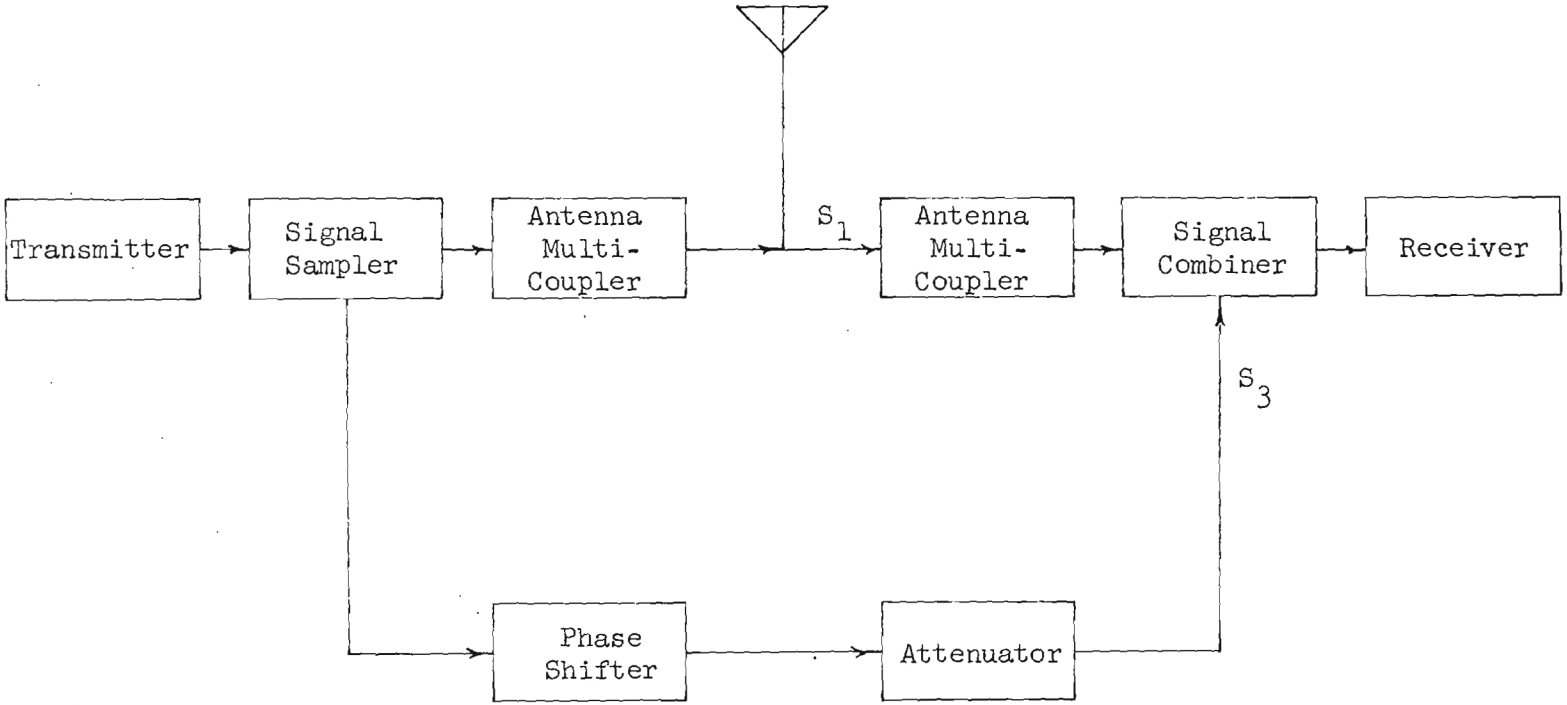

Figure 3. Block Diagram of RF Cancellation of Interference Involving Co-sited Transmitter-Receiver Pairs.

A simple type of phase shifter such as an appropriate length of transmission line may be used to adjust the path length so that $\theta = \pi$ radians. However, drift in the transmitter frequency or environmental effects such as temperature and humidity which detune the multicouplers slightly can result in a significant change in the phase of this signal at the receiver terminals. To maintain the proper phase relationship, a voltage controlled phase shifter with automatic tracking offers an attractive solution. The block diagram of a system to perform this function is shown in Figure 4. A portion of the interfering transmitter signal sample is fed to a mixer and heterodyned with a local oscillator to produce a 30 MHz IF signal. A portion of the signal plus interference is coupled to a second mixer where it is heterodyned with the local oscillator to produce another 30 MHz IF signal. The two 30 MHz signals are amplified, compared in a phase detector and the resulting phase error voltage is used to control the phase shifter. The manual shifter thus acts as a coarse phase control and is adjusted to obtain the phase required for initial cancellation of the interfering signal while the voltage controlled phase shifter corrects for the time varying changes to maintain the required phase shift.

In the system of Figure 4, a 200 to 400 MHz local oscillator is coupled to the mixers through a broad-band hybrid which serves to provide isolation between the "interference" and the "signal plus interference" input ports. Although not shown the two mixers also incorporate hybrid couplers to further isolate the local oscillator signal from the input ports. The local oscillator and input signal sum is fed into the base of the first stage and mixing is achieved in the base-emitter junction. The IF amplifier in the signal plus interference channel has a nominal gain of 75 db, which includes hybrid loss and conversion gain. Similiarly, the amplifier in the interference channel has a gain of 50 db. The gain is controlled by varying the DC collector

current with an external control. A gain variation of 60 db is provided for the signal plus interference channel and a 30 db variation is provided for the interference channel. The amplitude of the auxiliary signal may be adjusted with the signal sampler and the variable attenuator.

In many operational situations, the interfering transmitter and susceptible receiver are not located at the same site and a sample of the interfering signal is not available. For such cases, Figure 5 illustrates a technique which may be used. Since an auxiliary signal is not available, the phase shifter and amplitude adjustment must be of a different nature than those described in the system of Figure 3. In the sampling system of Figure 5, the difference in the phase shift around the sampling loop and the phase shift in the straight through path must be 180 degrees at the frequency of the interference signal but should be as small as possible (0 degrees, ideally) at the tuned frequency of the receiver. By the very nature of adjacent and co-channel interference, an abrupt phase change must occur over a narrow frequency range. A cavity resonator may be used to approximate the desired phase response because it exhibits a rate of change of phase with frequency that is directly proportional to Q. The rate of phase shift will directly determine the minimum frequency separation between the desired and interfering signals at which cancellation of the interference is possible. Since high Q cavity resonators are readily available, they represent a practical means of obtaining the rapid phase shift required.

The sampling loop can not be tightly coupled into the main line without attenuating the desired signal unnecessarily. Consequently, amplification is necessary within the sampling loop to permit the adjustment of the amplitude of the cancellation signal to match the amplitude of the interference signal at the point of re-entry.

In both of the previous systems, no closed loop feedback systems for continuous adjustments of amplitude are necessary because once

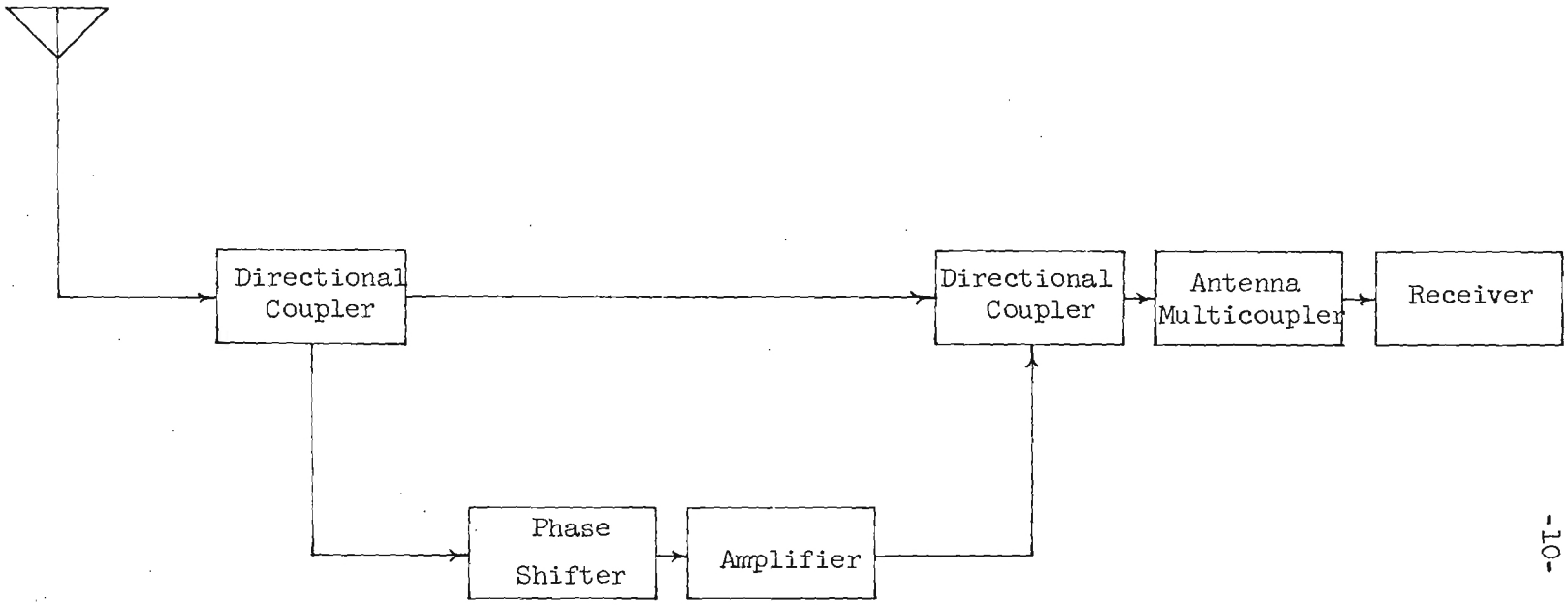

Figure 5. Simplified Block Diagram for Interference Cancellation in the Absence of an Auxiliary Signal.

initial adjustments are made and cancellation obtained, any subsequent phase and amplitude variations in the interfering signal source occur in the cancellation signal also. They are ultimately limited, however, to some required frequency separation between the desired and undesired signals because of the finite phase slope obtainable with practical resonators or because an auxiliary signal is not obtainable from the source.

In the absence of a signal sample from the source, the cancellation technique shown in the block diagram of Figure 6 permits closer spacing of the desired and undesired signals than is permitted with the system of Figure 5. The factors in this system which limit the frequency spacing between the desired and undesired are the gain-bandwidth characteristics of the phase lock loop and the relative amplitudes of the two signals. The technique illustrated by Figure 6 generates the cancellation signal by controlling the frequency, phase and amplitude characteristics of an auxiliary oscillator to match those of the interference signal. In this system, a sample of the interference is phase compared with the auxiliary signal. The error voltage is used to phase lock the auxiliary oscillator to the undesired signal to reproduce the frequency and phase characteristics of the undesired. Amplitude variations of the undesired are also detected and the resultant voltage used to control the amplitude of the auxiliary signal.

Broadband amplifier development:

The amplitude adjustment required in each of the cancellation techniques can be achieved through the use of an amplifier and/or an attenuator. In the system of Figure 3, an attenuation of the auxiliary will probably be necessary to obtain proper amplitude matching. The system of Figure 5, on the other hand, will require amplification of the cancellation signal to overcome the attenuation through the two couplers plus any loss exhibited by the phase shifter.

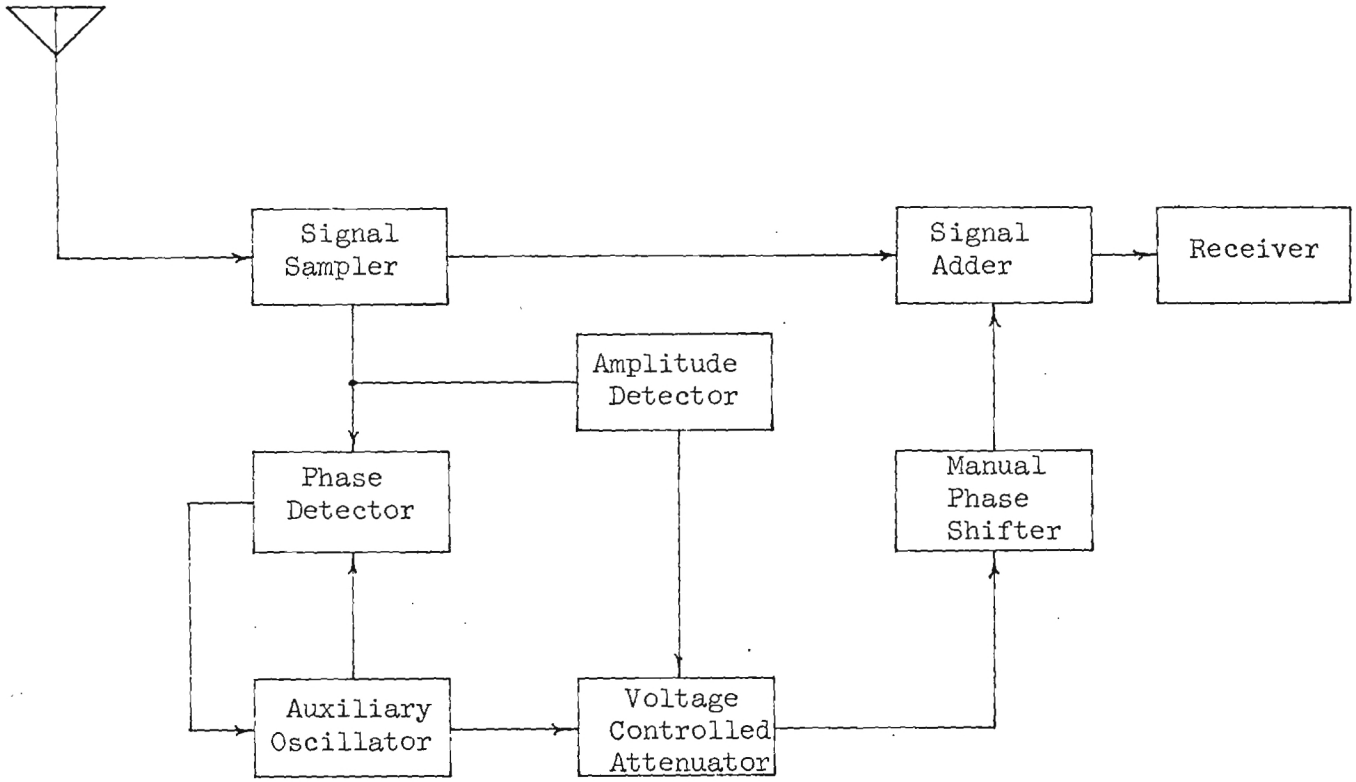

Figure 6. Simplified Block Diagram of the System for the Cancellation of AM Interference.

A straightforward approach is to provide more than adequate gain through an amplifier and provide for the amplitude adjustment with a variable attenuator following the amplifier.

The gain required in the amplifier can be estimated from the various losses in the sampling loop in the system of Figure 5. In a typical arrangement, coupling losses should not exceed 13 db in each coupler and 6 db should be a reasonable estimate of the losses in the remaining portions of the sampling loop. Therefore, not more than 32 db of gain should be required. Figure 7 is the circuit diagram of a transistor amplifier which was constructed to supply the necessary gain. Six grounded-base amplifier stages were constructed with wideband transformer coupling between stages. With appropriate capacitive trimming, flat gain response of 39 db was achieved from 200 to 400 MHz as shown in Figure 8.

Directional coupler development:

Prototype models of 10 db directional couplers were constructed from published design data.* The 10 db coupling value was chosen to provide an auxiliary signal of sufficient amplitude while avoiding excessive attenuation of the desired signal. Directional couplers were chosen for use in the system shown in Figure 5 in preference to other techniques, such as resistive coupling, because the directivity of the couplers provide high attenuation to any feedback components which would tend to cause oscillations around the loop. The 10 db coupling of the prototype unit behaves in the manner shown in Figure 9.

The development of the additional component parts necessary to evaluate the various RF cancellation techniques will continue during the next quarter. The construction of an electronically variable attenuator, a voltage controlled phase shifter, and an oscillator to cover the 200 to 400 MHz range will be initiated.

---

*G. L. Matthaei, L. Young and E. M. T. Jones, Microwave Filters, Impedance-Matching Networks and Coupling Structures, McGraw-Hill, (1964), New York, pp. 775-842.

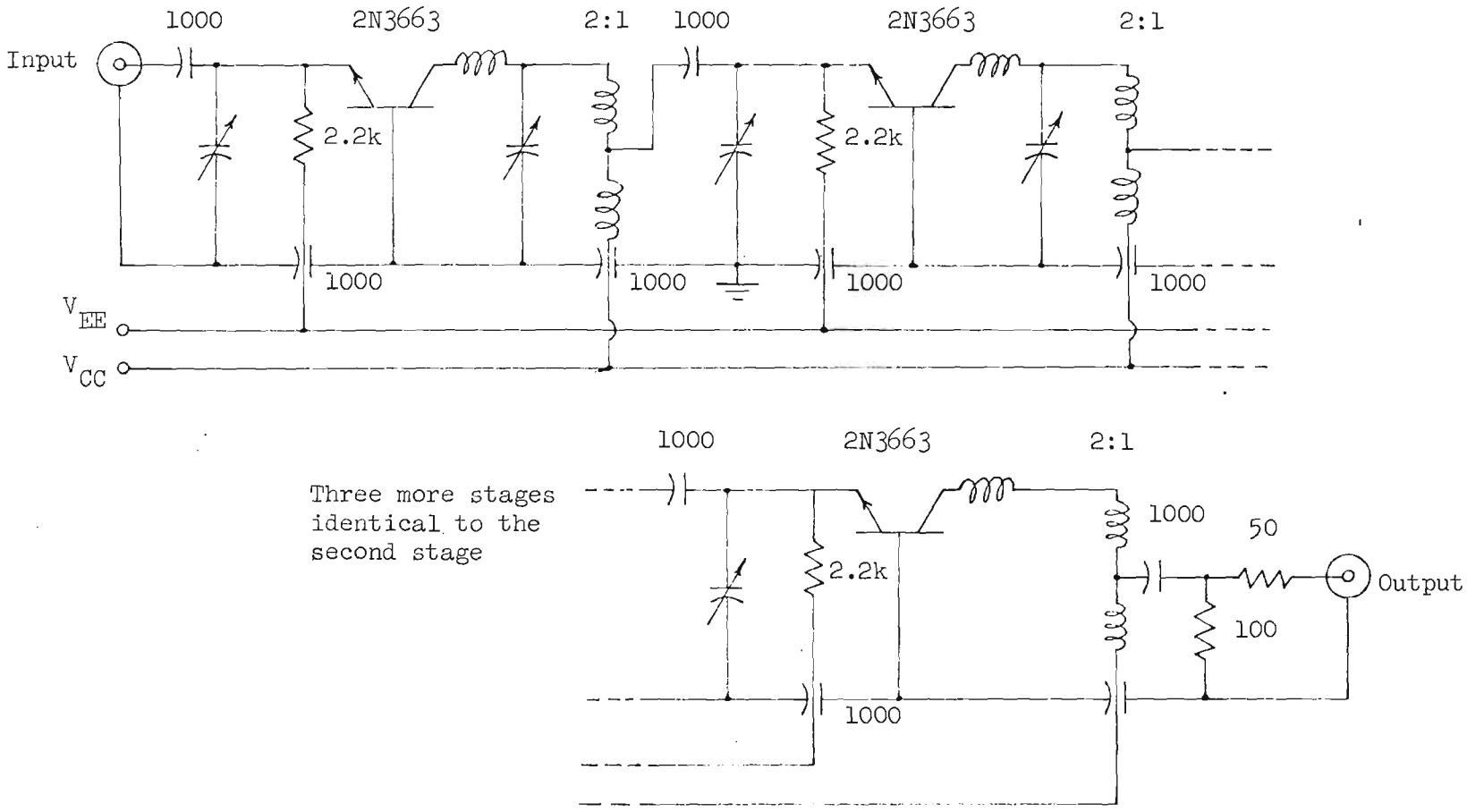

Figure 7. Schematic Diagram of a 200-400 MHz Transistor Amplifier.

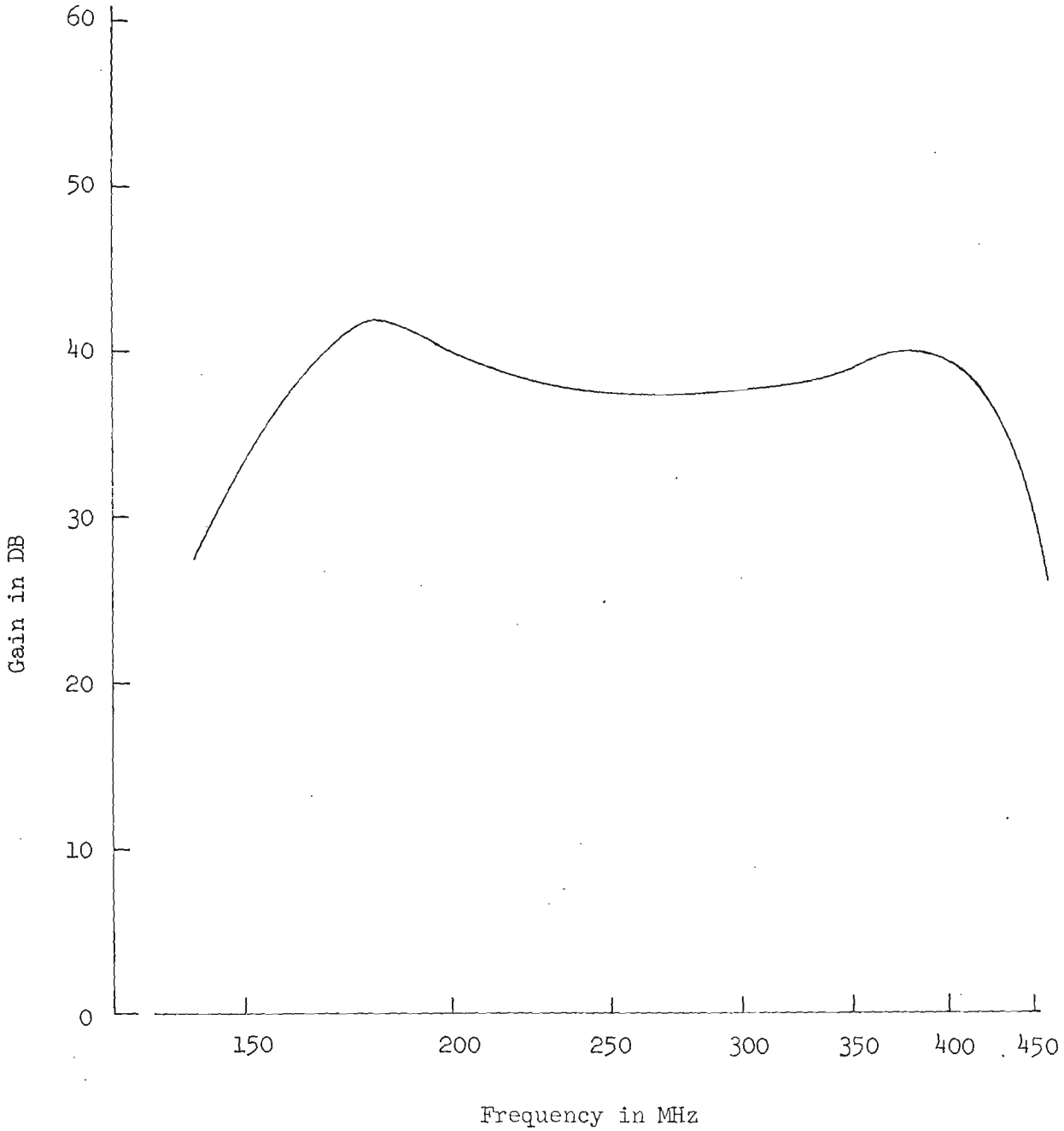

Figure 8. Gain Characteristics of the 200-400 MHz Transistor Amplifier.

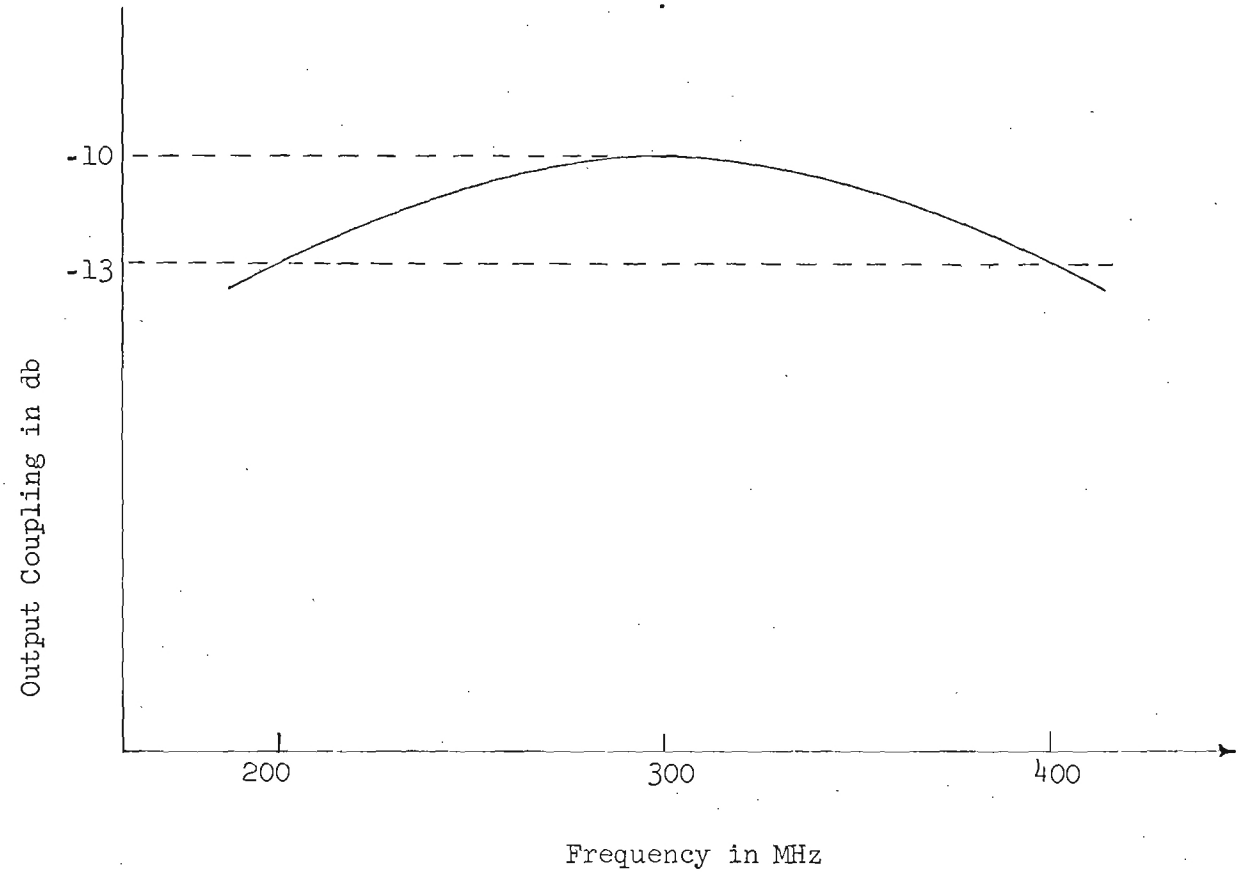

Figure 9. Coupling Characteristics of the 10 db Directional Coupler Prototype.

Final models of the 10 db directional couplers will also be constructed.

Quartz Crystal Studies:

During the first quarter, several simple reject filters comprised of passive circuit elements and a single crystal resonator were developed and evaluated. In order that the evaluation of each circuit be based only on the merits of the given circuit configuration, the same quartz crystal was used in each filter throughout the main test phase of the investigation. However, other crystals were tested and were found to give similar results.

Figure 10 is a schematic diagram of a simple bandpass filter which has a sharp rejection notch at the peak of the bandpass response. While the peak of the response occurs at the parallel resonant frequency of L and $(C + C_o)$, where C_o is the crystal parasitic capacitance, the sharp notch occurs at the series resonant frequency of the crystal. The depth of the notch depends directly on the ratio of the series resonant resistance of the crystal to the parallel resonant impedance of L and $(C + C_o)$.

The rejection characteristics of a 100 MHz crystal notch filter are shown in Figure 11. A large number of undesirable spurious responses are evident in the filter characteristics. If the desired signal falls within the region of these spurious responses, it may be subject to severe distortion and attenuation. Therefore, a crystal free of spurious responses or a circuit configuration capable of suppressing the spurious responses is needed. Since no spurious response free crystals were available for our initial investigation, efforts were directed toward circuit configurations capable of spurious response suppression.

The filter spurious responses may be suppressed by incorporating the crystal in a balanced bridge configuration. The bridge configuration takes advantage of the fact that normally the series resistance of the spurious responses are higher than the resistance at the main response.

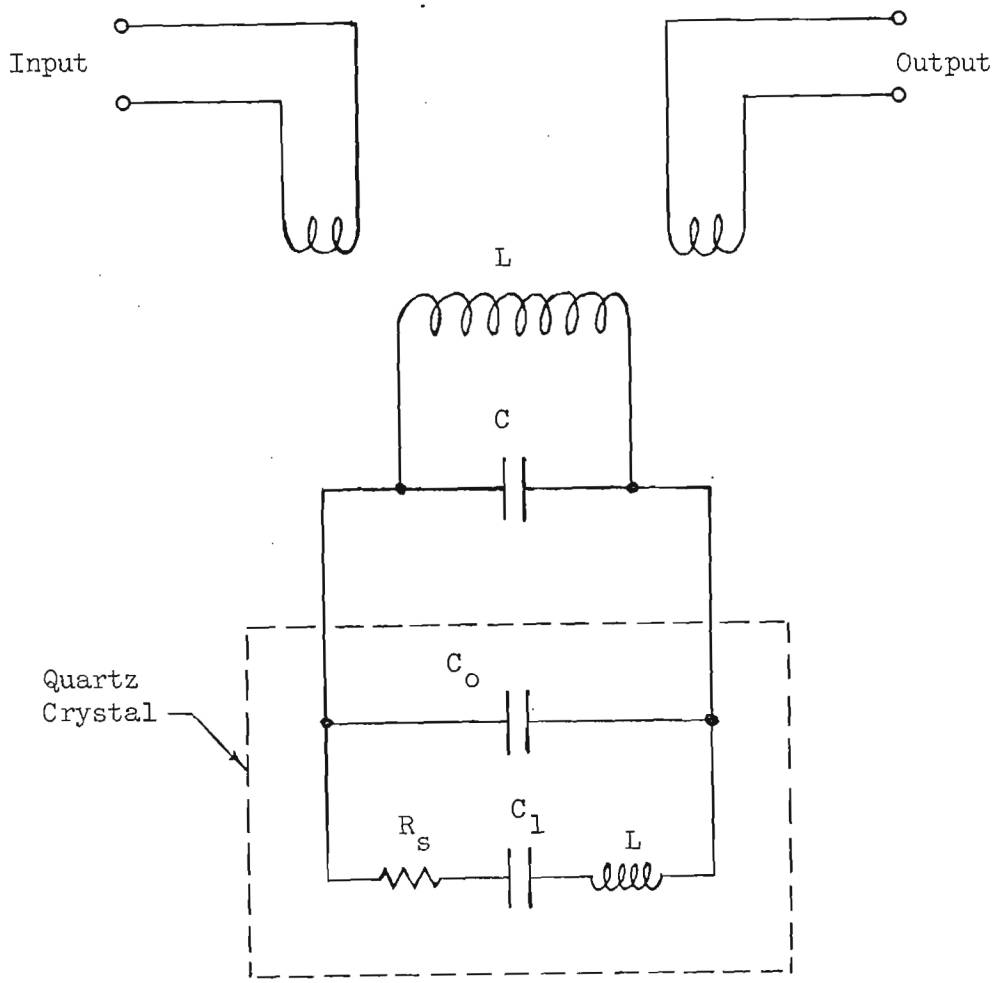

Figure 10. Simple Rejection Filter.

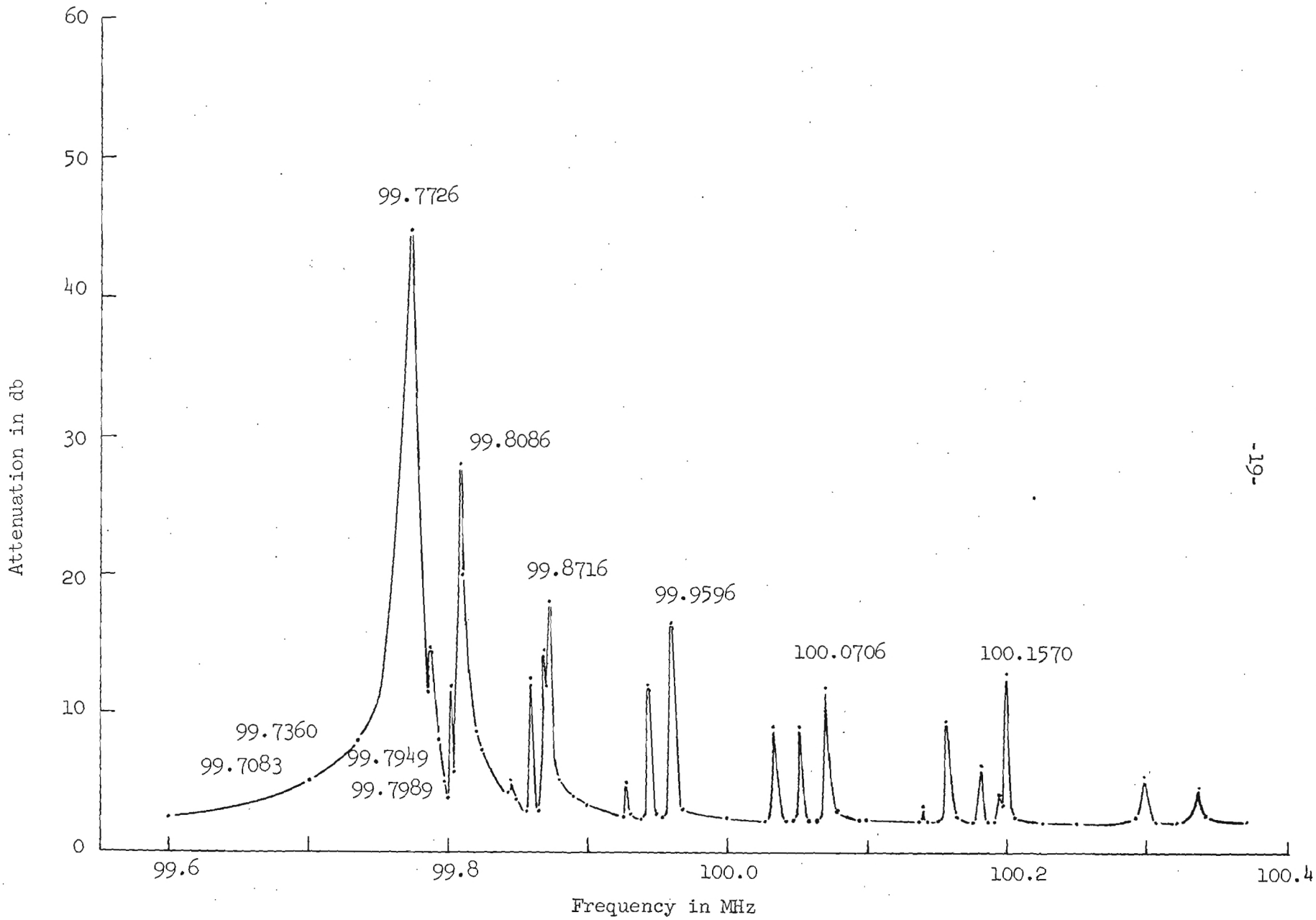

Figure 11. Rejection Characteristics of Simple Notch Filter.

By balancing the bridge at the resistance of the main response, the effectiveness of the main response is enhanced and the effects of the spurious responses are degraded.

The response characteristics at 100 MHz of a bridge type notch filter are shown in Figure 12 for the same crystal element as used in Figure 11. Note the improvement by several db of the ratio of the spurious responses to the desired response. An additional advantage is gained by the use of the bridge configuration in that the depth of the notch depends directly on the precision of the bridge balance instead of the ratio of the crystal resistance to the parallel resonant impedance of the tuned circuit.

Figure 13 illustrates the application of the bridge technique to provide a sharp notch in the vicinity of 220 MHz. Note that the maximum response ripple in the passband, 3 kc above and below the notch, is less than 2 db. In this region a desired signal would be subject to little attenuation from the notch filter. The passband insertion loss of the 220 MHz filter is on the order of 10 db compared to 3 db at 100 MHz. While part of the 7 db increase may be attributed to the larger resonant resistance of the crystal at the 220 MHz overtone frequency, the larger part of the insertion loss is probably due to the increase in core loss and decrease in transformer coupling which occurs at the higher frequencies.

The tabulation of crystal overtone responses in Table 1 indicates that the band reject crystal filters may be expected to give sharp notches at frequencies up to 400 MHz. The insertion loss is excessive at the higher overtone responses. However, this loss may be reduced by an improved circuit and transformer design. Although the rejection levels do not appear to be adequate at the higher overtone frequencies, greater amounts of rejection may be obtained through the use of a more precise bridge.

During the next quarter new crystal filter configurations will be investigated. The feasibility of incorporating several crystals into

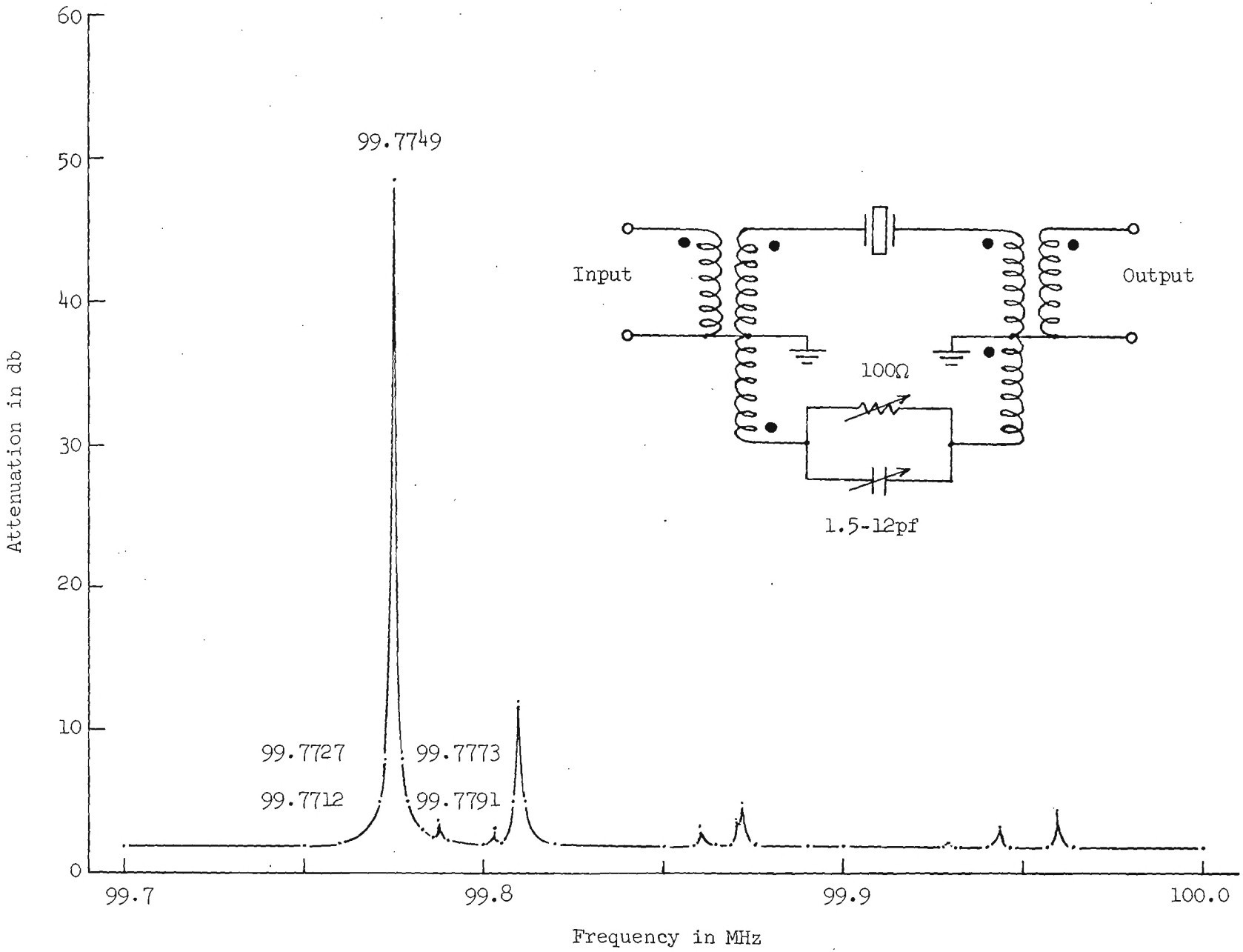

Figure 12. Rejection Characteristics of a Bridge Notch Filter.

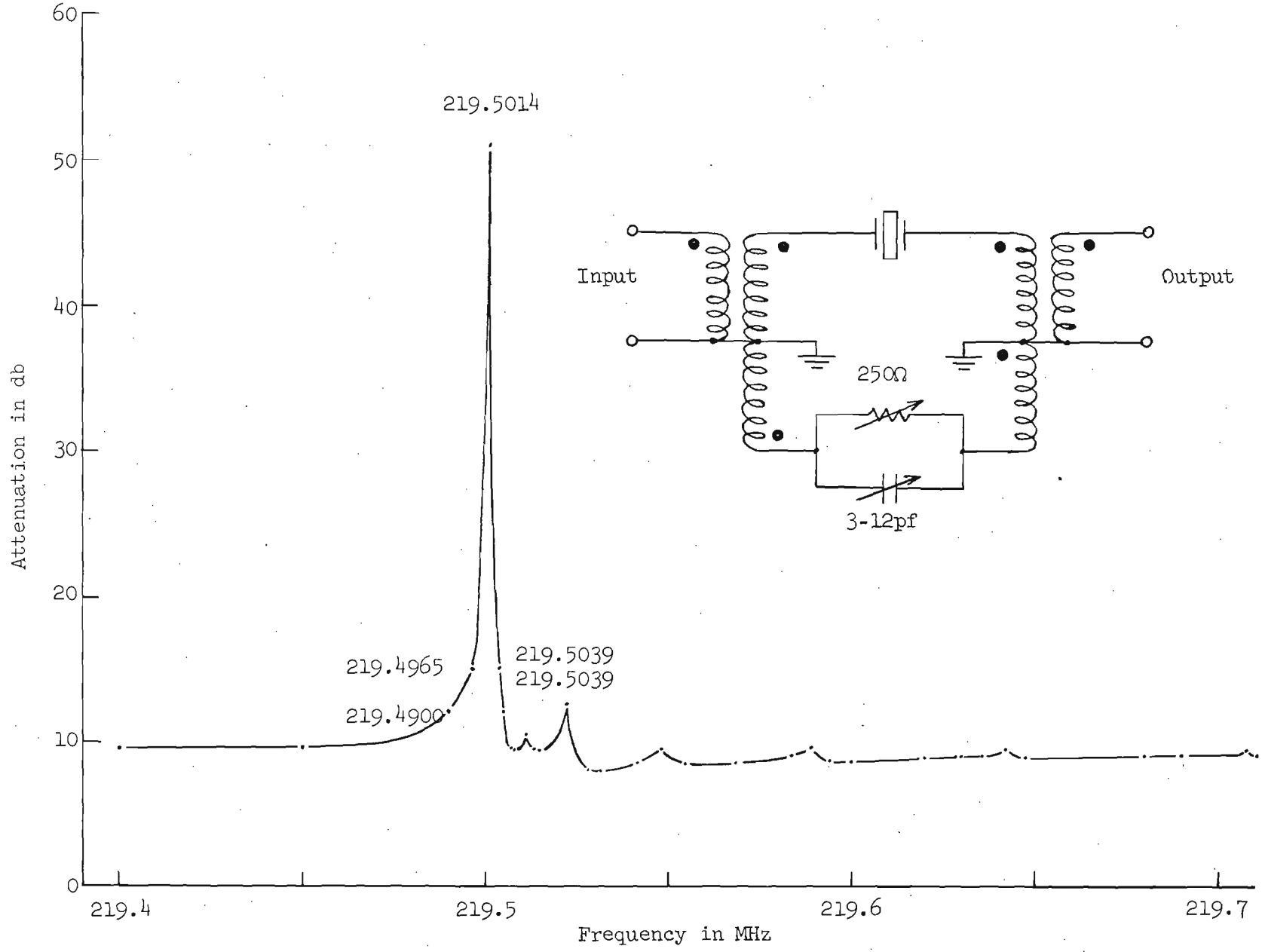

Figure 13. Rejection Characteristics of Bridge Notch Filter near 220 MHz.

TABLE 1

CHARACTERISTICS OF AN OUTPHASING BRIDGE BALANCED AT SEVERAL OVERTONE FREQUENCIES OF 20 MHz QUARTZ CRYSTAL

Crystal Overtone	Frequency (MHz)	Insertion Loss (db)	Rejection Level (db)	Approximate 3 db Bandwidth (kHz)	Approximate Q
3rd	59.8583	2.8	48	8.8	6,800
5th	99.7747	2.0	46	9.6	10,400
7th	139.6858	3.0	44	8.8	15,900
9th	179.5951	5.2	42	11.0	16,300
11th	219.5019	9.0	41	14.9	14,700
13th	259.4062	14.0	37	16.3	15,900
15th	299.3070	20.0	30	26.3	11,400
17th	339.2261	26.0	>25	44.4	7,700
19th	379.1300	28.0	>23	57.6	6,600

the design of a low pass filter to obtain a multiplicity of sharp rejection bands at the series resonant frequencies of the crystals will be studied. Further effort will be directed toward reducing the insertion loss and increasing the rejection levels of crystal notch filters in the 200-400 MHz region.

UHF Q multiplication techniques:

A straightforward approach to the improvement of the adjacent channel interference problem is to improve the selectivity of conventional resonant structures. One method of improving the selectivity of such structures is to increase their natural Q through the use of active devices. Although considerable effort has

been directed toward the problem of Q multiplication, the majority of successful attempts have been restricted to fairly low frequencies. The block diagram of Figure 14 illustrates a technique which overcomes the limitations of previous efforts and performs successfully at UHF as well as low frequencies.

To illustrate the behavior of the system of Figure 14, suppose a voltage, V_a, is applied to the input of the network at the junction of R_a and R_b. If the voltage transfer function of the network is represented by $A(\omega)$ and $R_b \gg R_c$ (where R_c is the equivalent output impedance), then the output voltage may be approximated by

$$V_o = V_a A(\omega) \quad . \tag{1}$$

Then the voltage, V_R, across R_b is

$$V_R = V_a - V_o = V_a - V_a A(\omega) \quad . \tag{2}$$

If the input impedance of the network $A(\omega)$ is high compared to R_b, the current, I_a, which flows through R_b is

$$I_a = \frac{V_R}{R_b} = \frac{V_a - V_a A(\omega)}{R_b} \quad . \tag{3}$$

The effective impedance, Z_a, of R_b in parallel with $A(\omega)$ is

$$Z_a = \frac{V_a}{I_a} = \frac{R_b}{1 - A(\omega)} \quad . \tag{4}$$

The voltage, V_a, is related to the input voltage, V_i, by

$$\frac{V_a}{V_i} = \frac{Z_a}{R_a + Z_a} = \frac{\dfrac{R_b}{1 - A(\omega)}}{R_a + \dfrac{R_b}{1 - A(\omega)}} \quad . \tag{5}$$

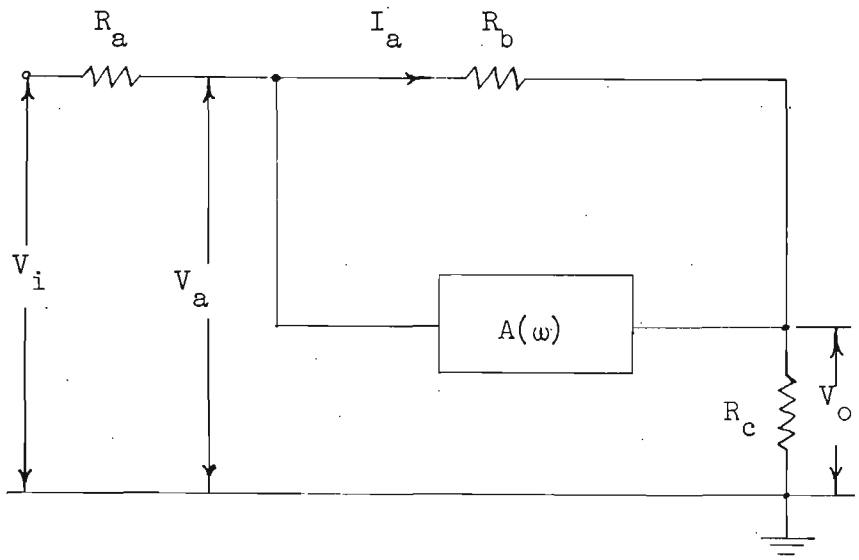

Figure 14. Simplified Diagram of Circuit for the Multiplication of the Q of a Network.

Expanding and rewriting (5), we get

$$\frac{V_a}{V_i} = \frac{1}{1 + \frac{R_a}{R_b}[1 - A(\omega)]} \quad . \tag{6}$$

Figure 15 shows the behavior of the ratio V_a/V_i as a function of frequency for various R_a/R_b ratios when $A(\omega)$ has a typical bandpass characteristic as shown by the dotted curve. The bandwidth narrowing properties of increasing R_a/R_b ratios is evident from this figure.

The effects of broadband gain or attenuation on the response behavior can be examined by analyzing the denominator of equation (6). For the voltage transfer function given by (6) to be stable, the following condition must be satisfied:

$$1 + \frac{R_a}{R_b}[1 - A(\omega)] > 0 \quad . \tag{7}$$

Upon expansion, equation (7) becomes

$$R_b + R_a - R_a A(\omega) > 0 \quad . \tag{8}$$

Therefore,

$$A(\omega) < 1 + \frac{R_b}{R_a} \tag{9}$$

is the condition which must be met for the network described by equation (6) to be stable. For example, consider the case where $\frac{R_b}{R_a} = 0.1$. Then $A(\omega)$ must not exceed 1.1 times its midband resonant value. For $A(\omega)$ between 1.0 and 1.1 the resonant peak value of the voltage ratio, V_a/V_i, will vary between one and infinity. The

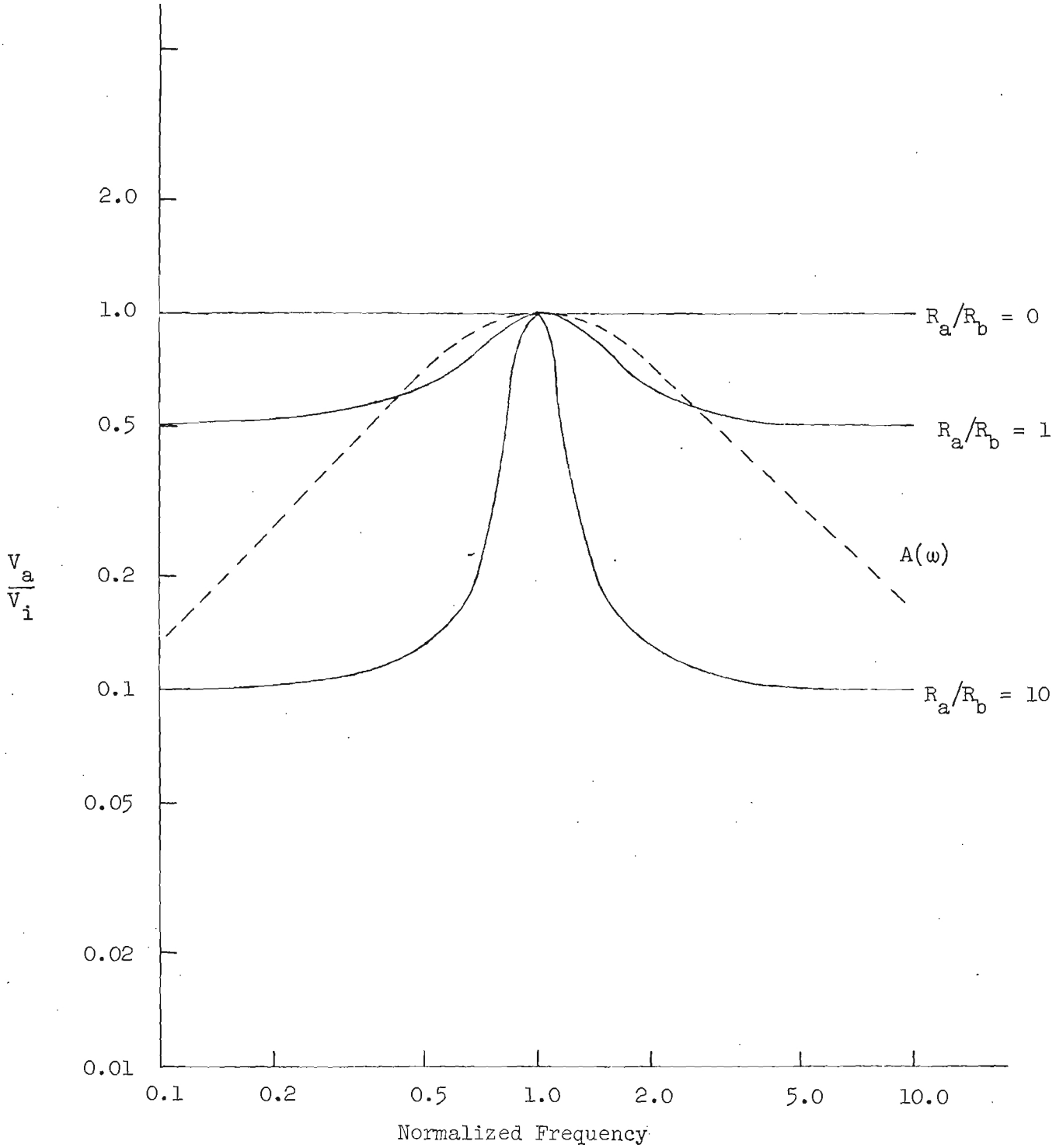

Figure 15. The Effects of the Ratio R_a/R_b on the Response Curve of $A(\omega)$.

variation of V_a/V_i with gain at resonance is effectively a variation of Q with gain.

The voltage, V_a, is further modified by the network, $A(\omega)$, to produce the output voltage, V_o. From equations (1) and (5),

$$V_o = V_a A(\omega) = \frac{\frac{R_b}{1 - A(\omega)}}{R_a + \frac{R_b}{1 - A(\omega)}} V_i A(\omega) \quad . \qquad (10)$$

Expanding equation (10), we obtain the expression which describes the Q multiplication technique:

$$\frac{V_o}{V_i} = \frac{R_b A(\omega)}{R_b + R_a [1 - A(\omega)]} \quad . \qquad (11)$$

The performance of the Q multiplication technique was verified at low frequencies by constructing the network which is illustrated in the block diagram of Figure 16. Two LC component combinations with a natural Q of 5 at 730 kHz were used to determine the frequency response characteristic, $A(\omega)$. The remaining elements of the network adjust the gain and impedance levels. The overall Q of the system as a function of the open loop gain at resonance is shown in Figure 17.

Figure 18 shows the narrowing of the 3 db bandwidth (Q multiplication) as the gain is varied. As the open loop exceeds unity, the system approaches an oscillatory condition. In fact, oscillations occur (bandwidth equal to 0 Hz) at a gain of 1.085 with a driving resistance, R_a in Figure 14, of 100 KΩ. The results of another series of tests conducted with a driving resistance of 10 KΩ are also shown in Figure 18. Note that the increased driving resistance results in a higher Q for a specified gain.

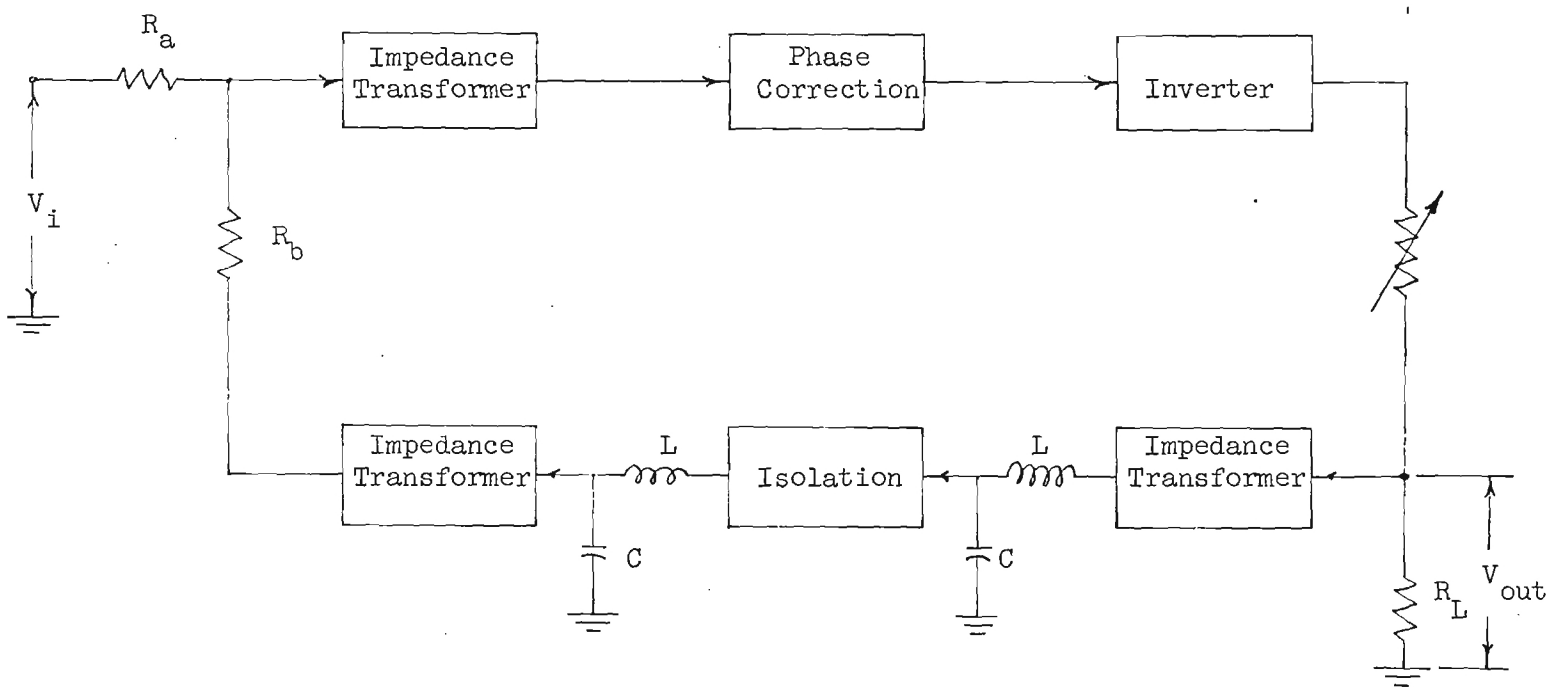

Figure 16. Block Diagram of A Network for the Multiplication of the Natural Q of Resonant Circuits at Low Frequencies.

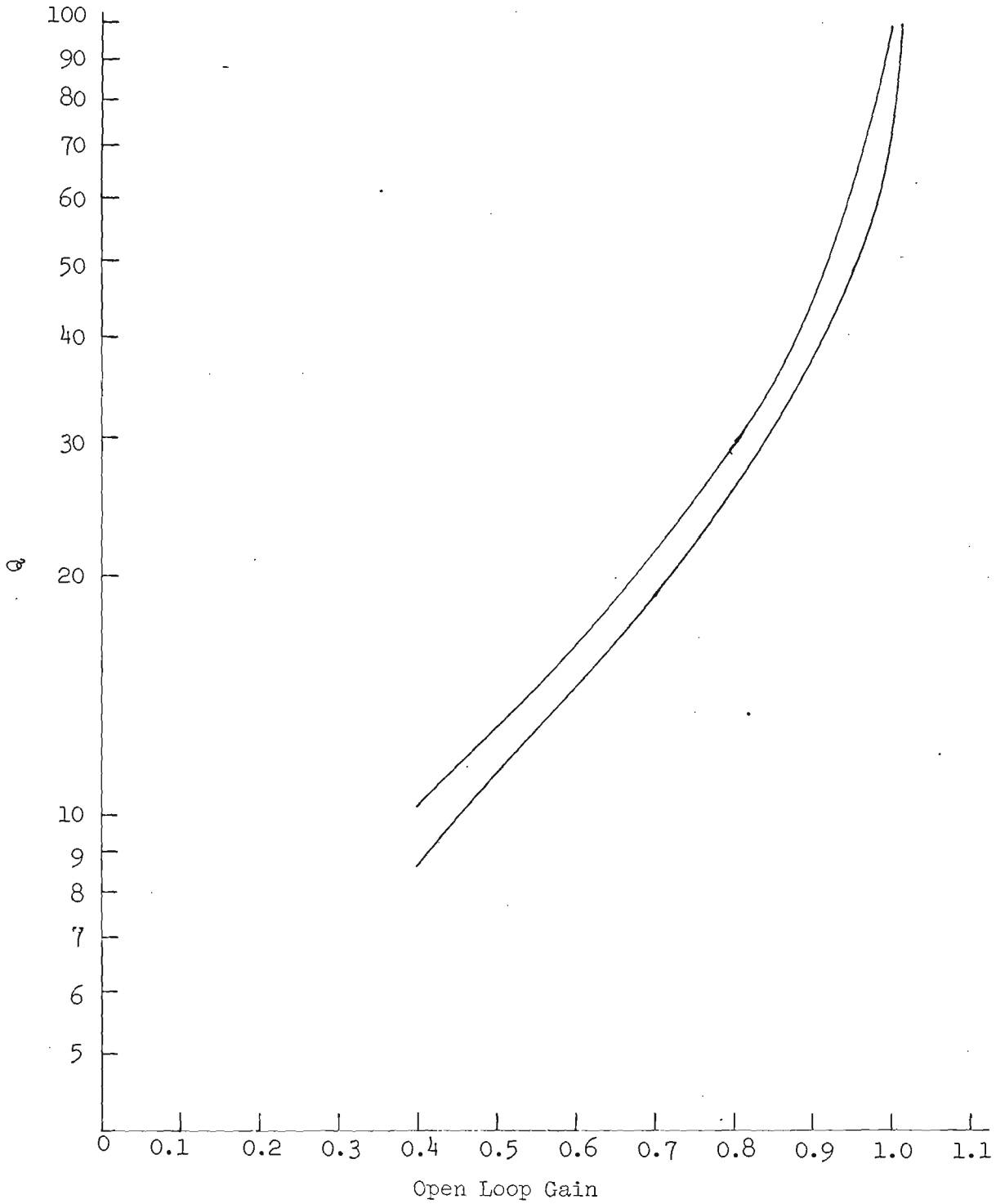

Figure 17. Q Versus Open Loop Gain.

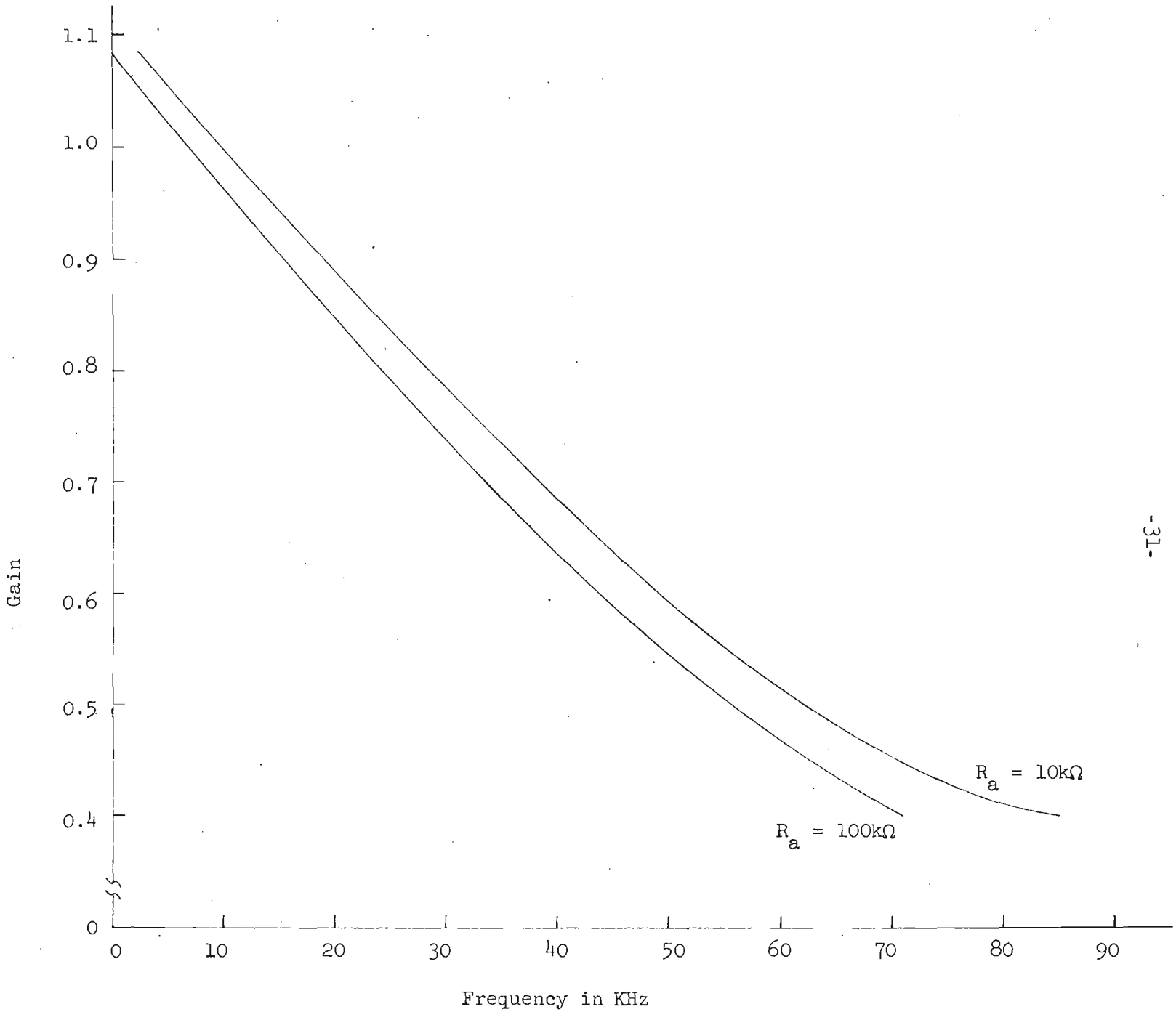

Figure 18. The 3 db Bandwidth as a Function of Open Loop Gain.

As a further test of the capabilities of the technique, a ceramic resonator, Clevite model TO-01, with a natural Q of 323 was substituted for the original low Q LC combination. The effective Q of the overall network was measured at various open loop gains. A gain of 0.84 resulted in an effective Q of 1900. This Q multiplication factor of 5.9 is the same as obtained with the low Q(Q = 5) test at a similar gain setting.

The block diagram of Figure 19 shows the equipment setup which was used to verify the technique at 220 MHz. The electronic counter and voltmeter are used to measure the response curves and are not part of the Q multiplication network. The 4:1 transformer is necessary to provide the proper impedance match to the input of the amplifier which drives the counter.

The two response curves of Figure 20 show the natural response of a coaxial cavity and its response after Q multiplication. The natural Q of the cavity resonator used in this test is approximately 1200. The Q of the multiplied response curve is approximately 10,000. In addition to the narrowing of the 3 db points, the skirt attenuation is also increased 10 db or more. Figure 21 is a graph of the Q versus gain as determined by the attenuator setting. Q's in excess of 70,000 were obtained. Naturally, the higher Q's are closer to the region of instability and are more difficult to obtain in the absence of fine control on the attenuator.

The analytical study of the described Q multiplication technique will be continued during the next quarter. More detailed experimental data will be obtained to describe the performance of the system up to 400 MHz. Exploration will continue into any active technique which promises to aid in the rejection of adjacent channel interference.

Work Schedule and Progress:

The progress of the work of this project is satisfactory and essentially in conformance to the projected work schedule.

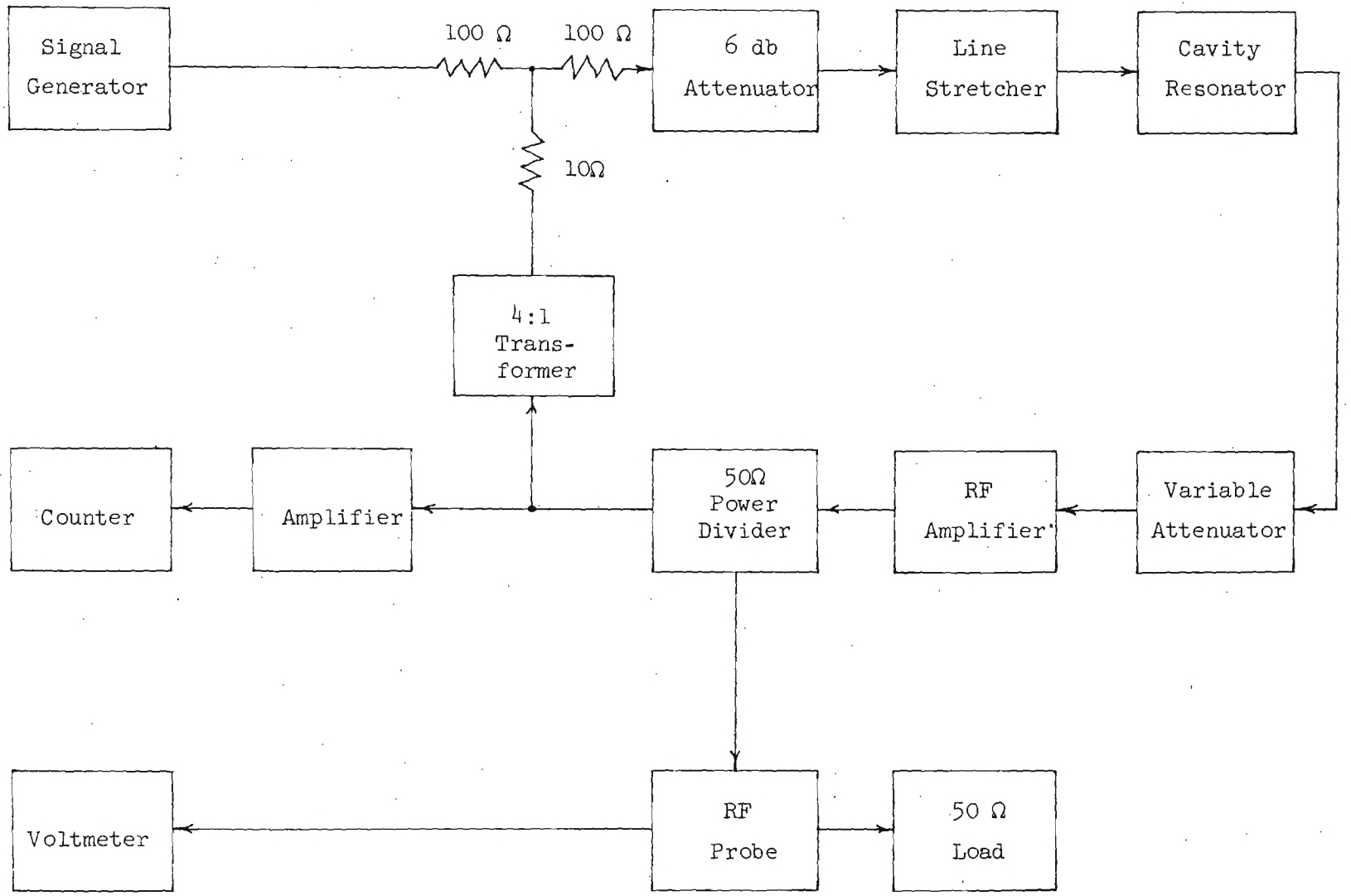

Figure 19. Block Diagram of Setup for the Verification of the Q-Multiplication Technique at 220 MHz.

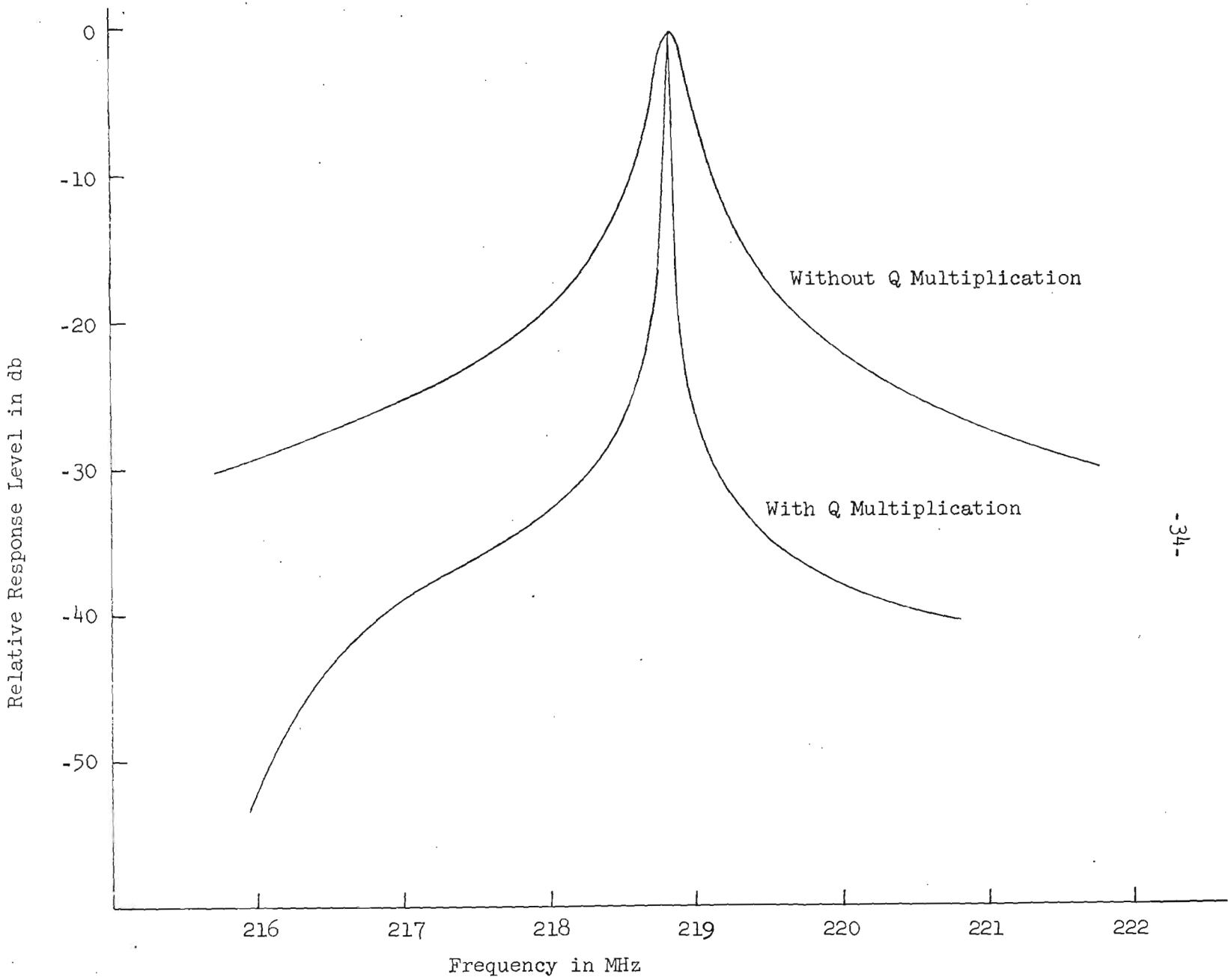

Figure 20. Response Curves of Coaxial Cavity with and Without Q-Multiplication.

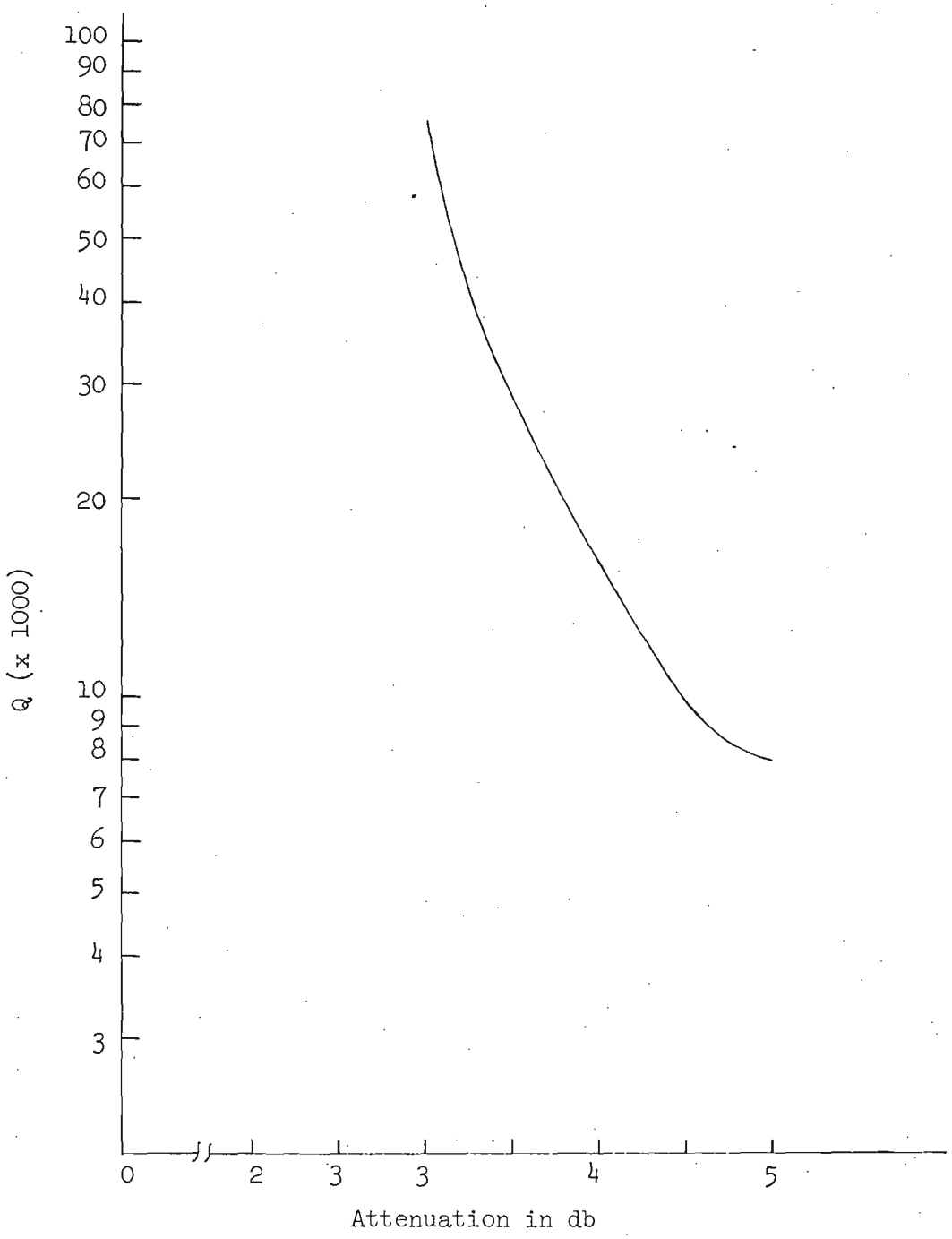

Figure 21. Q Versus the Loop Gain as Determined by Attenuator Setting.

Program for the Next Quarter:

The program for the next quarter will be essentially in conformance with that already outlined in the preceding paragraphs.

Personnel Changes:

During the past quarter, no significant personnel changes have taken place.

Engineering Man-hours:

The following number of engineering man-hours was devoted to this project effort during the past quarter:

Category	No. of Hours
Senior Research Engineer	60
Research Engineer	304
Assistant Research Engineer/ Graduate Research Assistants	656

Respectfully submitted:

Hugh W. Denny,
Project Director

Approved:

D. W. Robertson, Head
Communications Branch

GEORGIA INSTITUTE OF TECHNOLOGY
ENGINEERING EXPERIMENT STATION
ATLANTA, GEORGIA 30332

15 June 1967

Commander
Rome Air Development Center (EMKC)
Griffiss Air Force Base
New York 13440

Attention: EMCVI-2

Subject: Quarterly Status Report 2, Project A-987
"Interference Reduction Techniques Employing Active Devices"
Contract No. F30602-67-C-0066
Covering the period from 1 March 1967 to 31 May 1967

Dear Sir:

Objective:

To develop interference rejection networks employing a combination of active and passive techniques to obtain improved rejection of co-channel and adjacent channel interference.

Technical Program:

During the past quarter the technical effort of this project has continued in three principal areas. These areas are: (1) the application of RF cancellation techniques at UHF, (2) the evaluation of quartz resonators as interference filter elements at VHF, and (3) an investigation of UHF Q multiplication techniques. The activities and results obtained in these areas are discussed in the following paragraphs.

RF Cancellation Techniques:

The development of several components necessary for the realization of the cancellation techniques described in the first quarterly report was emphasized during the second quarterly period. The construction of the automatic phase control system for the cancellation of co-sited interference was essentially completed. Two directional couplers and an amplifier for the 200-400 MHz range were constructed and evaluated in addition to a current controlled attenuator for the same frequency range.

Several difficulties in the original system necessitated certain design changes which are shown in the block diagram of Figure 1. Initially a 200 to 400 MHz transistorized local oscillator was constructed but the performance was not satisfactory because of poor frequency stability and excessive harmonic content in the output. This poor performance was a result of the low output impedance of the oscillator transistors in the UHF region which excessively loaded the oscillator tuned circuit. Proper impedance matching between the transistor and the tuned load at each frequency of operation could have alleviated these problems. However, over an octave bandwidth, proper impedance match was difficult to maintain because of the wide variation in transistor parameters. Replacing the transistors with a Nuvistor vacuum tube gave a considerable improvement in both frequency stability and harmonic suppression.

Some instability was encountered in the original power dividing system which fed the local oscillator signal to the 30 MHz IF subchassis. This difficulty was avoided by constructing two balanced mixers with high speed switching transistors on the local oscillator subchassis. Confining the local oscillator signal to one subchassis and separating the mixers from the IF amplifiers improved the system stability by dividing the total 30 MHz gain between the two subchassis.

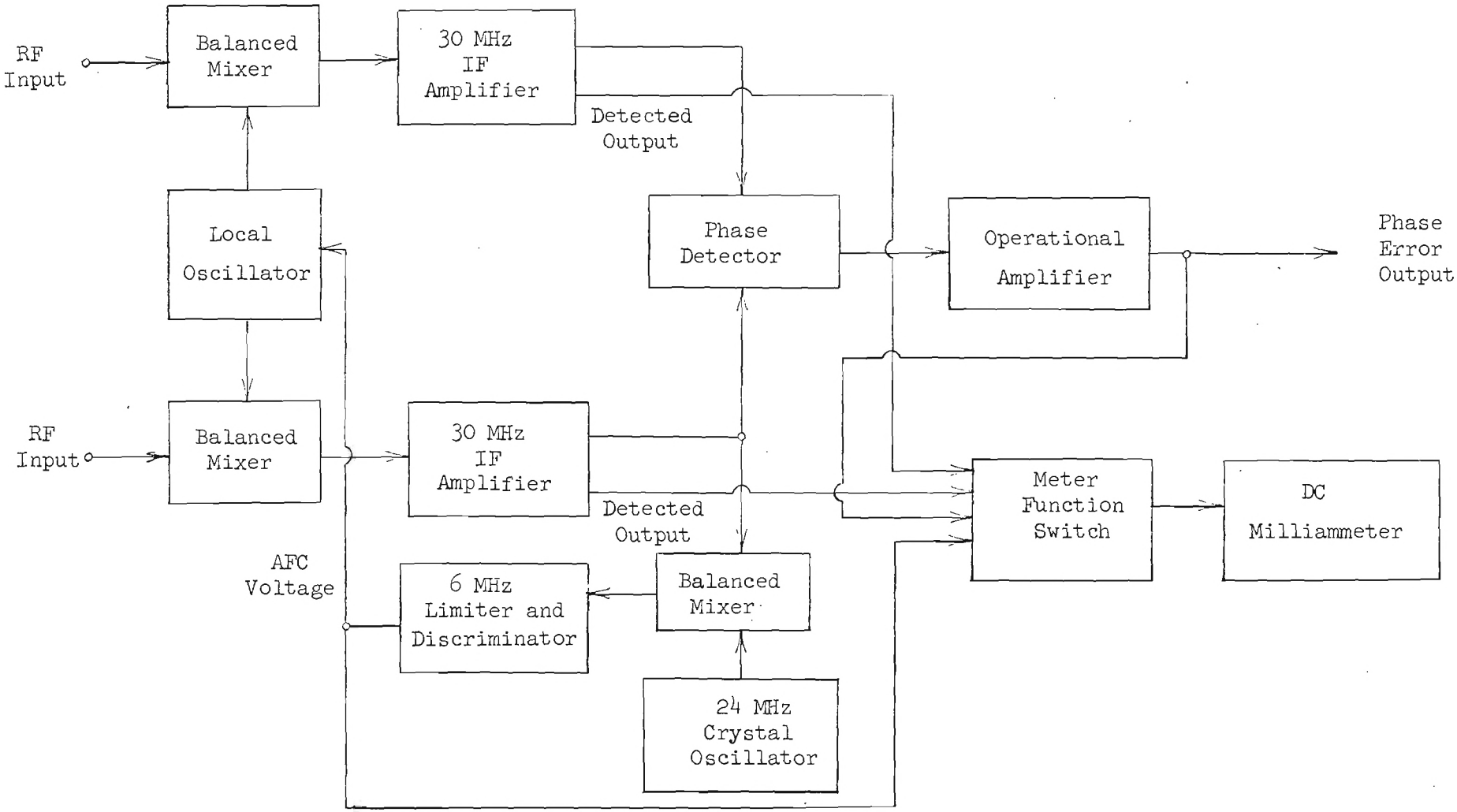

Figure 1. Automatic Phase Control System.

The stability of the local oscillator is an important factor in controlling the phase of the cancellation signal since any drift in the frequency of the local oscillator with respect to the RF input signal can produce a differential phase shift through the two IF amplifiers with a resulting phase error. The stability of the local oscillator was greatly improved through the use of an automatic frequency control loop. Figure 1 shows how a portion of the 30 MHz IF signal is heterodyned with a 24 MHz signal from a crystal controlled oscillator. The resulting 6 MHz IF signal is fed to a limiter and discriminator to provide an error signal to control the frequency of the local oscillator.

Design and construction of the automatic phase control system for the cancellation signal is now complete. Alignment and check-out of the system will be completed in the next quarter and extension of this system to the cancellation of AM signals will be initiated.

Wideband Amplifier:

Further tests were conducted on the wideband amplifier described in the first quarterly report. Primarily, the power output level at which saturation begins to occur was determined. This power level limits the magnitude of the interfering signal which can be cancelled, and it is also a limiting factor on the power level that can be handled by the Q multiplier. For example, complete cancellation of a signal can not be obtained if the required power level exceeds the unsaturated capabilities of the amplifier. Once the amplifier saturates, the output signal is no longer an exact duplicate of the input and does not match the amplitude and phase characteristics of the signal to be cancelled.

Figure 2 shows the output power as a function of the input power for the six stage, grounded base amplifier described in the first quarterly report. The distortion added to the signal by the amplifier

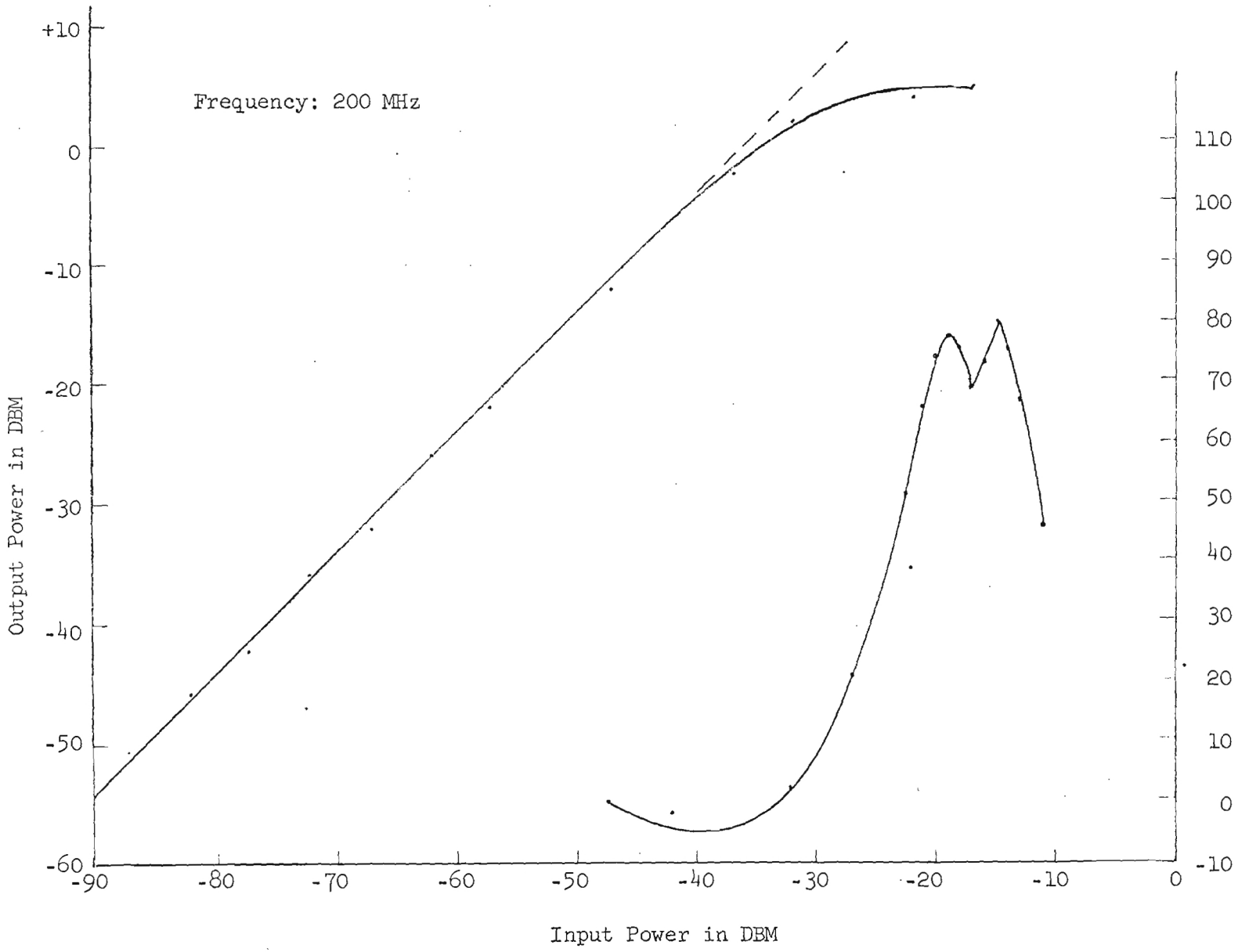

Figure 2. Wideband Amplifier Performance As A Function of Input Power.

is also shown. Good correlation exists between the input power level at which saturation occurs and the power level at which distortion shows a marked increase. For instance, at an input level of about -32 dBm, the output ceases to linearly follow the input and a significant increase in distortion is noticeable near this same power level.

Another grounded base amplifier was constructed with four stages of gain. In an attempt to provide a higher nonsaturated output level, the output stage was constructed with a 2N3866 transistor. This transistor was selected because its collector dissipation rating is much higher than that of the 2N918 or 2N3663 used in the original amplifier. A lower gain was obtained in this amplifier than in the previous model because of the fewer number of stages. In spite of the increased output capacity of the amplifier, the undistorted output power was not significantly improved over the initial unit. This lack of improvement indicates that the power handling capability of the output stage is set by the signal level at the input to the final stage rather than by the available output swing of the final stage. To avoid excessive distortion, the driving voltage across the base-to-emitter junction of the output transistor must be less than about 200 mv. In a grounded base amplifier, the input is applied directly across the base-to-emitter junction. For a 50 ohm impedance level a 200 mv signal corresponds to an input power to the final stage of approximately -3 dBm. Since the gain of the output stage is about 6 dB, the maximum undistorted output power level is in the neighborhood of + 3 dBm.

This discussion indicates that the grounded base amplifier appears to be unable to handle output levels much in excess of 0 dBm. In order to provide for those situations that may require power levels above 0 dBm, amplification techniques with higher output capabilities will continue to be investigated.

Current Controlled Attenuator:

Both the cancellation filter and the UHF Q multiplier require a variable gain control which has good UHF characteristics. A current controlled diode attenuator makes an excellent gain control for this application in that it can be constructed in a small physical configuration and can be continuously varied over a wide range. A current controlled attenuator was constructed in a manner similar to that outlined in Hewlett-Packard Application Note 912. A PIN diode was used as the resistive element in an attenuator because it exhibits a wide range of rf resistance as a function of bias current. This variable resistance property was incorporated into a π network whose performance is demonstrated in Figures 3 and 4. Figure 3 shows the attenuation at 300 MHz as a function of control current while Figure 4 shows the attenuation behavior over the frequency range of 200 to 400 MHz for three different current settings. The VSWR remained under 2:1 over the same frequency range for the various settings.

The AM cancellation system discussed in the first quarterly report requires that the auxiliary signal have its amplitude characteristics duplicate those of the interfering signal. The current controlled attenuator offers promise as a possible method for performing this function if the attenuation can be varied at an audio rate. Further tests of the attenuator are planned to evaluate this possibility.

Directional Couplers:

Two models of an octave-bandwidth, 10 dB directional coupler were constructed in final form. Typical performance as provided by each unit is shown in Figure 5.

VHF Crystal Interference Filters:

The use of quartz crystals as VHF interference filters continued to be investigated during the second quarter. The principal

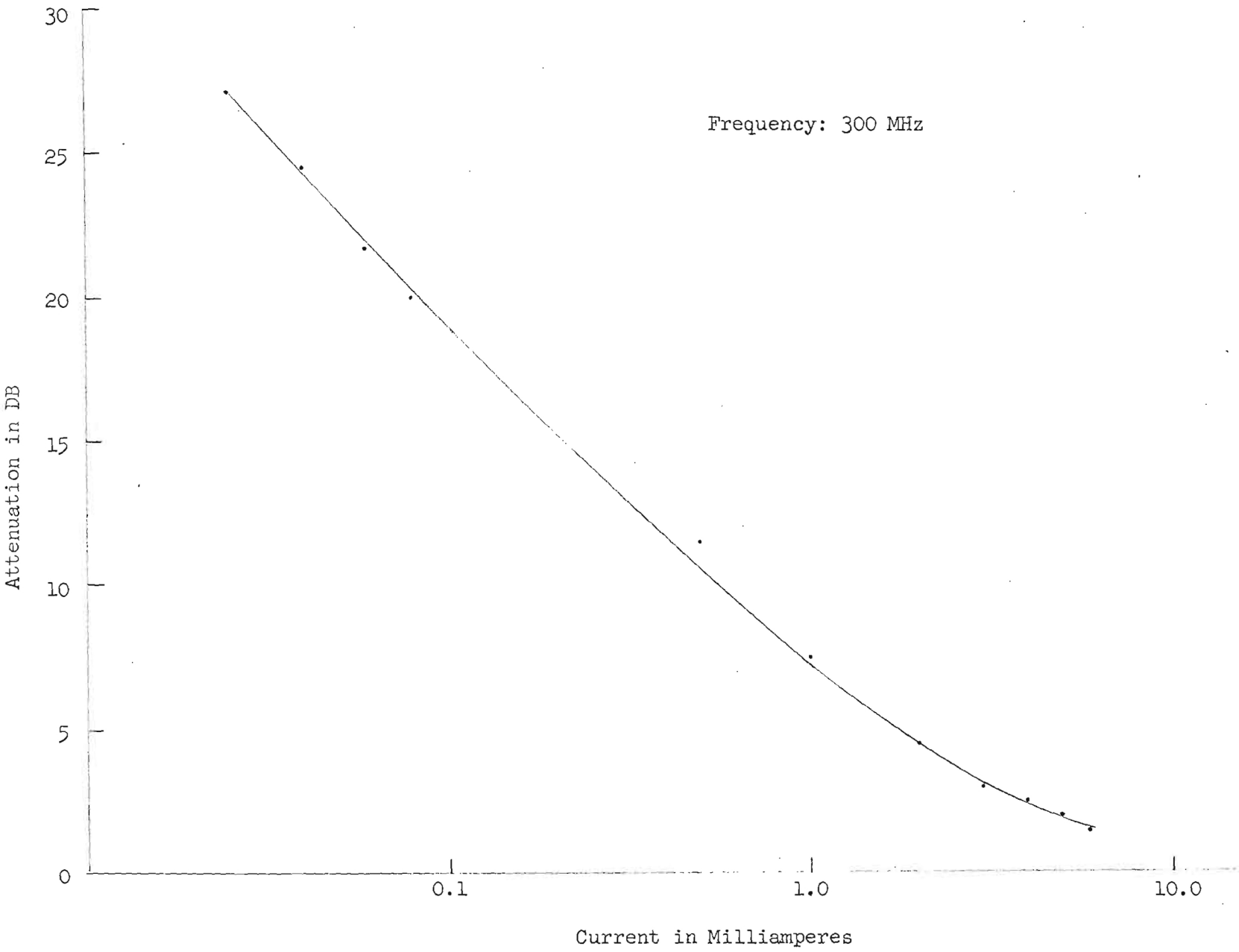

Figure 3. Attenuation Versus Bias Current of PIN Diode Attenuator.

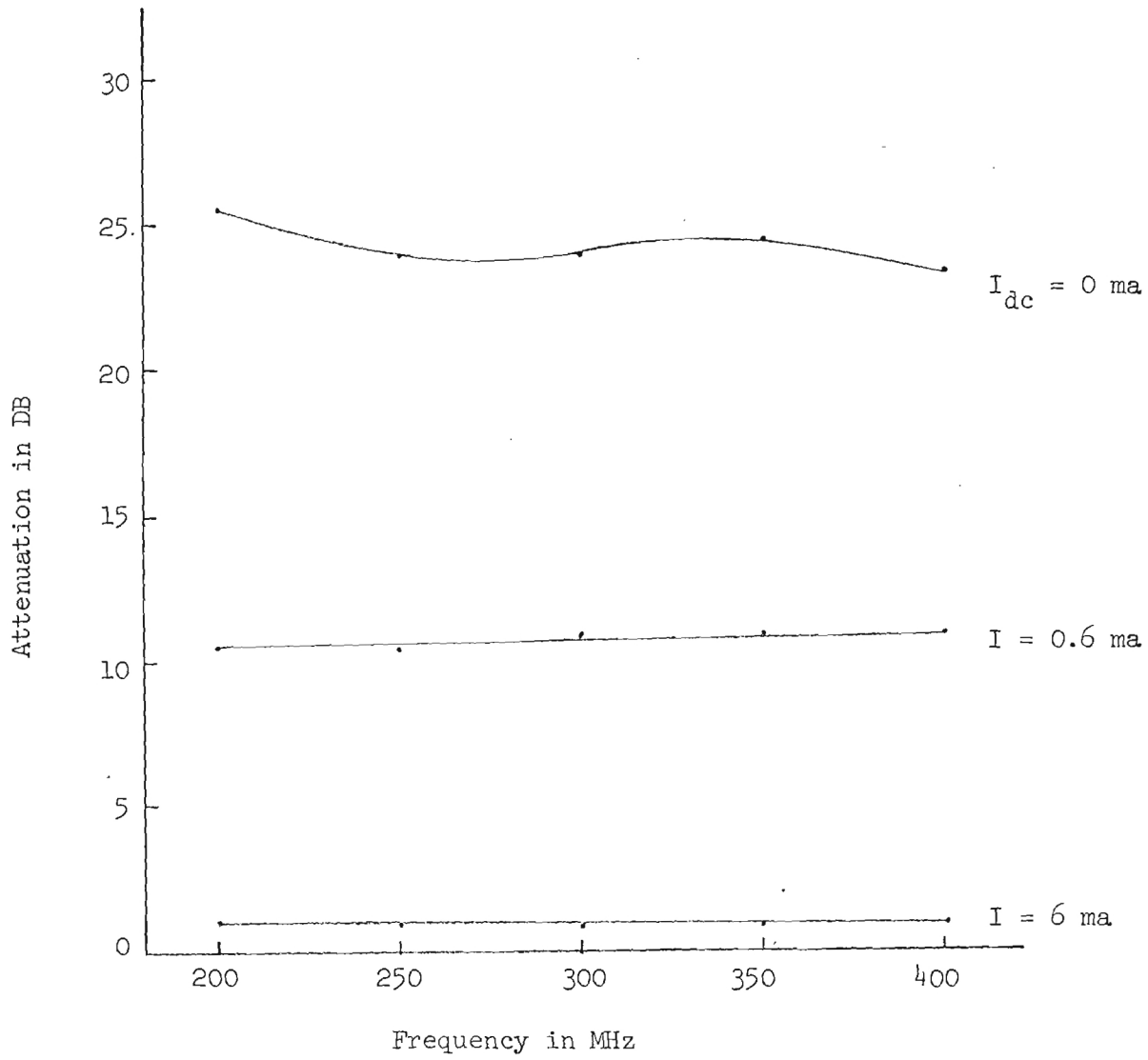

Figure 4. Attenuation Versus Frequency Characteristics of PIN Diode Attenuator.

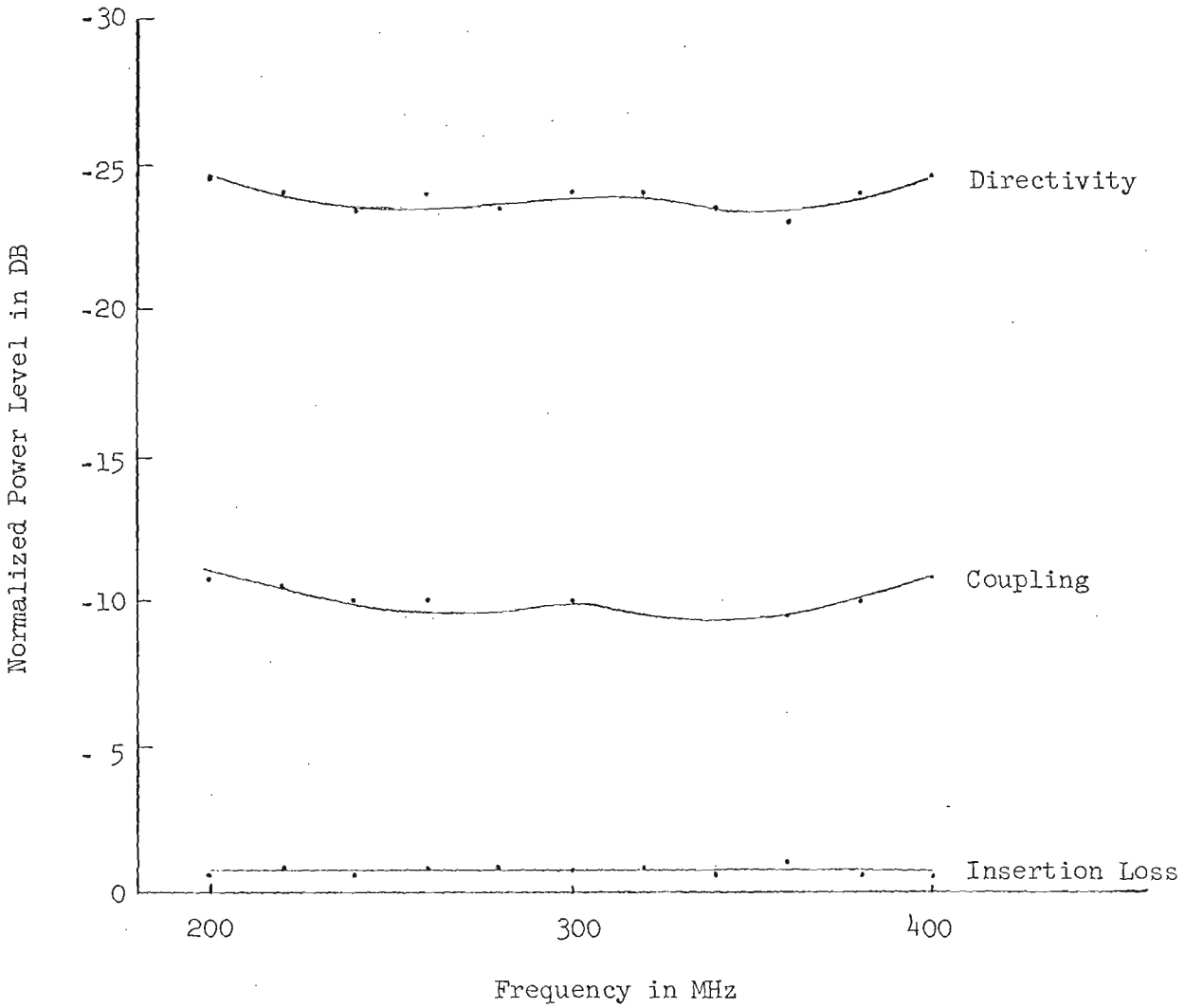

Figure 5. Characteristics of Directional Coupler.

areas of investigation were (1) the reduction of the off resonance insertion loss of bridge notch filters above 200 MHz and (2) the integration of crystal elements into high-pass and low-pass filter configurations. A filter using the parallel resonant impedance of the crystal was briefly investigated and a study was made of the characteristics of crystal elements in series.

The incorporation of a crystal into a balanced bridge configuration has been previously shown to produce a filter with good rejection levels at the notch frequency and good suppression of spurious responses, although at frequencies above 200 MHz, the preliminary models exhibited an excessive insertion loss outside the notch frequency. The original balanced bridge notch filter had an insertion loss of 28 dB at 380 MHz. To find out what part of this insertion loss was due to transformer losses, the insertion loss of the filter was measured with the bridge unbalanced. The measured loss of 18.5 dB at 380 MHz indicated that the transformers were contributing a large part of the loss. The original transformers were replaced with low loss UHF transformers constructed in the manner described by Ruthroff in the Proceedings of the IRE, volume 47, No. 8, August 1959. Using these new transformers, the insertion loss was still 19.5 dB at 260 MHz. These results indicate that other factors were responsible for the high value of loss.

Further study of the bridge configuration has shown that the insertion loss is related to the series resonant impedance of the crystal at the overtone response frequency. With a crystal in one arm of the bridge and an impedance in the other arm matched to the series resonant impedance of the crystal and the shunt capacity of the holder, cancellation of the signal in the frequency range of crystal resonance produces an effective notch filter. Off resonance, the crystal becomes a high impedance which unbalances the bridge. The resistance and capacitance necessary for balancing the crystal resonant impedance remain in series with the signal path and determine the off resonance insertion loss of the filter. In general, at the higher overtone responses, the series

resonant impedance increases and the overall insertion loss of the filter rises. In the next quarter, an attempt will be made to overcome the effect of high series resonant resistance of the crystals by incorporating the crystal in a hybrid structure.

One limitation of crystal filters as an interference reduction technique is the lack of flexibility because of their fixed tuned characteristics. A way of circumventing this limitation is to have available a large number of crystals with response frequencies appropriate to the interference environment. For maximum flexibility in meeting changes in the environment, the crystal elements should be interchangeable with minimum perturbation to the overall performance of the filter. The bridge configuration is limited in this regard as it must be balanced at each frequency of operation. A possible approach to the realization of a crystal filter with increased flexibility is to incorporate some of the crystal parameters into the integral design of a broadband filter configuration such as a high-pass or low-pass. For example, the shunt capacity, C_o, is primarily a function of the holder and can be integrated into the filter design. Then, as crystals of this holder group are interchanged to obtain responses at different frequencies, the overall bandpass response will not be materially changed.

Figure 6 illustrates the manner in which the crystal shunt capacity has been incorporated into a low-pass filter. The crystal resonant impedance shunts the transmission path through the filter at the series resonant frequency. The amount of attenuation through the filter at crystal resonance is dependent upon the ratio of the characteristic impedance of the filter to the series resonant impedance of the crystal. Consequently, the impedance level of the filter should be at the maximum practical value and the series impedance of the crystals should be as low as possible. The performance of a low-pass filter designed for a 200 ohm characteristic impedance is shown in Figure 6. Note the decrease in the attenuation at the higher overtone response frequencies

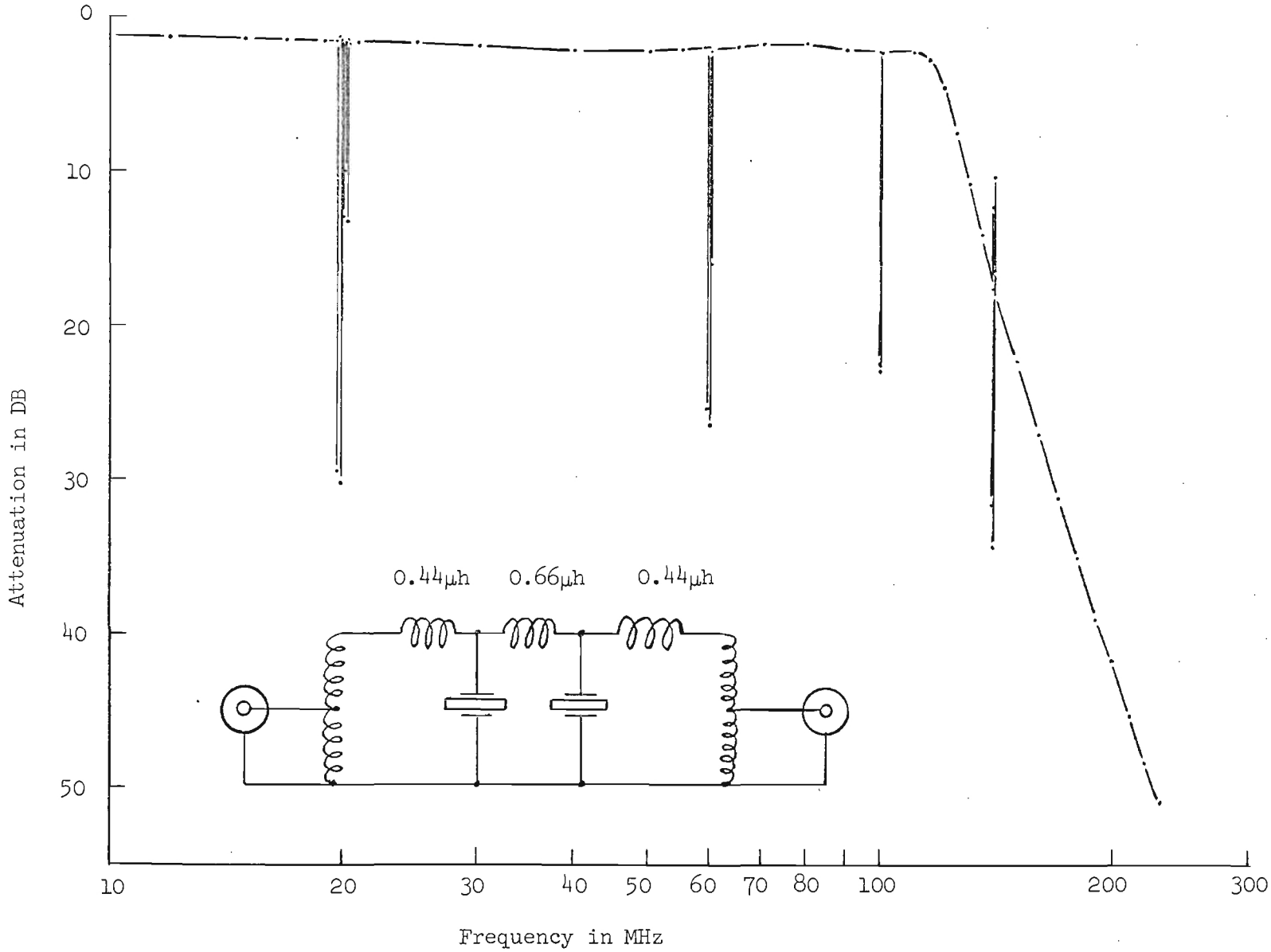

Figure 6. Rejection Characteristics of Lowpass Filter.

which is caused by the higher impedance of the crystal.

A crystal resonator is characterized by a number of parallel resonant frequencies which alternate between the conventional overtone and spurious response frequencies. The impedance level at parallel resonance is high compared to the series impedance. This high impedance can be used to obtain narrow bands of high insertion loss in the pass band of a high-pass filter. A high-pass filter was constructed which exhibited rejection ratios of greater than 20 dB at 100 MHz. The rejection ratio rapidly deteriorated to a negligible value at 200 MHz indicating a limited applicability of this technique above 100 MHz.

Two quartz crystals having the same fundamental response will not, in general, exhibit the same pattern of spurious responses. If the spurious response frequencies are not the same at the particular frequency where one crystal has a low impedance path, the other crystal should exhibit a high impedance path. It might be expected then, that a filter containing two series crystal elements having the same fundamental response frequency would have fewer spurious responses than a single crystal filter. To verify this concept, two crystal elements were incorporated into the design of a bandpass filter. Figure 7 shows the transmission characteristics of the filter with the crystals in series. Also shown for comparison purposes are the transmission characteristics of the filter with each crystal individually. Rather than effecting a reduction in spurious responses, the series operation of the crystals actually displayed a number of spurious responses approximately equal to the sum of the responses of both units. Consequently, cascading two crystal elements of the same fundamental frequency does not offer a very attractive means for reducing the number of spurious responses.

An investigation of the application of active circuits, including negative resistance and negative capacity, to the improvement of the interference rejection capabilities of crystal resonators will be

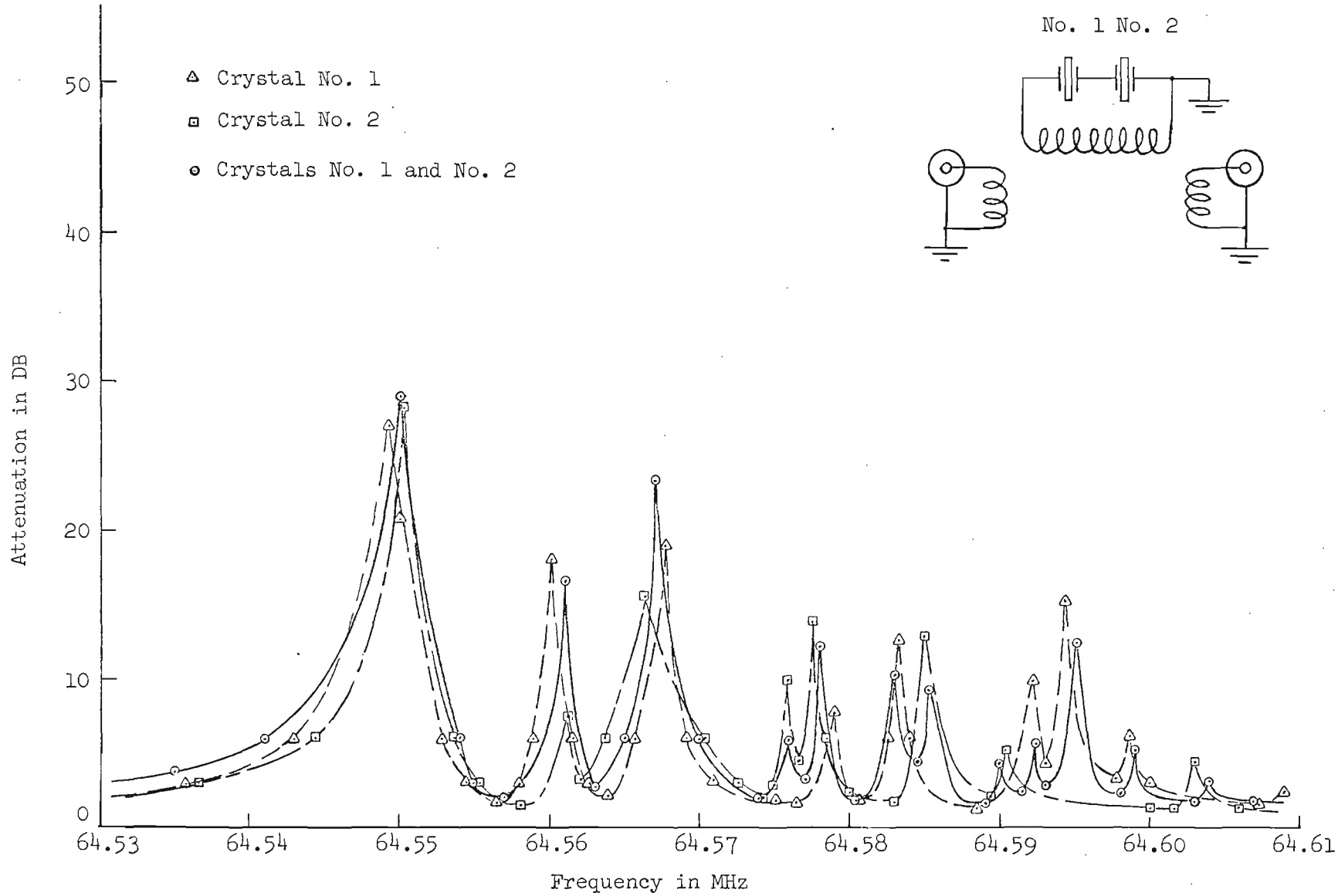

Figure 7. Rejection Characteristics of Two Crystals in Simple Notch Filter.

studied during the next quarter. Also, an examination of possible techniques for a tunable crystal filter is planned.

Analysis of the Q Multiplier:

The general analysis of the Q multiplier technique was continued during the second quarter. A multiplication factor, M_f, was defined in terms of network elements and its behavior with changes in the network was explored. The applicability of the analysis to the multiplication of the Q of a double tuned resonator was considered.

Figure 8 is a simplified block diagram of the Q-multiplication technique. The determination of the multiplication factor, M_f, may be developed in a straightforward manner by first defining a function, G(s), as

$$G(s) = A \frac{2\zeta\omega_o s}{s^2 + 2\zeta\omega_o s + \omega_o^2} \quad . \qquad (1)$$

Equation (1) is the generalized expression for a second order response function and is representative of the transmission function, in terms of the complex frequency, s, of a cavity resonator. The quantity ζ is related to the Q of the resonator by

$$\zeta = \frac{1}{2} Q \quad . \qquad (2)$$

In Quarterly Status Report No. 1 the transfer function of the overall Q multiplier network was derived as

$$T(s) = \frac{G(s)}{1 + \frac{R_a}{R_b} [1 - G(s)]} \quad . \qquad (3)$$

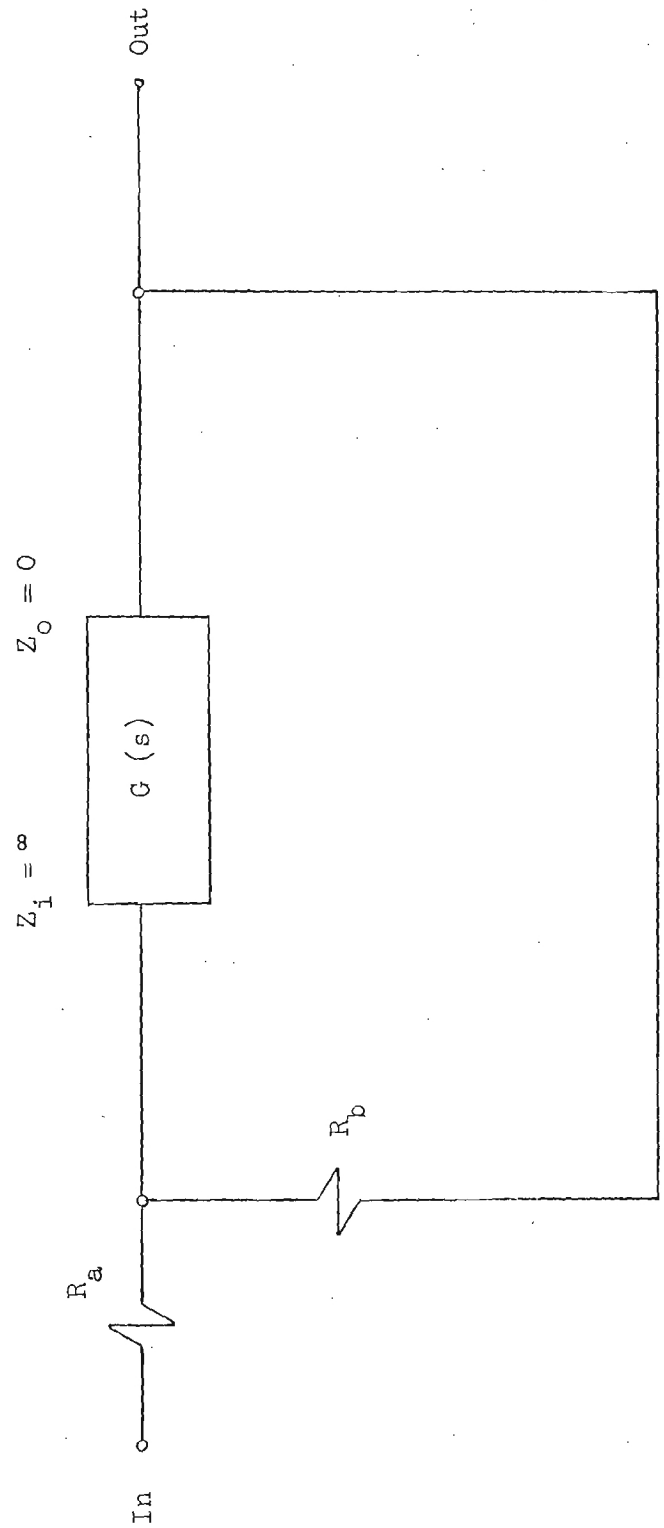

Figure 8. Simplified Block Diagram of Q Multiplier.

Substituting G(s) from equation (1) into (3) gives

$$T(s) = \frac{R_b}{R_a + R_b} \left\{ \frac{2A\zeta\omega_o s}{s^2 + \frac{[R_b + R_a(1-A)]\, 2\zeta\omega_o s}{R_a + R_b} + \omega_o^2} \right\} \quad . \quad (4)$$

Although expressions (1) and (4) are of the same form, they do differ in that the constant multiplier and the coefficient of s in the denominator are not the same.

By analogy with equation (1) the multiplied Q of the response function of equation (4) can be defined as:

$$Q' = \frac{R_a + R_b}{[R_b + R_a(1-A)]\, 2\zeta} \quad . \quad (5)$$

Defining the ratio of the multiplied Q to the natural Q as the multiplication factor, M_f, gives

$$M_f = \frac{Q'}{Q} = \frac{R_a + R_b}{R_b + R_a(1-A)} \quad . \quad (6)$$

Figure 9 shows the variation of M_f with the gain, A, for various values of $\frac{R_a}{R_b}$. Note that each curve is asymptotic to some value of A. This particular gain is the critical value at which the circuit becomes unstable.

Perhaps a more useful form for the multiplication factor is in terms of the change in bandwidth rather than in terms of Q. For example, suppose a cavity resonator with some natural Q is available. Then, the 3 dB bandwidth, Δf, at a particular frequency, f, is

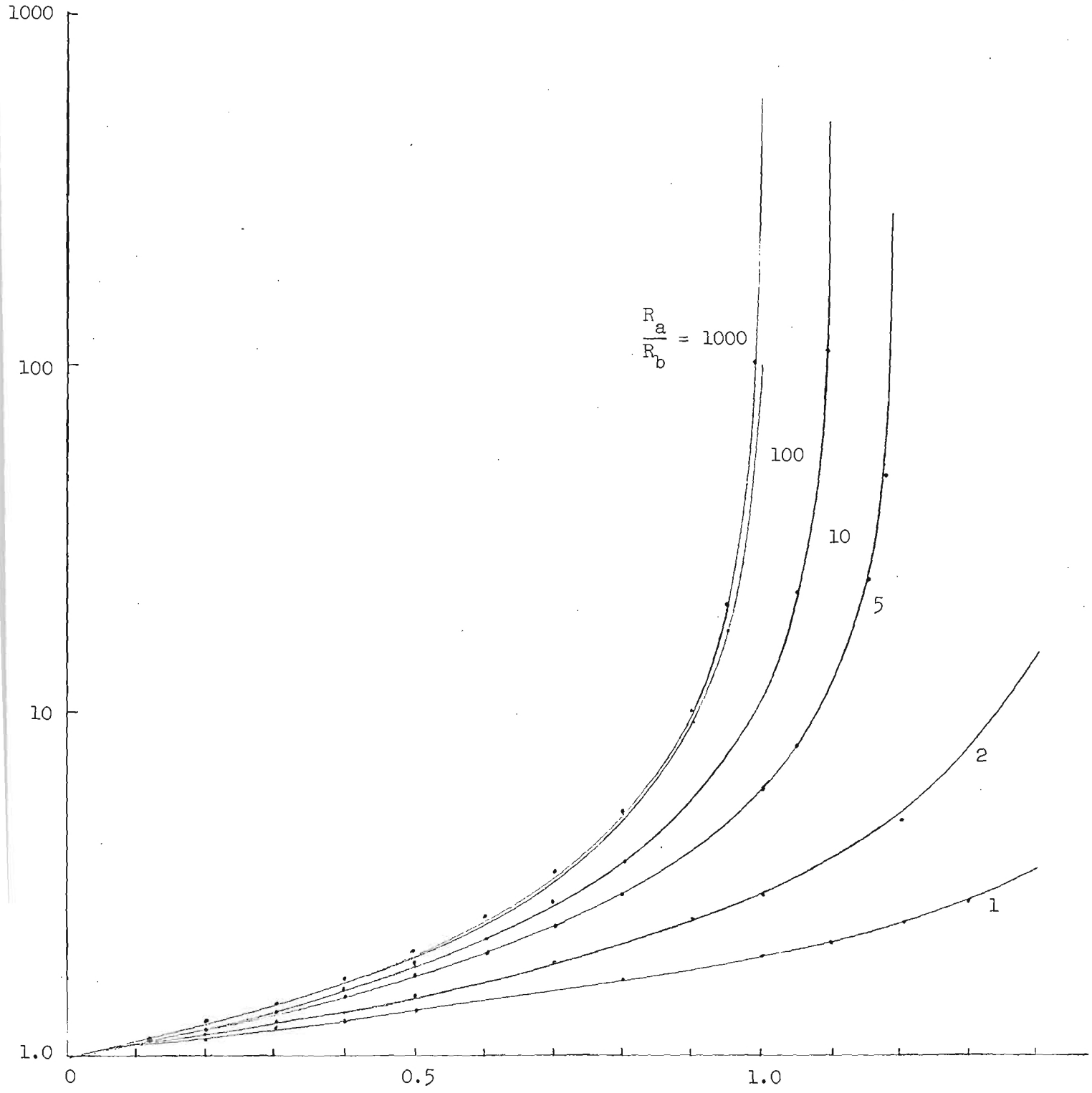

Figure 9. M_f Versus Gain For Selected Values of $\frac{R_a}{R_b}$.

$$\Delta f = \frac{f}{Q} \quad . \tag{7}$$

If the Q of the resonator is multiplied, the modified bandwidth is

$$\Delta f' = \frac{f}{M_f Q} \quad . \tag{8}$$

If a normalized bandwidth, $\bar{B}$, is defined such that

$$\bar{B} = \frac{\Delta f'}{\Delta f} \quad , \tag{9}$$

then it follows from (7) and (8) that

$$\bar{B} = \frac{1}{M_f} \quad . \tag{10}$$

Figure 10 shows the variation of the normalized bandwidth as a function of open loop gain for various values of $\frac{R_a}{R_b}$. The unmodified bandwidth, $A = 0$, is represented as 100 percent.

In actual practice, changes in system gain and phase, can be expected to cause bandwidth variations. In order to separate the effects of changes in the magnitude and phase of the loop gain on the normalized bandwidth, $\bar{B}$, equation (6) can be written in the form

$$M_f = \frac{R_a + R_b}{R_b + R_a[1 - |A| P(\theta)]} \quad , \tag{11}$$

where $|A|$ and $P(\theta)$ are the magnitude and phase of the loop gain, A. Substituting (11) in (10) gives

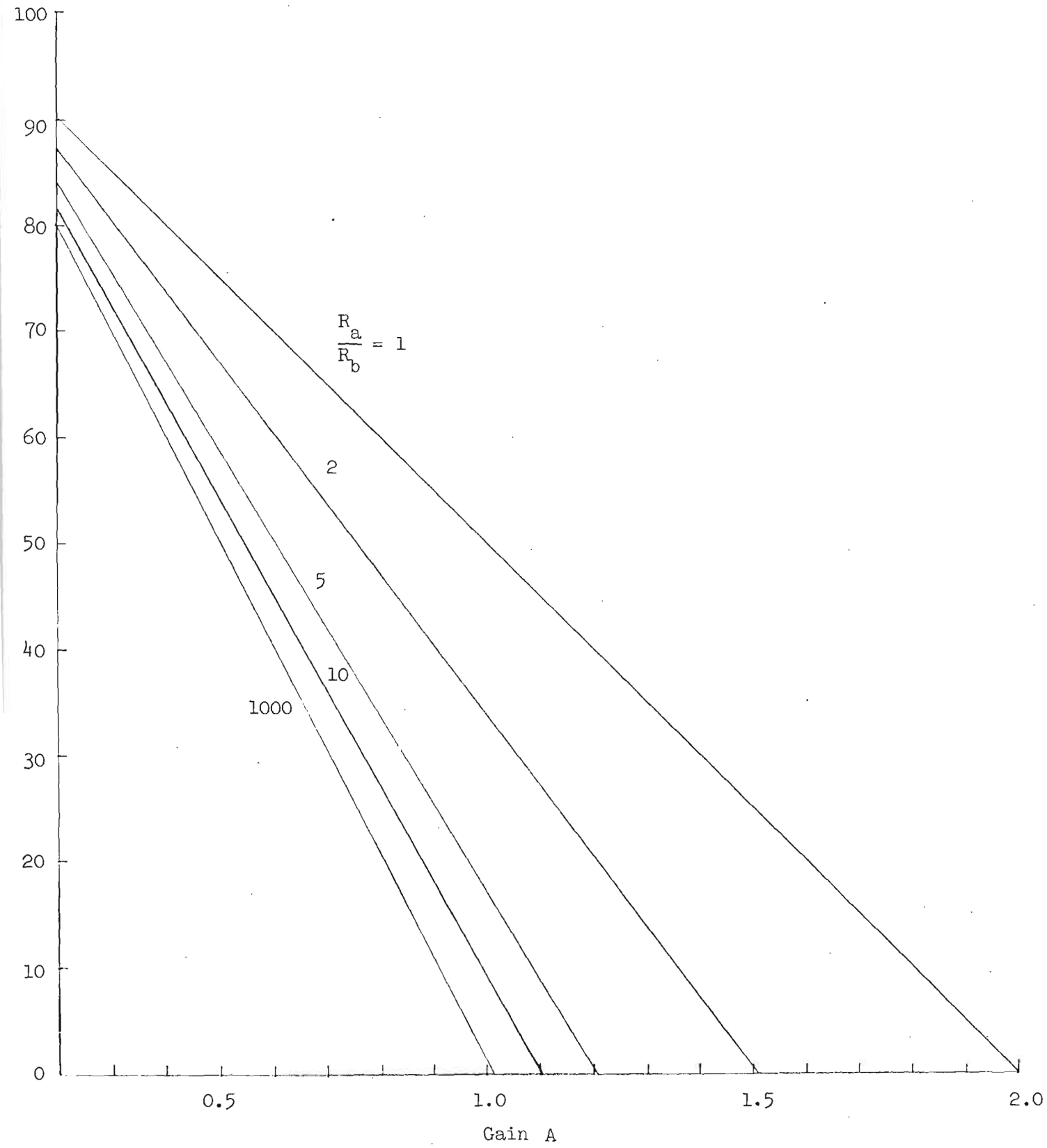

Figure 10. Normalized Bandwidth Versus Gain for Selected Values of $\frac{R_a}{R_b}$.

$$\bar{B} = \frac{1}{M_f} = \frac{R_b + R_a[1 - |A| P(\theta)]}{R_a + R_b} \quad . \qquad (12)$$

The variation of the normalized bandwidth due to changes in gain or phase that may be caused by environmental factors such as temperature, humidity, and others can now be described by differentiating (12) to obtain an expression for the total differential, $d\bar{B}$. Performing the necessary differentiation gives

$$d\bar{B} = - \frac{R_a}{R_a + R_b} \left[P(\theta)\, d|A| + |A| dP(\theta)\right] \quad . \qquad (13)$$

As an example, suppose the phase function is adjusted so that $P(\theta) = 1.0$ and suppose that $dP(\theta) = 0$. Changes in $\bar{B}$ because of changes in $|A|$ are then given by:

$$d\bar{B} = - \frac{R_a}{R_a + R_b} d|A| \quad . \qquad (14)$$

Equation (14) defines the slope of the curves of Figure 10. Suppose, for a ratio $\frac{R_a}{R_b} = 1$, the loop gain in the system changes 10 per cent. The resulting change in bandwidth is 5 per cent.

Application of Q Multiplication to a Double Tuned Circuit:

A double tuned circuit may be adjusted to exhibit a flat amplitude response with skirt selectivity better than that obtainable with a single tuned circuit. It seems reasonable that the application of the Q multiplication technique to a double tuned circuit would result in a filter with a flat pass band and very steep skirt selectivity. To test this idea, a double tuned circuit with a phase and amplitude

response characterized by the solid lines of Figure 11 was inserted into the Q multiplication network. The typical response of the resulting network, shown by the dashed line in Figure 11, does not have the desired shape. An examination of the loop phase conditions showed that the distortion in the shape of the response was due to the mismatch between the phase response through the double tuned circuit and the phase response around the feedback loop. Referring to equation (3), it can be seen that the maximum transmission level through the overall network occurs when the phase shift around the loop is 360 degrees. To duplicate the response characteristics of the double tuned circuit, the phase response of the feedback path must exhibit a region of no change in phase shift with frequency which coincides with the bandpass region of the filter. The phase shifter used in the Q multiplier does not provide this type of response.

During the next quarter, evaluation and analysis of the VHF multiplication technique will continue. The development of component parts for a demonstration prototype system will continue. A wide band phase shifter for the 200 to 400 MHz range will receive particular attention.

Work Schedule and Progress:

The progress of the work of this project is satisfactory and essentially in conformance to the projected work schedule.

Program for the Next Quarter:

The program for the next quarter will be essentially in conformance with that already outlined in the preceding paragraphs.

Personnel Changes:

During the past quarter, no significant personnel changes have taken place.

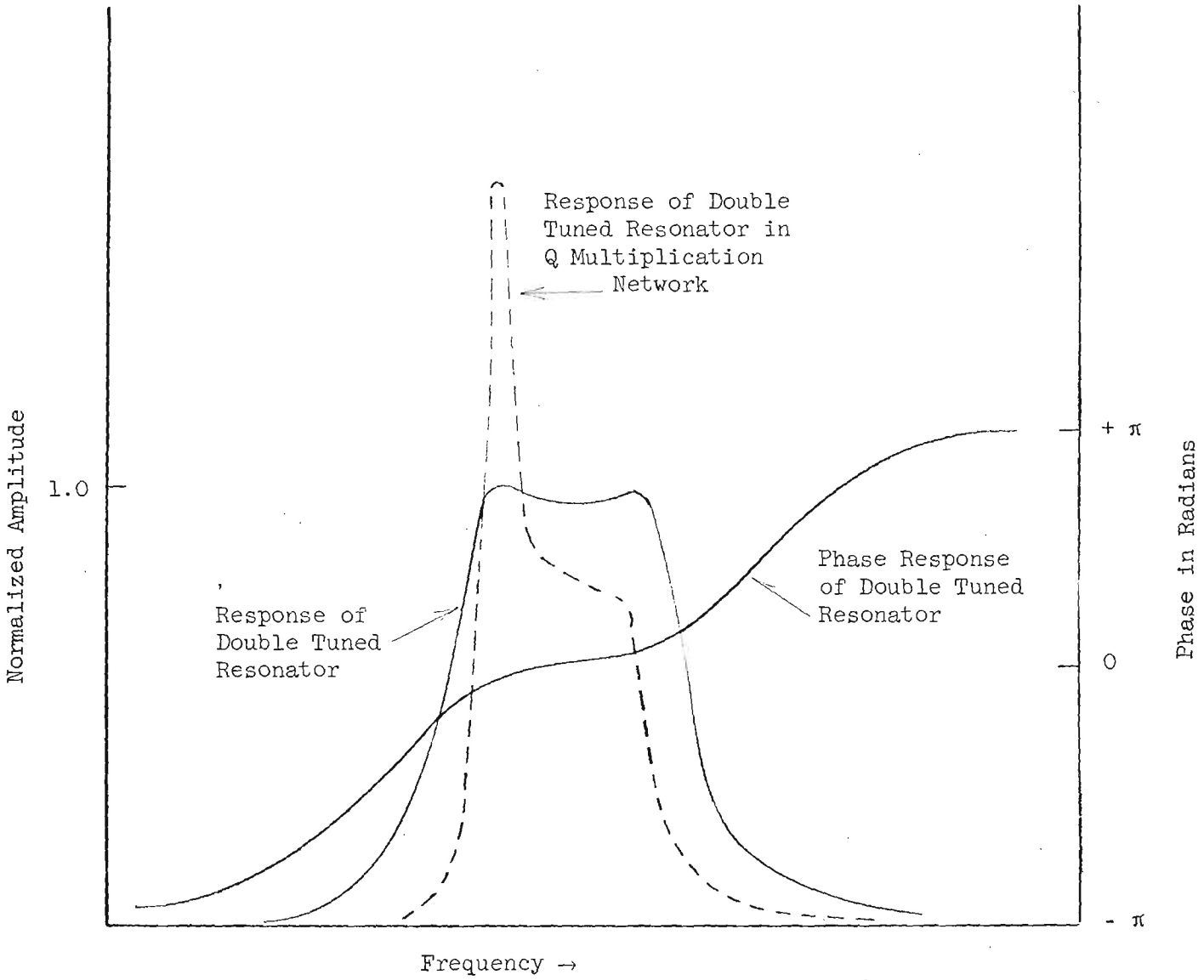

Figure 11. Representation of the Behavior of a Double Tuned Resonator in the Q Multiplication Network.

Engineering Man-hours:

The following number of engineering man-hours was devoted to this project effort during the past quarter:

Category	No. of Hours
Senior Research Engineer	192
Research Engineer	485
Assistant Research Engineer/ Graduate Research Assistants	1291

Respectfully submitted:

Hugh W. Denny
Project Director

Approved:

D. W. Robertson, Head
Communications Branch

GEORGIA INSTITUTE OF TECHNOLOGY
ENGINEERING EXPERIMENT STATION
ATLANTA, GEORGIA 30332

15 September 1967

Commander
Rome Air Development Center (EMKC)
Griffiss Air Force Base
New York 13440

Attention: EMCVI-2

Subject: Quarterly Status Report 3, Project A-987
"Interference Reduction Techniques Employing Active Devices"
Contract No. F30602-67-C-0066
Covering the period from 1 June 1967 to 31 August 1967

Dear Sir:

Objective:

To develop interference rejection networks employing a combination of active and passive techniques to obtain improved rejection of co-channel and adjacent channel interference.

Technical Program:

During the past quarter the technical effort of this project has continued in three principal areas. These areas are: (1) the application of RF cancellation techniques at UHF, (2) the evaluation of quartz resonators as interference filter elements at VHF, and (3) an investigation of UHF Q multiplication techniques. The activities and results obtained in these areas are discussed in the following paragraphs.

RF Cancellation Techniques:

The development of experimental systems for the active cancellation of interference signals was continued during the third quarter. Emphasis was directed primarily toward techniques appropriate to the operational situations of (1) the availability of a sample of the interfering signal at other than the receiver terminals and (2) the more general situation where an isolated sample is not available. The automatic phase control system described in Quarterly Status Report 2 was designed to develop a cancellation signal from an isolated sample. Early in the quarter, construction of this system was completed and performance data was obtained. For the general situation where the interfering source is not sufficiently close by to obtain a sample of its signal, a complete system which includes the ability to extract the interfering signal is required. To meet this need, the development of an active cancellation filter for AM signals was initiated this quarter.

The modifications which were discussed in Quarterly Status Report 2 made significant improvements in the performance of the automatic phase control system. The replacement of the local oscillator transistor with a Nuvistor vacuum tube improved the free running frequency stability to approximately 5 parts in 10^6, averaged over a one minute time interval. With AFC applied, the AFC loop gain was sufficient to increase the stability to 5 parts in 10^8 when locked to an input signal derived from a frequency standard. AFC between the local oscillator and the reference input signal was obtained at signal levels as low as 5μV.

The two 30 MHz IF amplifiers were constructed with transistors having forward AGC characteristics which permitted IF gain control through the use of a potentiometer mounted on the front panel. The net gain of the interference channel amplifier was variable from 15 dB to 38 dB, and the range of the signal plus interference channel

amplifier gain was from 33 dB to 57 dB. Both channels exhibited similiar bandwidths of 1.5 MHz.

Filtering of the phase detector output voltage was accomplished with a low pass filter with a variable cutoff frequency. Selection of cutoff frequencies of 2.5, 10, 100 or 1000 Hz was provided through a front panel switch. The phase detector was followed by a operational amplifier with a maximum gain of 60 dB which allowed an increase of the maximum phase detector error voltage to ±10 Volts for an RF input signal of -85 dBm at the signal plus interference port.

Following the completion of the automatic phase control system, emphasis was directed to the design and contruction of the UHF AM cancellation filter. Since several of the components of the two systems perform similiar functions, many of the designs developed for the automatic phase control system were applied directly to the AM cancellation filter.

The block diagram of figure 1 illustrates the operational features of the cancellation filter. A sample of the interference signal is obtained from the output side of the summation junction to provide the error signal for a dual closed loop system. The level and phase of interference signal out of the junction provides a reference voltage which is used to adjust the amplitude and phase characteristics of the cancellation signal.

The AM cancellation filter consists of two 200-400 MHz double conversion receivers sharing a common local oscillator. The RF input signal is fed to a cascode Nuvistor preselector which has approximately 15 dB of RF gain and establishes the system noise figure. The amplified RF signal and the cancellation signal are heterodyned in balanced mixers with the first local oscillator to produce 30 MHz first IF signals. Two 30 MHz amplifiers provide a gain of 58 dB with a nominal bandwidth of 1 MHz. The transistors used in these amplifiers have a forward AGC characteristic which permits external control of the gain

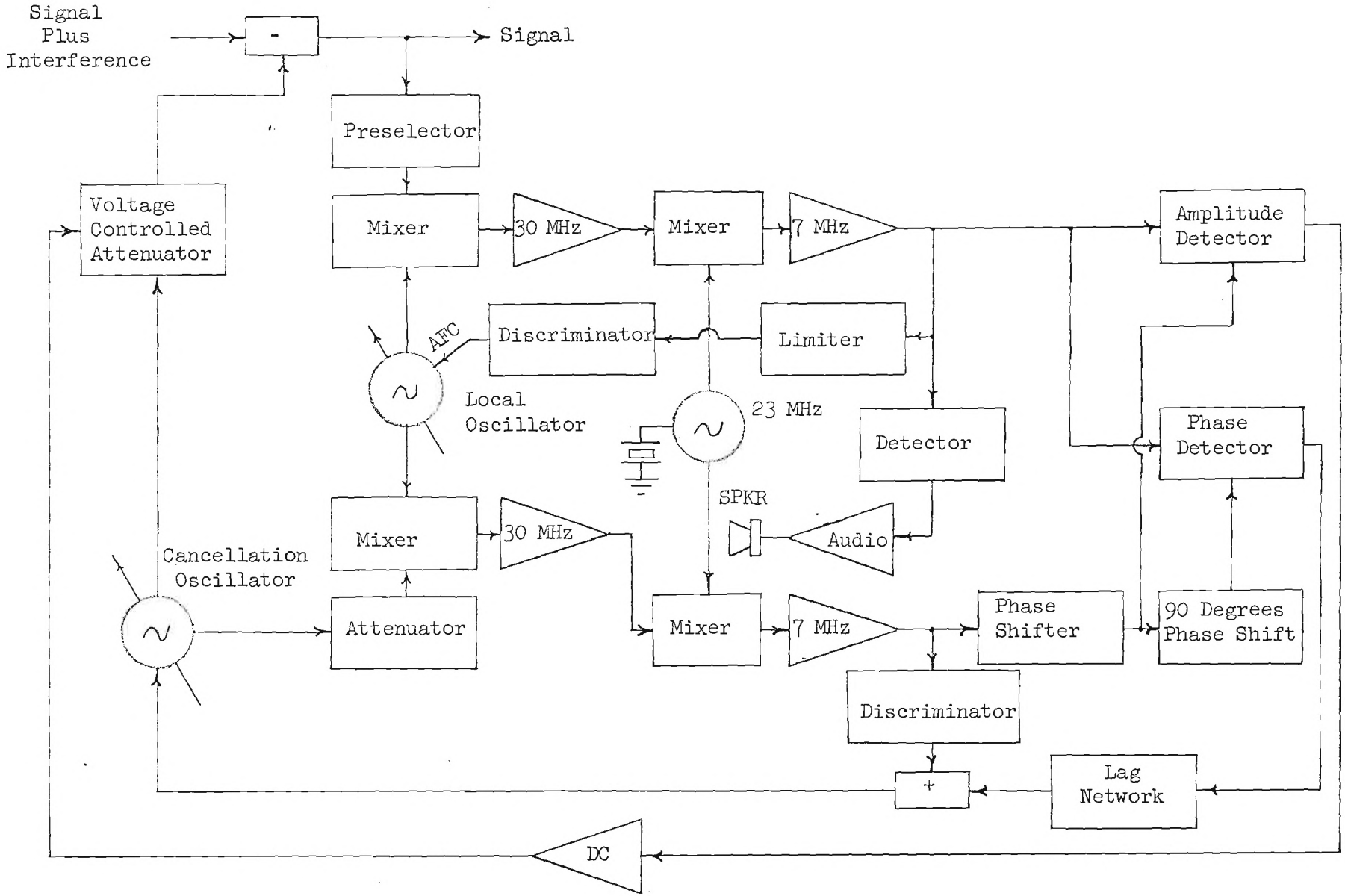

Figure 1. UHF AM Cancellation Filter.

by varying the DC collector current.

The two 30 MHz signals are heterodyned with a 23 MHz, crystal controlled, second local oscillator to produce 7 MHz second IF signals. An additional gain of 50 dB is supplied by the second IF amplifiers over a bandwidth of 100 KHz. A portion of one of the 7 MHz output signals is used to develop an AFC voltage for controlling the frequency of the first local oscillator. An AFC voltage for the cancellation oscillator is obtained from the other 7 MHz signal. This signal is applied to a discriminator to develop an error signal which aids in the acquisition of phase lock of the cancellation signal to the interfering signal. The outputs from the two 7 MHz IF amplifiers are phase compared and the resultant phase error voltage is added to the AFC voltage and both are applied to the cancellation oscillator.

The adjustable phase shifter at the output of the 7 MHz IF amplifier in the cancellation oscillator loop has a range in excess of 360 degrees. Adjustment of the phase of the 7 MHz IF signal results in the phase of the cancellation oscillator being shifted by the same amount since the phase lock loop maintains a quadrature relationship between the two 7 MHz IF signals. A fixed 90 degree phase shift, as shown on the block diagram of figure 1, results in the 7 MHz inputs to the amplitude detector being in phase since the two phase detector signals are in quadrature.

The output of the amplitude detector is coupled to the DC amplifier which increases the signal amplitude to a level sufficient to drive a voltage controlled attenuator. The voltage controlled attenuator incorporates HPA 3001 PIN diodes to vary the level of the cancellation oscillator signal in accordance with the output of the amplitude detector. As a result, the level of the cancellation oscillator is made to follow the amplitude variations of the interfering signal. Therefore, by proper phase adjustment and initial

level adjustment, the modulated interfering signal can be suppressed.

In the final quarter, construction of the AM cancellation filter will be completed and evaluation tests performed.

Further developmental work is also planned on the feed-forward cancellation filter which was discussed in Quarterly Status Reports 1 and 2.

VHF Crystal Interference Filters:

The investigation of quartz crystals as VHF interference filters continued during the third quarter. Particular emphasis was placed on (1) the integration of a crystal in a hybrid structure, and (2) the application of active circuits, including negative resistance and negative capacity, for improvement of the rejection capabilities of crystal resonators.

The incorporation of a crystal into a balanced bridge configuration has been previously shown to produce a filter having rejection levels approaching 50 dB at the notch frequency with good suppression of spurious responses. However, at frequencies above 200 MHz the preliminary models exhibited excessive insertion loss outside the notch frequency. This insertion loss was attributed in part to the transformer losses.

State-of-the-art broadband hybrid junctions exhibit lower loss characteristics in the VHF region than conventional transformers. Therefore, a crystal notch filter was constructed using a hybrid junction in the manner shown in figure 2. In the hybrid junction, a signal applied to the summing port is split between the two side arm ports. Any impedance mismatch at the side arms reflect the signals to the output difference port. With one side arm containing the crystal and the other side arm containing an impedance matched to the series resonant impedance of the crystal and the shunt

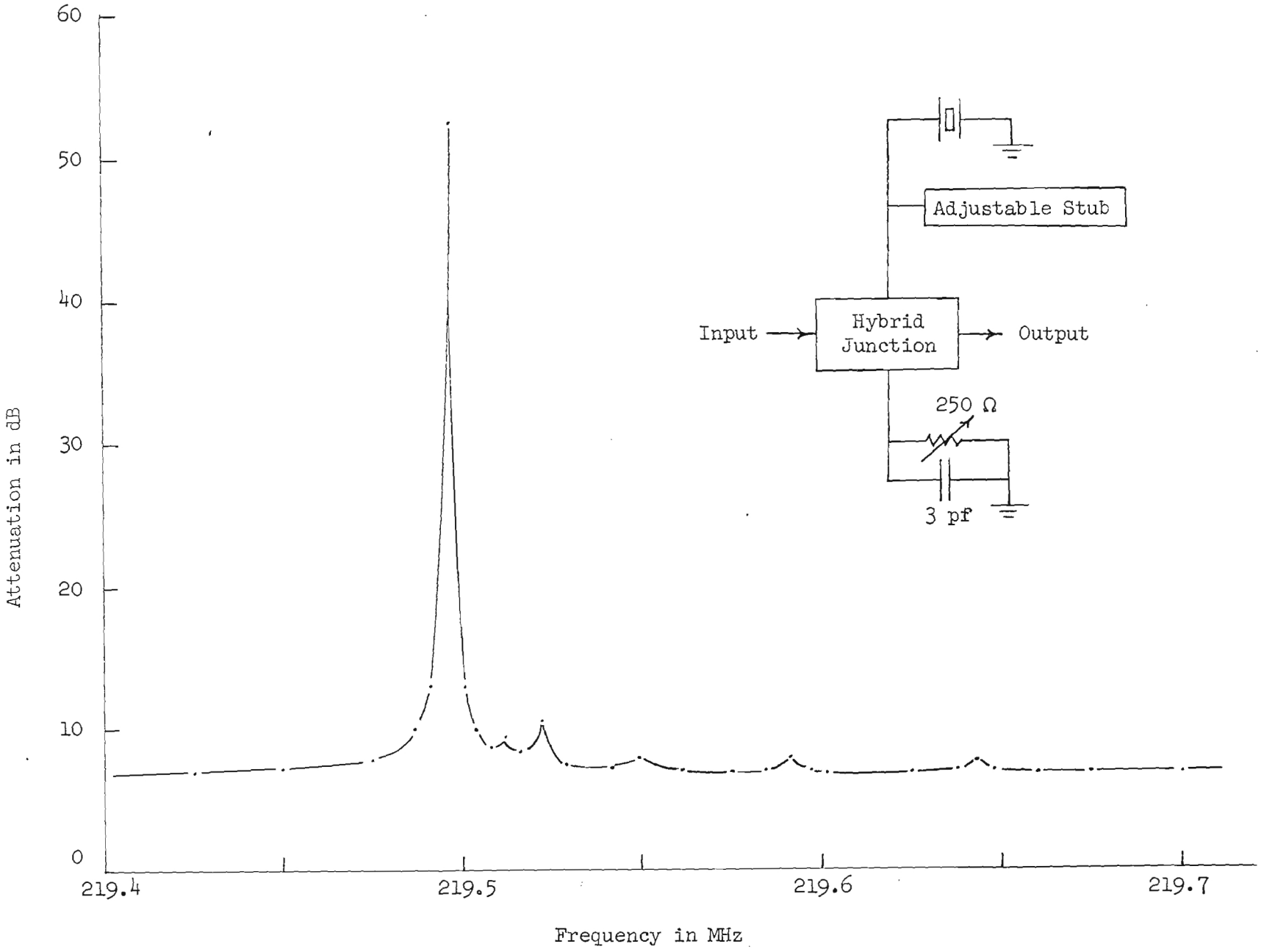

Figure 2. Rejection Characteristics of Hybrid Filter.

capacity of the holder, cancellation of the signal at the crystal resonant frequency produces a notch characteristic as shown by the response curve of figure 2. Off resonance, the crystal exhibits a high impedance which unbalances the hybrid. The off-resonance insertion loss of the filter is determined by the amount of hybrid unbalance created by the off resonance crystal impedance. The 7 dB insertion loss is a 3 dB improvement over the 10 dB insertion loss of the preliminary bridge configuration discussed in Quarterly Status Report 2.

The depth of the notch obtainable with the balanced hybrid bridge filter depends upon the precision of match between the side arm impedances. The pass band insertion loss, however, depends upon the degree of mismatch between these impedances. Minimum insertion loss with maximum rejection at the notch frequency will, consequently, be obtained with a crystal unit of lowest series resonant impedance. The low balancing impedance required to produce the notch characteristic at crystal resonance then exhibits a large mismatch to the crystal off-resonance impedance which results in a lower insertion loss.

This fact was verified by lowering the 250 ohm potentiometer setting. At minimum resistance, the pass band insertion was reduced to 3.5 dB at the 220 MHz measurement frequency. Naturally, this procedure unbalanced the bridge and degraded the notch rejection value but it showed that a lower value of crystal resonant impedance is necessary to reduce the pass band insertion loss of the notch filter configuration.

These results provide further evidence that the insertion loss and the rejection ratio of VHF crystal reject filters are limited in most cases by the holder capacitance and the series resonant impedance of the crystal. Consequently, a reduction in either or both of these crystal parameters is desirable. The application of active circuit techniques to the reduction of these parameters was

initiated during the third quarter. Two basic methods were investigated. One method used an active network to produce a negative resistance which supplied some of the energy losses in the crystal. A second approach used the active network to produce a negative capacitance to cancel a portion of the crystal holder capacitance.

An active circuit which exhibits a negative impedance characteristic is shown in figure 3. The impedance between terminals 1 and 2 is given by

$$Z_{12} \approx \frac{Z_f + 68}{1 - A} \qquad (1)$$

where Z_{12} and Z_f are expressed in ohms and A is the gain of the RF amplifier. If the feedback element is a capacitance, C_f, whose reactance is large compared to 68 ohms then the impedance, Z_{12}, appears to be a capacitance of value $C_f/(1-A)$, which is negative when $A > 1$.

A lowpass filter similar to the one described in the second quarterly report was designed to test the application of the negative capacitance. The two shunt elements of the filter were designed to be 2 pf each. One of the capacitors was replaced with a 100 MHz crystal in parallel with the negative capacitance circuit of figure 2. When the negative capacitance circuit was adjusted to partially cancel the 6.5 pf crystal holder capacitance, a periodic peak and null pattern of the type shown in figure 4 was obtained. This pattern is apparently the result of the constant time delay around the feedback loop of the negative capacitance circuit. Since the phase of the feedback signal increases with frequency, the proper phase relation with the input signal occurs only at periodic frequencies. At other frequencies the negative impedance circuit will generate both positive and negative real values of impedance. These results indicate that the proper phase relations required for a negative capacitance circuit in the VHF region can be maintained only

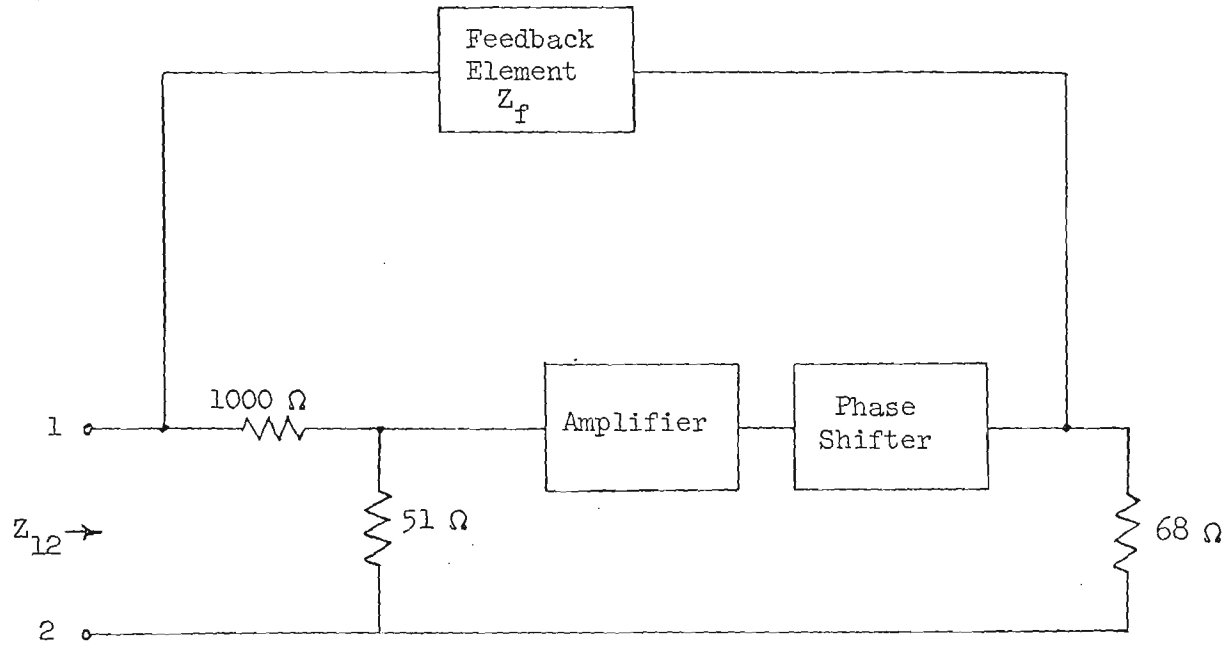

Figure 3. Block Diagram of Network Used to Generate a Negative Impedance.

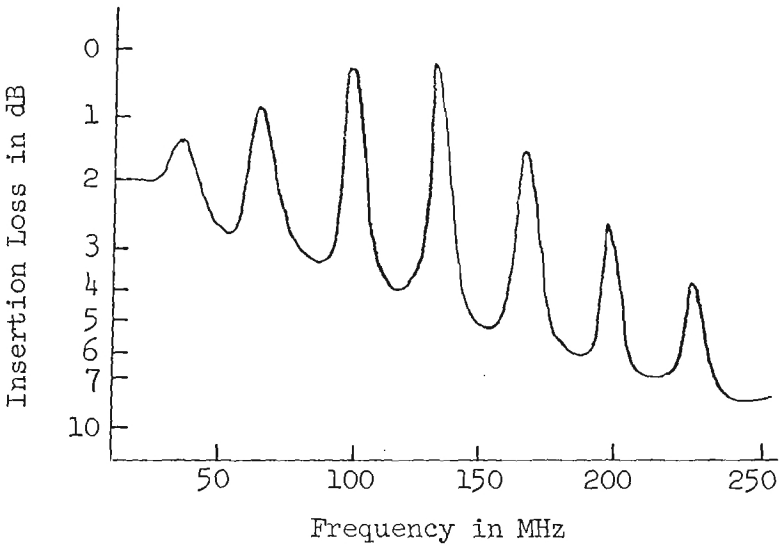

Figure 4. Effect of Negative Capacitance Network on Transfer Characteristic of a Low-Pass Filter.

over a narrow frequency band without elaborate broadband phase compensation networks.

The negative impedance circuit of figure 3 may also be used to realize a negative resistance. The peak and null behavior which limits the application of negative capacitance does not restrict the negative resistance application since the frequency range is narrowly restricted to the crystal resonant frequency region.

The application of the negative resistance circuit in parallel with the crystal element was tested in several preliminary circuits including the simple rejection filter, the bridge notch filter, and the hybrid filter. In each case there was no significant improvement in the filter rejection characteristics. In fact, an increase in the insertion loss of each filter resulted which was probably due to the shunt loading of the crystal by the active circuit at frequencies outside the crystal resonance region. These results do not encourage further study of the shunt negative resistance method.

Next quarter the application of a negative resistance in series with the crystal element will be studied. Additional active techniques will be studied to include a bandpass filter which utilizes Q multiplication techniques.

UHF Q Multiplication Techniques:

The development of a working model of the UHF Q multiplier was continued during the third quarter. Primary emphasis was placed on the development of a compact, voltage controlled phase shifter compatible with the other elements of the multiplication network. This type of phase shifter is desirable for the development of a relatively compact system.

An ideal phase shift network permits the phase of the signal through the network to vary without affecting the amplitude of the signal. A simple technique which is commonly used in the UHF and

VHF regions is a variable length of transmission line. Transmission line phase shifters are practically ideal in that the amplitude of the signal is not affected. However, in the 200 to 400 MHz range, they become rather large since the amount of phase shift obtainable is directly related to their physical length. For example, at 300 MHz, a length variation of 50 centimeters is necessary to obtain at least 180 degrees of phase shift. Since one of the primary objectives in developing the Q multiplication technique is to realize large effective Q's in smaller physical systems, long lengths of transmission lines are not desired. Consequently a primary aim in the development of a phase shifter was to develop a device that is more compatible with the overall Q multiplication concept. Additionally, a voltage tuning capability was also desired to simplify operational adjustments.

A length of transmission line is an example of an all-pass network, that is, the amplitude of the transfer function is a non-varying function of frequency while the phase does vary as a function of frequency. The pole-zero (p-z) plot of an elementary all pass function is shown in figure 5. The transfer function represented by this p-z plot is

$$T(s) = \frac{s - z_1}{s - p_1} = \frac{s - \sigma_1}{s + \sigma_1} \quad . \tag{2}$$

Evaluating (2) at $s = j\omega_1$, point A, yields

$$T(j\omega_1) = \frac{j\omega_1 - \sigma_1}{j\omega_1 + \sigma_1} \quad . \tag{3}$$

The amplitude of the transfer function as a function of frequency is

$$|T(j\omega)| = \frac{|j\omega_1 - \sigma_1|}{|j\omega_1 + \sigma_1|} = \frac{\sqrt{\omega_1^2 + \sigma_1^2}}{\sqrt{\omega_1^2 + \sigma_1^2}} = 1 \quad . \tag{4}$$

Note that as point A moves to a new frequency, $s = j\omega_2$, the value of $|T(j\omega)|$ remains unity.

The net phase shift, θ_T, through the network of the signal at frequency ω_1 is given by

$$\theta_T = \theta(z_1) - \theta(p_1) = \pi - \alpha - \alpha = \pi - 2\alpha = \pi - 2 \tan^{-1} \frac{\omega_1}{\sigma_1} \quad . \quad (5)$$

It can be seen from equation (5) that as the frequency of point A moves from ω_1 to another frequency ω_2 a change in phase through the network occurs.

The objective of a phase shifter, however, is to vary the net phase between two points in a transmission path at a fixed frequency (point A not moving as above) with minimum perturbation to the amplitude. If instead of the fixed p-z pair of figure 5, suppose a pair of complex poles and zeros move on a line parallel to the $j\omega$ axis as shown in figure 6. The transfer function of this p-z function is

$$T(s) = \frac{(s - z_1)(s - z_1^*)}{(s - p_1)(s - p_1^*)} = \frac{(s - \sigma_1 - j\omega_2)(s - \sigma_1 + j\omega_2)}{(s + \sigma_1 - j\omega_2)(s + \sigma_1 + j\omega_2)} \quad . \quad (6)$$

The amplitude of $T(s)$ evaluated at $s = j\omega_1$ can be shown to be

$$|T(j\omega)| = \frac{\left(\sqrt{\sigma_1^2 + (\omega_1 + \omega_2)^2}\right)\left(\sqrt{\sigma_1^2 + (\omega_2 - \omega_1)^2}\right)}{\left(\sqrt{\sigma_1^2 + (\omega_1 + \omega_2)^2}\right)\left(\sqrt{\sigma_1^2 + (\omega_2 - \omega_1)^2}\right)} = 1 \quad . \quad (7)$$

Equation (7) shows that as the complex poles and zeros move up and down parallel to the $j\omega$ axis, the amplitude is invariant.

The net phase shift at point A is

$$\theta_T = \theta(z_1) + \theta(z_1^*) - \theta(p_1) - \theta(p_1^*) \quad . \quad (8)$$

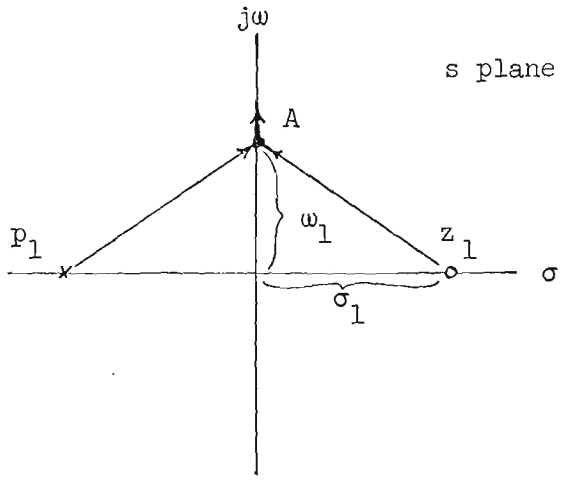

Figure 5. Pole-Zero Plot of Simple All-Pass Network Function.

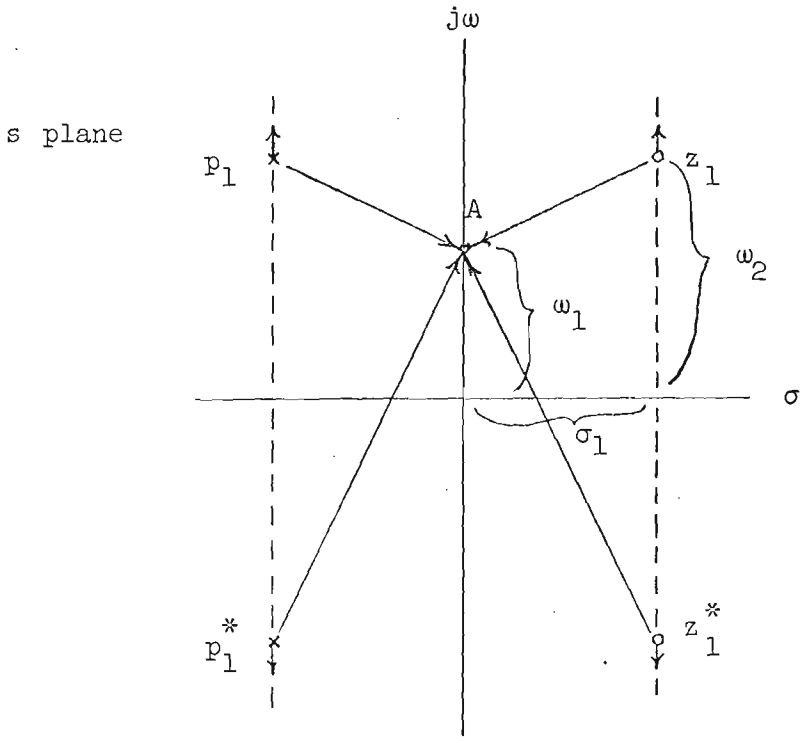

Figure 6. Pole-Zero Plot of An Ideal Phase Shifter.

From Equation (6) an expression for the total phase shift can be obtained which is

$$\theta_T = \tan^{-1}\left(-\frac{\omega_1 - \omega_2}{\sigma_1}\right) + \tan^{-1}\left(-\frac{\omega_1 + \omega_2}{\sigma_1}\right) - \tan^{-1}\left(\frac{\omega_1 - \omega_2}{\sigma_1}\right) - \tan^{-1}\left(\frac{\omega_1 + \omega_2}{\sigma_1}\right) \quad . \tag{9}$$

Equations (7) and (9) verify that the p-z configuration of figure 6 represents the network function of an ideal phase shifter since the phase angle but not the amplitude of the transfer function is a function of frequency.

Another way of expressing equation (6) is

$$T(s) = \frac{s^2 - \frac{\omega_o}{Q}s + \omega_o^2}{s^2 + \frac{\omega_o}{Q}s + \omega_o^2} \quad . \tag{10}$$

Being an improper fraction, T(s) may be written as one plus a proper fraction:

$$T(s) = 1 + \frac{P(s)}{N(s)} \quad , \tag{11}$$

or

$$T(s) - 1 = \frac{P(s)}{N(s)} \quad . \tag{12}$$

Performing operation (12):

$$\frac{P(s)}{N(s)} = \frac{s^2 - \frac{\omega_o}{Q}s + \omega_o^2}{s^2 + \frac{\omega_o}{Q}s + \omega_o^2} - 1 = \frac{-2\frac{\omega_o}{Q}s}{s^2 + \frac{\omega_o}{Q}s + \omega_o^2} \quad . \tag{13}$$

The form of the expression (13) for $P(s)/N(s)$ is immediately recognized as the second order response such as that obtained with a conventional LC circuit. Consequently, this analysis indicates that a practical phase shifter should be obtainable with the proper combination of relatively simple networks. Figure 7 is a simplified diagram of such a combination.

Figure 8 is a detailed block diagram of a voltage controlled phase shifter which was constructed for the frequency range of 300 to 350 MHz. The input signal is divided into two paths of equal amplitude with the power divider. Channel one consists of a wideband amplifier with appropriate resistive padding to provide constant gain over the desired frequency range. Channel two contains a voltage controlled, single tuned amplifier with appropriate buffers to stabilize the input and output impedance of the channel as the tuning is varied. From equation (13) the net gain at resonance through the tuned amplifier channel must be twice that of the other channel and the net phase difference between the two must be 180 degrees. Consequently, the net gain of channel two is adjusted to be twice the gain of channel one. To insure that 180 degrees of phase difference is maintained at the summing junction over the desired frequency range, a short piece of transmission line is incorporated in channel one to equalize the time delay through both channels.

The success at obtaining a gain ratio of 2:1 with a phase difference of 180 degrees between both channels is illustrated in figure 9. The operational characteristics of the complete phase shifter are shown in figure 10 and 11. Figure 10 shows the phase shift as a function of control voltage at selected frequencies from 275 MHz to 350 MHz. Note that greater than 180 degrees of phase adjustment is possible over the entire frequency range. Figure 11 shows the variations in total gain through the device as a function of control voltage, i.e. phase shift, at 300, 325, and 350 MHz.

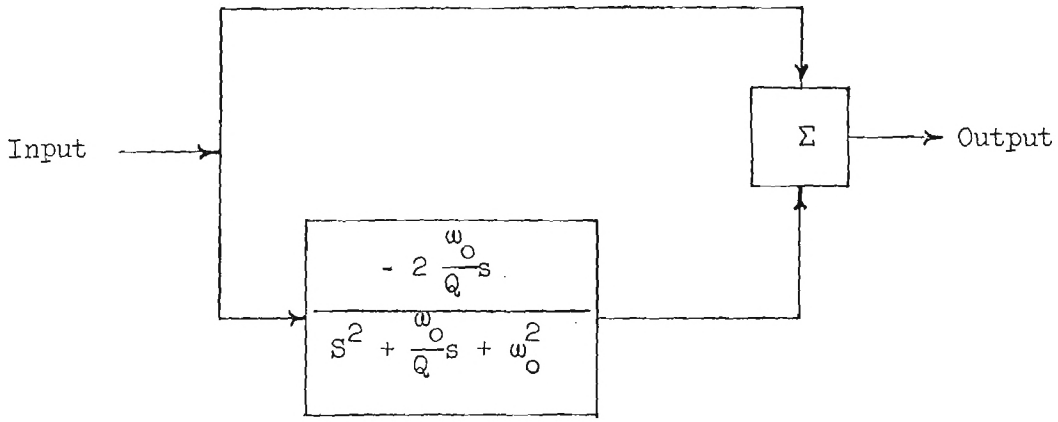

Figure 7. Block Diagram Showing the Necessary Combination of Simple Networks to Realize an Ideal Phase Shifter.

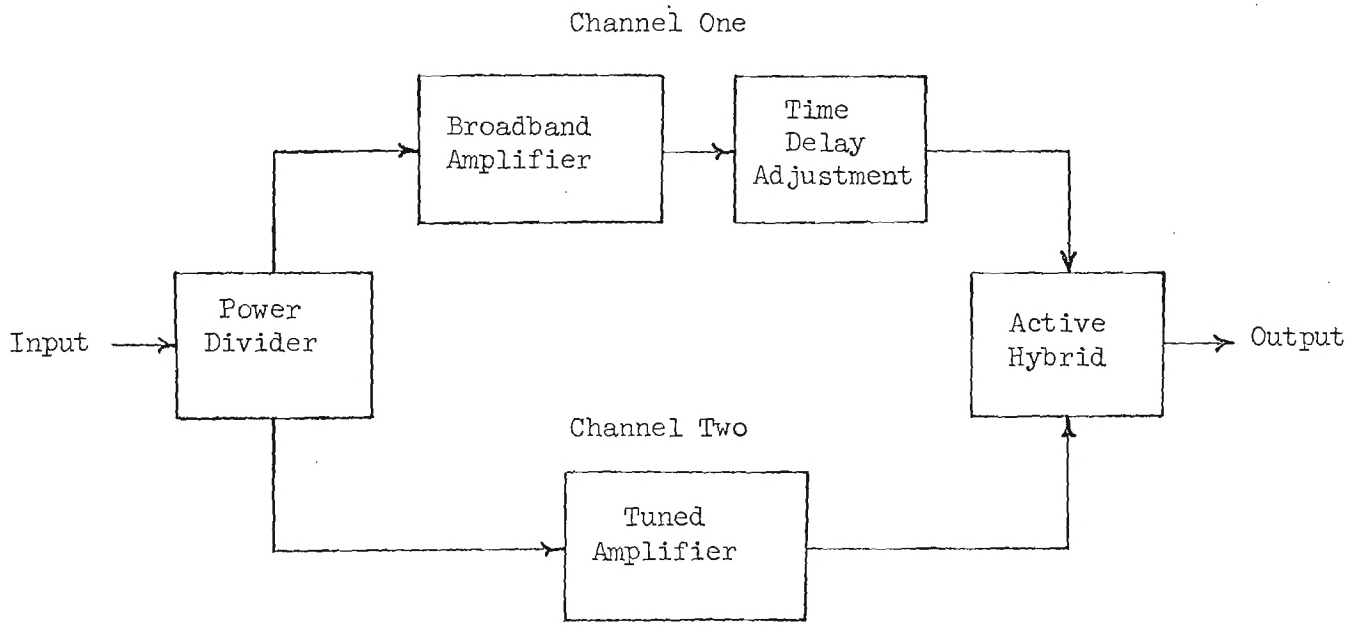

Figure 8. Block Diagram of Voltage Controlled Phase Shifter.

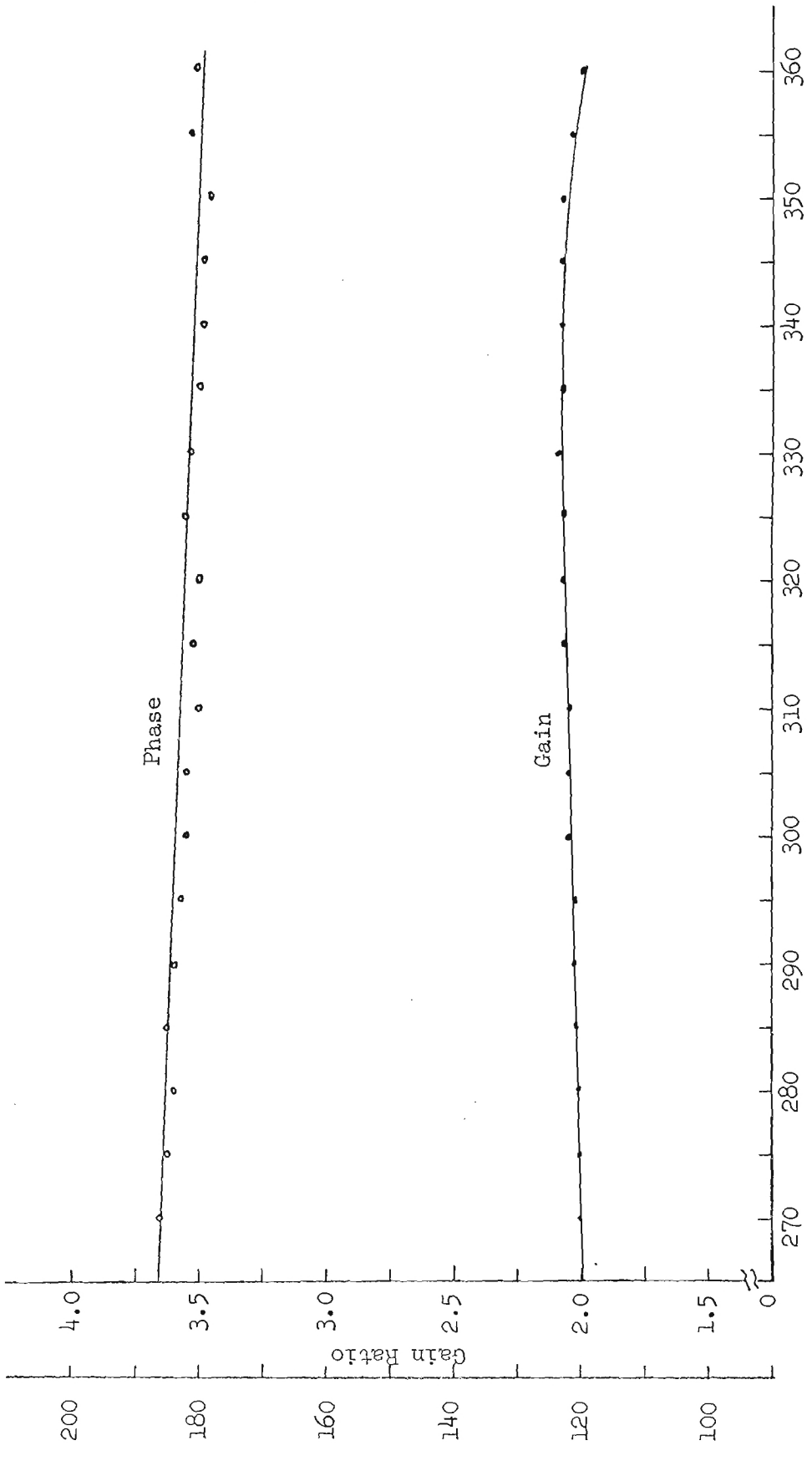

Figure 9. Gain Ratio and Phase Difference Between the Channels of the Phase Shifter.

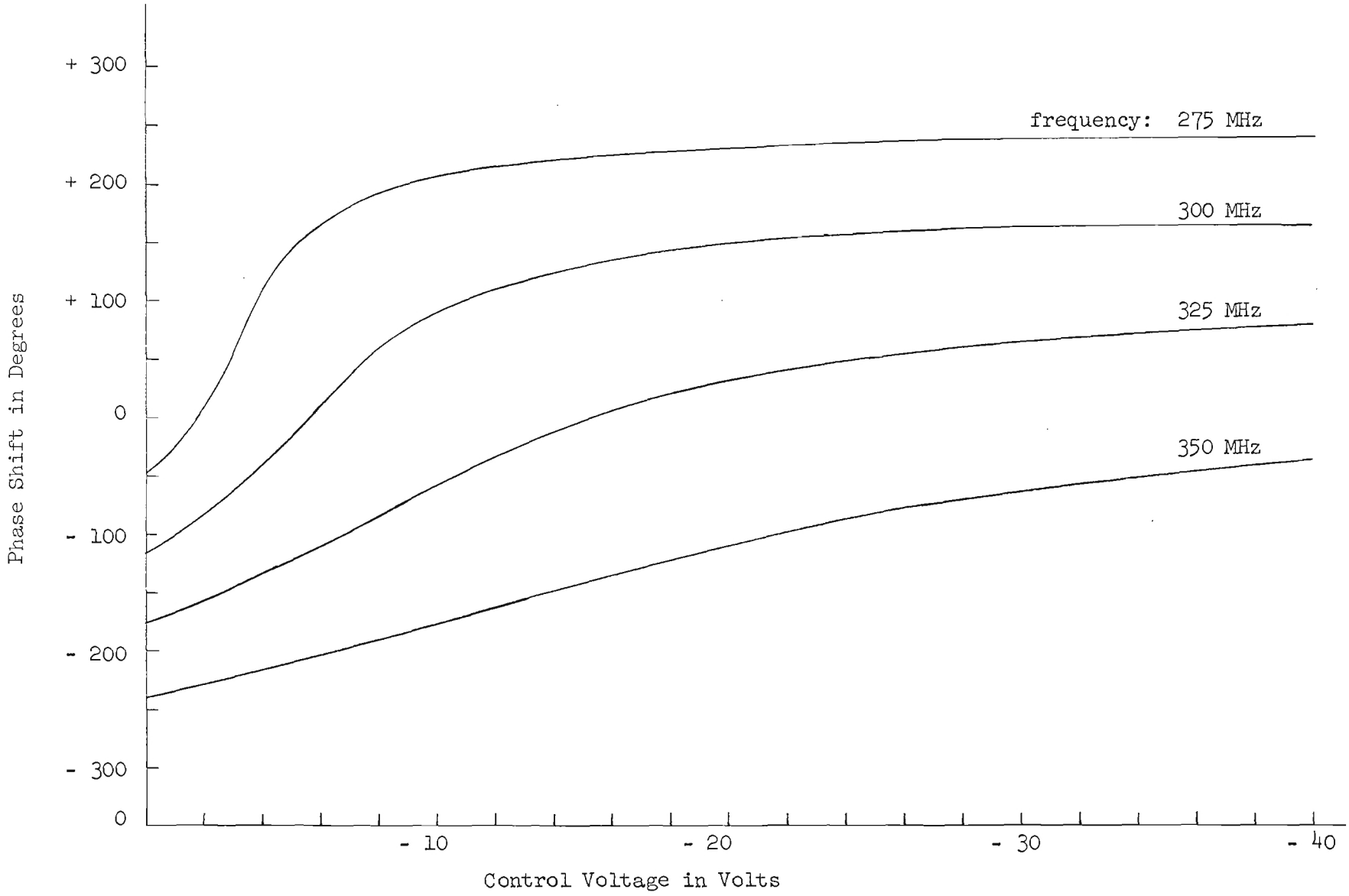

Figure 10. Phase Shift versus control voltage from 275 to 350 MHz.

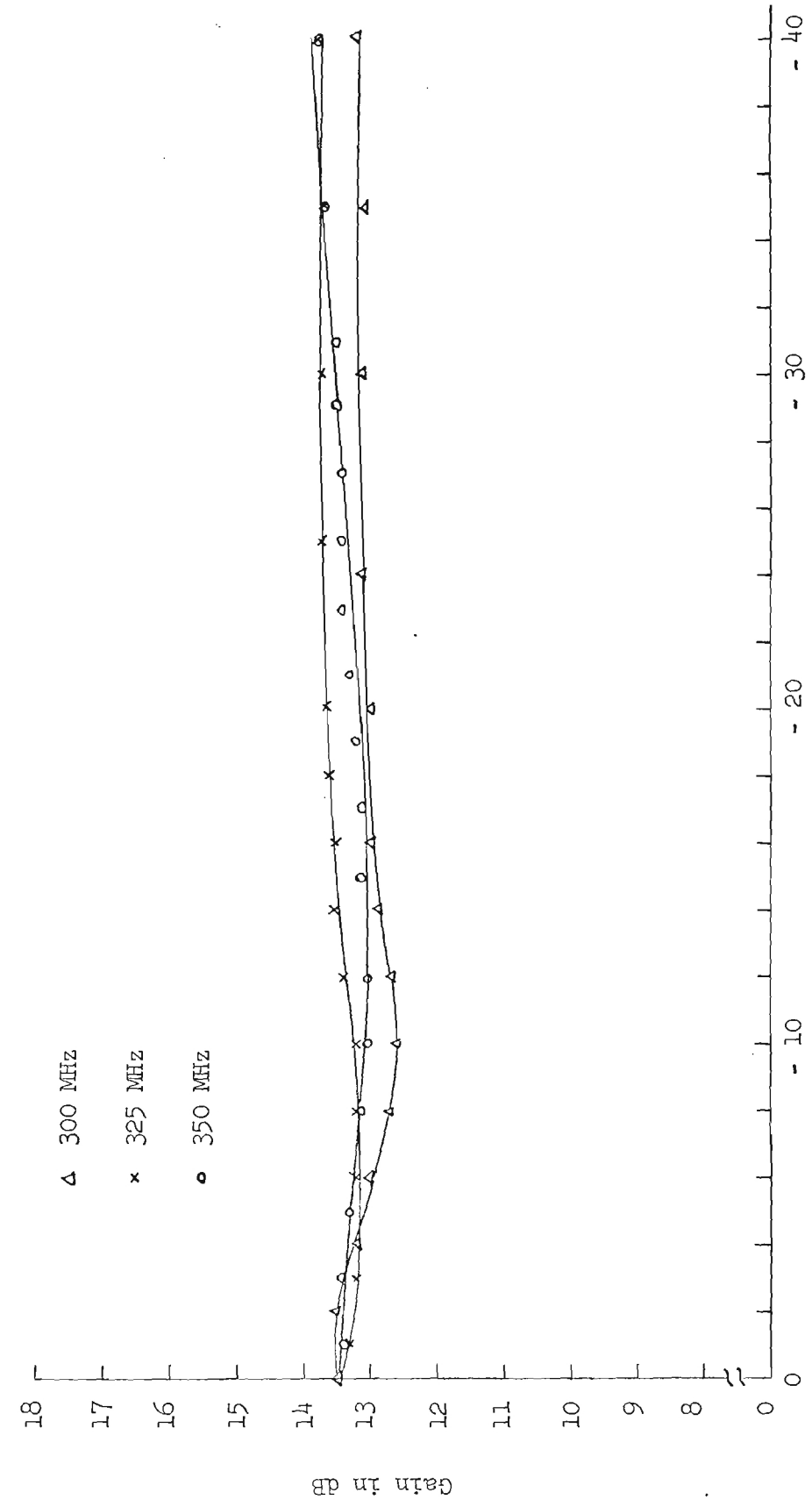

Figure 11. Gain versus Control Voltage Characteristics.

An improved version of a previously constructed coaxial cavity which is to provide the basic resonant circuit for the Q multiplication network is presently under construction for incorporation into the working model. Mechanical assembly of the UHF active filter will be completed and performance data will be obtained during the next quarter.

Work Schedule and Progress:

The progress of the work of this project is satisfactory and essentially in conformance to the projected work schedule.

Program for the Next Quarter:

The program for the next quarter will be essentially in conformance with that already outlined in the preceding paragraphs.

Personnel Changes:

During the past quarter, no significant personnel changes have taken place.

Engineering Man-hours:

The following number of engineering man-hours was devoted to this project effort during the past quarter:

Category	No. of Hours
Senior Research Engineer	173
Research Engineer	475
Assistant Research Engineer/ Graduate Research Assistants	1193

Respectfully submitted:

Hugh W. Denny
Project Director

Approved:

D. W. Robertson, Head
Communications Branch

A-987

RADC-TR-68-8
Final Report

INTERFERENCE REDUCTION TECHNIQUES EMPLOYING ACTIVE DEVICES

Hugh W. Denny
Robert A. Byers
Carl R. Driskell
Charles S. Wilson
Georgia Institute of Technology

TECHNICAL REPORT NO. RADC-TR-68-8
February 1968

Rome Air Development Center
Air Force Systems Command
Griffiss Air Force Base, New York

INTERFERENCE REDUCTION TECHNIQUES EMPLOYING ACTIVE DEVICES

Hugh W. Denny
Robert A. Byers
Carl R. Driskell
Charles S. Wilson

Georgia Institute of Technology

AFLC, GAFB, N.Y., 28 Mar 68-159

FOREWORD

This final report was prepared by Hugh W. Denny, Robert A. Byers, Carl R. Driskell and Charles S. Wilson of Georgia Institute of Technology, Atlanta, Georgia, under Contract F30602-67-C-0066, project number 4540, task number 454003. Reporting period covered 1 December 1966 to 30 November 1967. RADC project engineer is George A. Long (EMCVI-2).

This report has been reviewed and is approved.

Approved:

GEORGE A. LONG
Interf Analysis & Control Sec
Vulnerability Reduction Br

Approved:

RICHARD M. COSEL
Colonel, USAF
Chief, Communications Division

FOR THE COMMANDER:

for IRVING J. GABELMAN
Chief, Advanced Studies Group

ABSTRACT

This report discusses the development and performance of several techniques employing active devices for the reduction of adjacent and co-channel interference in receivers. For operational situations where the interfering source is co-sited with the receiver, an automatic phase control system is described which detects the differential phase shift between the interference path and the direct path from the source and supplies a phase corrected signal for cancellation of the interfering signal. For the more general situation where the interference is not a cosite source, a feed forward system and a dual loop, phase locked system were developed. For 60 kHz spaced signals at 300 MHz, the feed forward system typically provides 55 dB suppression to CW interference and 40 dB suppression to AM interference. The dual loop cancellation system, which generates an auxiliary signal to cancel the interfering signal, is shown to be capable of suppressing an interfering signal by 50 dB when the interference signal is greater than an audio bandwidth from the desired signal. The improved performance of passive preselectors that can be obtained through Q multiplication is demonstrated with a Q multiplier device for the UHF region. Effective Q's of approximately 7,000 with relatively small coaxial cavities are realized with this device. Active and passive circuit configurations which incorporate the extremely narrow passbands of quartz crystals are discussed. When used as band stop filters, interference rejection levels greater than 50 dB are possible with these filters.

TABLE OF CONTENTS

LIST OF FIGURES

LIST OF FIGURES - Continued

LIST OF FIGURES - Continued

EVALUATION

The objective of this effort was to develop specialized amplifiers using such techniques as Q multiplication and negative feedback which produce extremely narrow bandpass and band reject filters. These filters are to be used in solving specific interference problems especially those in the UHF region from 225 MHz to 400 MHz and more specifically adjacent channel interference due to too close spacing of transceiver frequencies.

The feasibility of Q multiplication at UHF has been demonstrated in this contract. However the model developed requires considerable improvement in power handling capability and noise figure before becoming a practical device.

The rejection capabilities of crystal notch filters have been thoroughly explored and, unless better crystals are produced, further reduction of their insertion loss is highly improbable.

To summarize, some very useful techniques in Q multiplication, phase shifting, and interference cancellation have resulted which can be utilized in specific interference situations.

GEORGE A. LONG
Interf Anal & Control Sec
Vulnerability Reduction Branch

SECTION I

INTRODUCTION

The rapidly expanding demand for more communication channels in a fixed amount of available spectrum space has resulted in the assignment of communications channels with very little frequency separation. At the same time, the advancing state-of-the-art in receiver design has continued to lower the minimum signal level that can be detected. This combination of close channel spacing and increased sensitivity has created serious adjacent channel interference problems.

An insight into the nature of the adjacent channel interference problem can be gained by the consideration of a typical operational situation. In the UHF region of 200 to 400 MHz, transmitters capable of producing output powers of 200 watts (+ 53 dBm) or more are quite common and typical receivers in this frequency range have sensitivities of -100 dBm. An operational situation might be that as illustrated in figure 1, where a receiver is tuned to a relatively weak (-90 dBm) signal at 201 MHz while the strong undesired signal is at 200 MHz. Operational conditions often require that transmitters and receivers share the same antenna. In that case, if a 10 dB signal-to-noise ratio is required in the receiver's rf stage to prevent excessive information loss, then the interfering signal must be attenuated 153 dB to -100 dBm. The typical receiver preselector can be expected to provide approximately 50 dB of attenuation to the undesired signal and an additional 20 dB of attenuation is typically supplied by antenna multicouplers. The remaining 83 dB of attenuation necessary to reduce the + 33 dBm signal out of the multicoupler to the -50 dBm permitted at the receiver's antenna terminals requires a filter technique exhibiting an effective attenuation slope of 16,600 dB per octave for an equivalent low-pass or high-pass configuration.

In the past, selective filters, employing only passive elements, have been effective in reducing or eliminating the undesirable effects of large adjacent channel signals. However, in some situations, such as that discussed above, passive selective devices are often unable to provide the required rejection to the interfering signal. In these situations, other techniques must be sought.

This report discusses the findings of a study program which emphasized the application of active devices and techniques to the reduction of adjacent channel interference. The general areas of investigation were:

1) cancellation of the undesired signal;
2) multiplication of the Q of passive devices; and
3) the application of quartz resonators as interference suppression filters.

The suppression of a strong CW signal by subtracting a phase locked auxiliary signal was demonstrated under a previous contract.[1] Efforts to

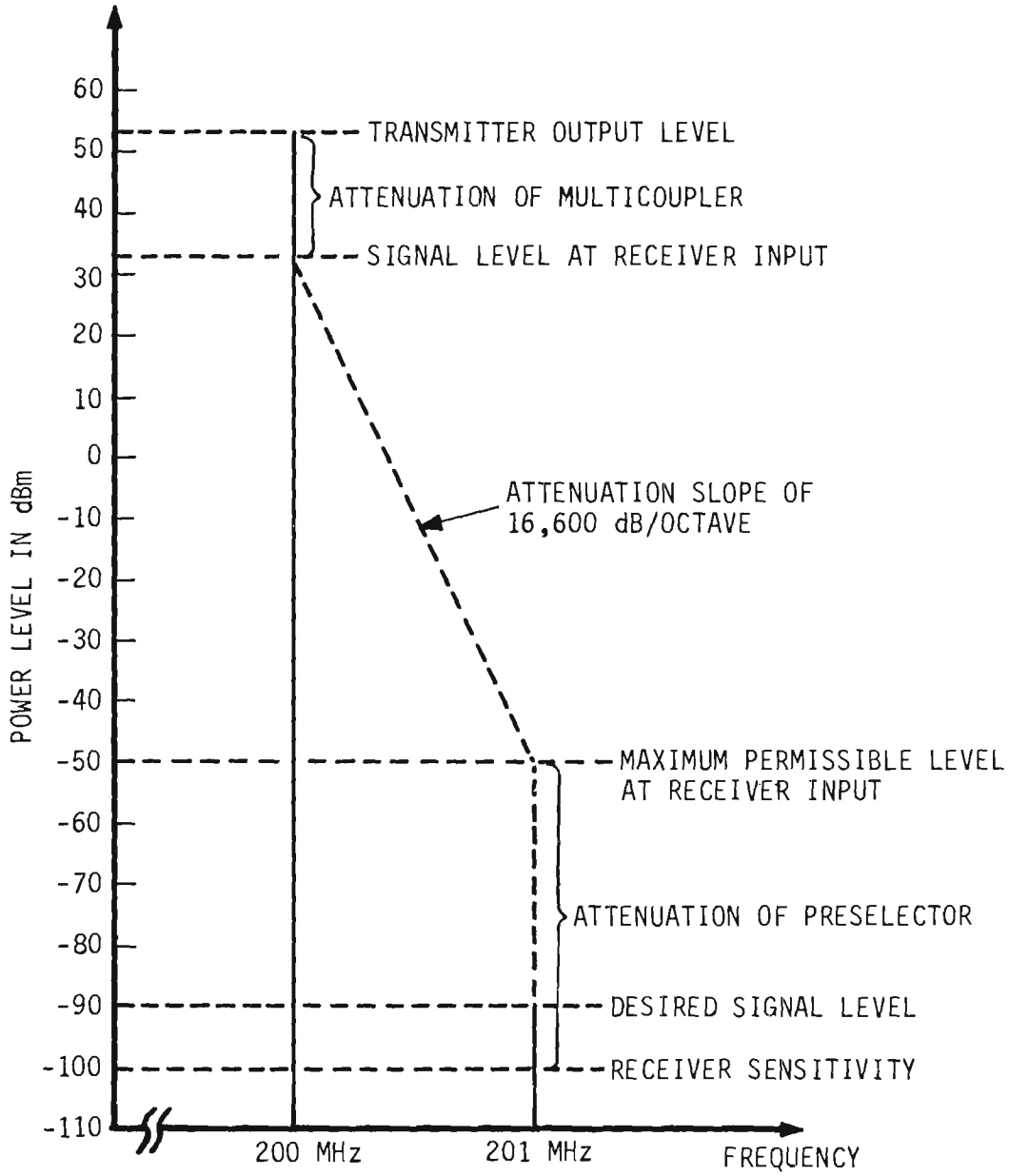

Figure 1. Illustration of Typical Adjacent Channel Interference Situation.

adapt this device to the suppression of AM signals were successful. The performances of an automatic phase control system and a feed forward system add considerable impetus to the active cancellation approach for the suppression of AM signals in the 225 to 400 MHz region.

At low frequencies, particularly in the audio range, the application of active devices to counter the inherent circuit losses associated with passive devices has permitted a high degree of selectivity to be obtained in resonant structures. This principle of Q multiplication was successfully extended to the UHF region where extremely high Q responses with moderately sized passive devices were obtained.

Because of their very narrow passbands, quartz crystal resonators present an attractive approach to the problem of differentiating between two very closely spaced signals. Several active and passive circuit configurations incorporating crystal resonators were evaluated for interference suppression capabilities.

The description and evaluation of these techniques for the suppression of adjacent channel interference is contained in this report.

SECTION II

INTERFERENCE CANCELLATION

The adjacent channel interference problem may be conveniently represented by the vector diagram of figure 2. A low level desired signal, represented by the short vector, S_1 is effectively masked by the high level undesired signal which is represented by the longer vector, S_2. Although the two signals are close in frequency, they are not at the same frequency. Consequently, the angular velocities of rotation of the two vectors are not equal. Cancellation of the undesired signal may be obtained by combining an auxiliary signal, represented by the dotted vector, S_3, with the original two signals. The auxiliary signal must identically match the undesired signal in amplitude and frequency and the phase angle between the two must be maintained at π radians.

Three possible cancellation techniques were investigated. The characteristics of the operational situation will determine which of these approaches is most appropriate for a specific interference problem.

A. Automatic Phase Control System

If the interfering transmitter or antenna is physically located nearby, a sample of the interference signal may be obtained and directed to the receiver in the manner shown in figure 3. Referring to the vector diagram of figure 2, the solid vector, S_2, represents the interference signal that reaches the receiver through the antenna lead, and the dotted vector, S_3, represents the signal on the auxiliary path.

Appropriate phase and amplitude corrections must be performed on the signal sample for cancellation of the undesired signal before entering the receiver front end. The angular frequencies, ω_2 and ω_3, of S_2 and S_3 are identical but the phase shift through the two paths will not necessarily be the same. For cancellation, a net difference of 180 degrees must exist in the phase shift through the two paths. A simple type of phase shifter such as an appropriate length of transmission line may be used to adjust the path length so that $\theta = \pi$ radians. However, drift in the transmitter frequency or environmental effects such as temperature and humidity which detune the multicouplers slightly can result in a significant change in the phase of this signal at the receiver terminals. To maintain the proper phase relationship, a voltage controlled phase shifter with automatic tracking offers an attractive solution. The block diagram of a system to perform this function is shown in figure 4. A portion of the interfering transmitter signal sample is fed to a mixer and heterodyned with a local oscillator to produce a 30 MHz IF signal. A portion of the signal-plus-interference is coupled to a second mixer where it is heterodyned with the local oscillator to produce another

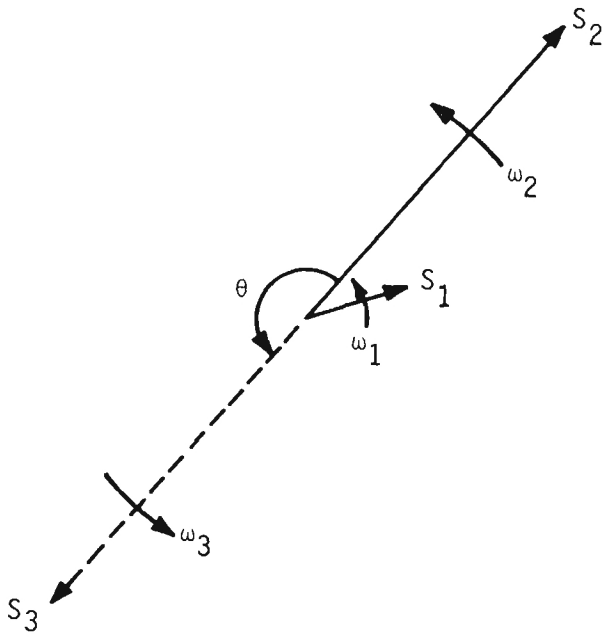

Figure 2. Vector Diagram Illustrating the Principles of the RF Cancellation Technique.

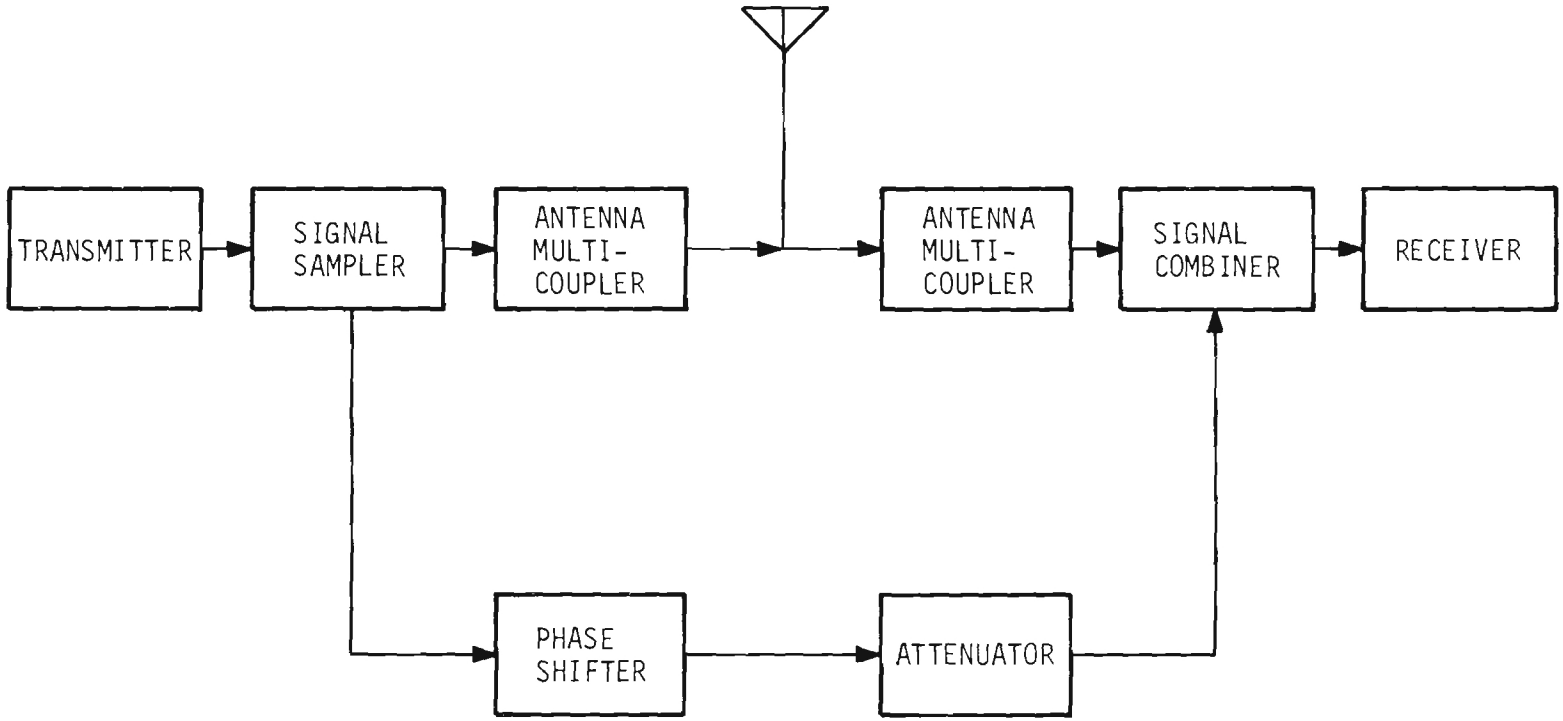

Figure 3. Block Diagram of RF Cancellation Technique for Co-sited Transmitter-Receiver Pairs.

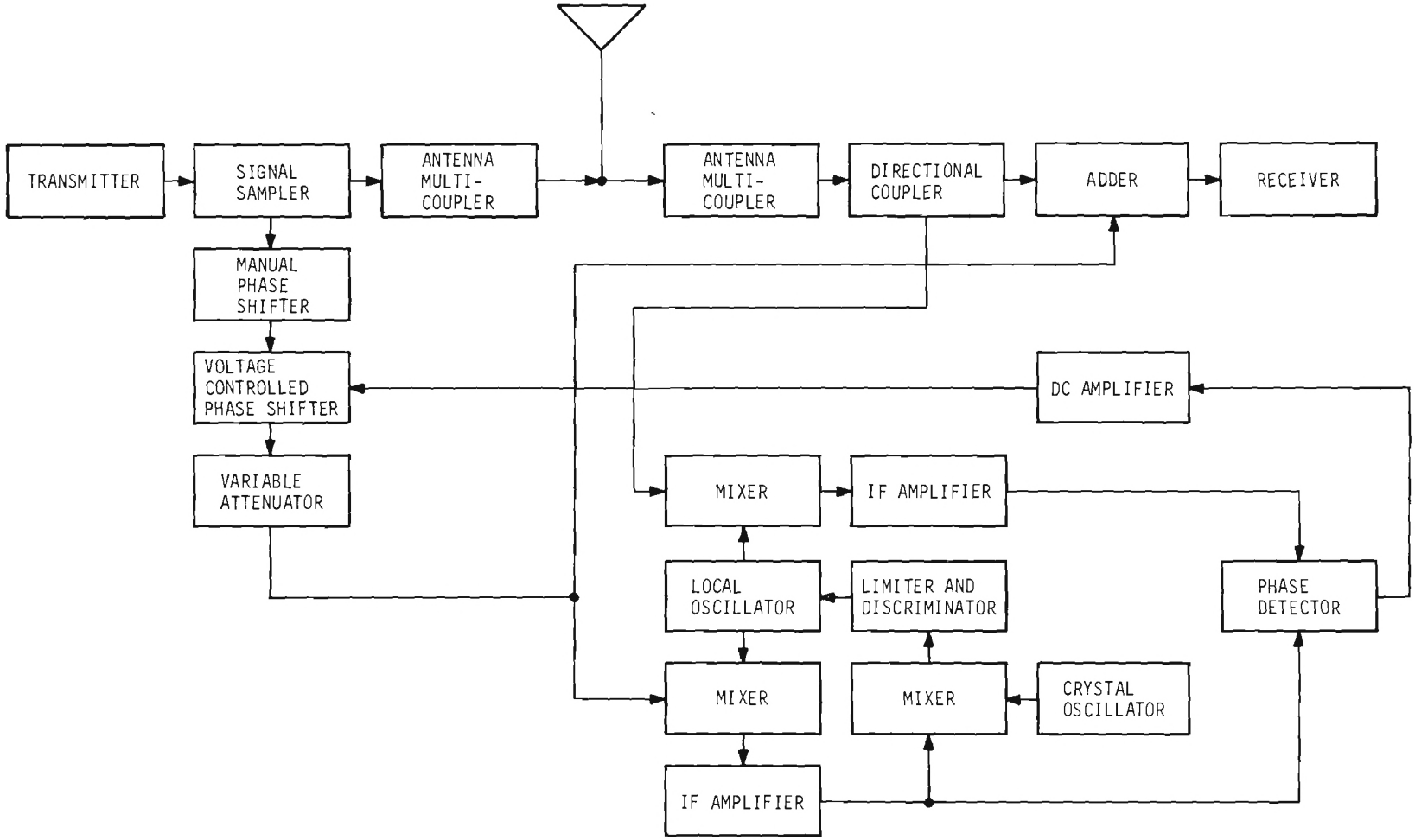

Figure 4. Block Diagram of Automatic Phase Control System.

30 MHz IF signal. The two 30 MHz signals are amplified, compared in a phase detector and the resulting phase error voltage is used to adjust the phase shifter. A manual shifter acts as a coarse phase control and is adjusted to obtain the phase required for initial cancellation of the interfering signal. The voltage controlled phase shifter corrects for incremental changes to maintain the required phase shift.

Initially, a 200 to 400 MHz transistorized local oscillator was employed in a configuration which directed portions of the local oscillator signal through a broad band hybrid to the two 30 MHz IF subchassis for mixing. Unfortunately, this system exhibited poor local oscillator frequency stability. Poor stability of the local oscillator can cause an erroreous phase error voltage to be generated since any drift in the frequency of the local oscillator with respect to the RF input signal can produce a differential phase shift through the two IF amplifiers. The low output impedance of the local oscillator transistors excessively loaded the tuned circuit. The low impedance could not be properly matched over the octave bandwidth because of the wide variation in transistor parameters. Consequently, a Nuvistor vacuum tube version of the local oscillator was incorporated into the system and the free running frequency stability of the output signal was improved to approximately 5 parts in 10^6 when averaged over a one minute time interval. The instabilities were reduced further by constructing the two balanced mixers on the local oscillator subchassis. By separating the mixers from the IF amplifiers, total 30 MHz gain is divided between two subchassis. An automatic frequency control (AFC) loop added further improvements to the local oscillator stability. A portion of the 30 MHz IF signal is heterodyned with a crystal controlled 24 MHz signal in the manner shown in figure 4. The resulting 6 MHz IF signal is fed to a limiter and a discriminator which provide an error signal to control the frequency of the local oscillator. With AFC applied, the AFC loop gain was sufficient to increase the stability to 5 parts in 10^8 when locked to an input signal derived from a frequency standard. AFC between the local oscillator and the reference input signal was obtained at signal levels as low as 5μV.

The two 30 MHz IF amplifiers were constructed with transistors having forward AGC characteristics which permitted IF gain control through the use of a remote potentiometer. The net gain of the interference channel amplifier was variable from 15 dB to 38 dB, and the adjustable range of the signal-plus-interference channel amplifier gain was from 33 dB to 57 dB. Both channels exhibited similiar bandwidths of 1.5 MHz.

Filtering of the phase detector output voltage was accomplished with a low-pass filter with a variable cutoff frequency. Selection of cutoff frequencies of 2.5, 10, 100 or 1000 Hz was provided through a front panel switch. The phase detector was followed by a operational amplifier with a maximum gain of 60 dB which allowed an increase of the maximum phase detector error voltage to $\pm$ 10 Volts for an RF input signal of -85 dBm at the signal-plus-interference port.

The completed automatic phase control device for the RF cancellation system is shown in the photograph of figure 5.

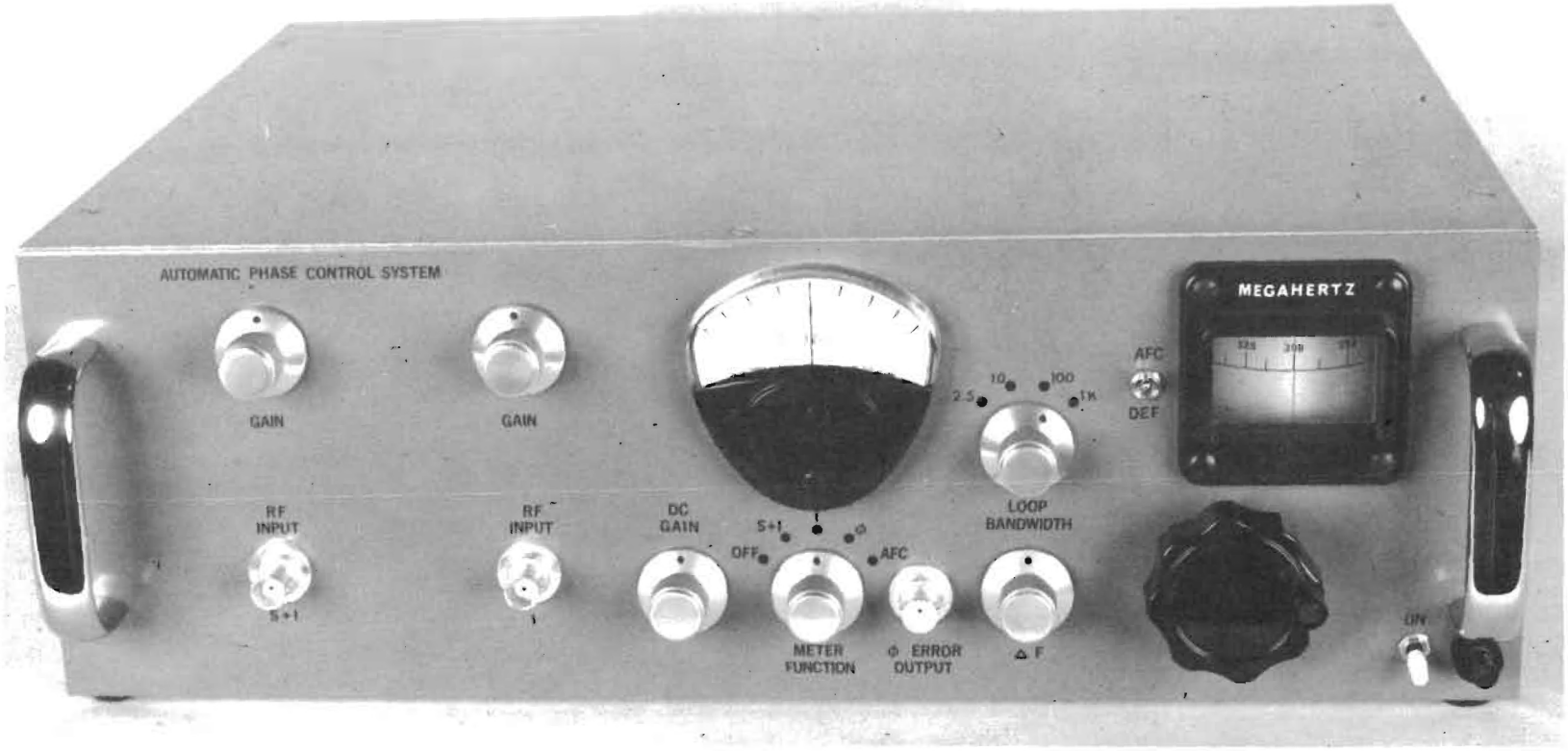

Figure 5. Photograph of Automatic Phase Control Device.

B. Feed Forward System

In many operational situations, the interfering transmitter and susceptible receiver are not located at the same site. In these situations, the acquisition of a sample of the interfering signal at its source is either impossible or impractical. For such cases, a sample of the interfering signal must be obtained at the antenna, appropriately modified in an auxiliary feed forward path, and subsequently recombined with the original signal for cancellation prior to the receiver. A simplified block diagram of this type of system is shown in figure 6.

In the feed forward system, the difference in the phase shift around the sampling loop and the phase shift in the straight through path must be 180 degrees at the frequency of the interference signal but should be as small as possible (0 degrees, ideally) at the tuned frequency of the receiver. Since the two frequencies are close together, an abrupt phase change in the auxiliary path must occur over a narrow frequency range. The rate of phase shift directly determines the minimum frequency separation between the desired and interfering signals at which cancellation of the interference is possible. A cavity resonator is appropriate for approximating the desired phase response because it exhibits a rate of change of phase with frequency that is directly proportional to Q. Since high Q cavity resonators are readily available, they represent the most practical means for obtaining the required rapid phase shift.

The sampling loop can not be tightly coupled into the main line without attenuating the desired signal unnecessarily. Consequently, amplification is necessary within the sampling loop to permit the adjustment of the amplitude of the cancellation signal to match the amplitude of the interference signal at the point of cancellation. The gain of the amplifier in the system is sufficient to overcome the attenuation through the two couplers plus any losses exhibited by the phase shifter.

With a broadband transistor amplifier in the system, greater than 60 dB suppression of a CW signal was obtained by cancellation. However, only about 40 dB of suppression of an AM signal was possible. The capability of the feed forward system to suppress an AM signal is directly related to the linearity of the transfer characteristics of the amplifier. The amplifier nonlinearities prevent the components of the amplified interference sample from exactly matching the components of the original signal and thus complete cancellation can not be obtained in practice.

The output level at which saturation of the amplifier occurred was approximately 0 dBm. With a 10 dB coupler as the summation device, the system is restricted to the cancellation of interfering signals at levels of less than -10 dBm. In an attempt to provide a higher power handling capability, another broadband amplifier was constructed with a transistor of higher collector dissipation in the output stage. In spite of the increased output capacity of the amplifier, the undistorted output power was not significantly improved over the initial unit.

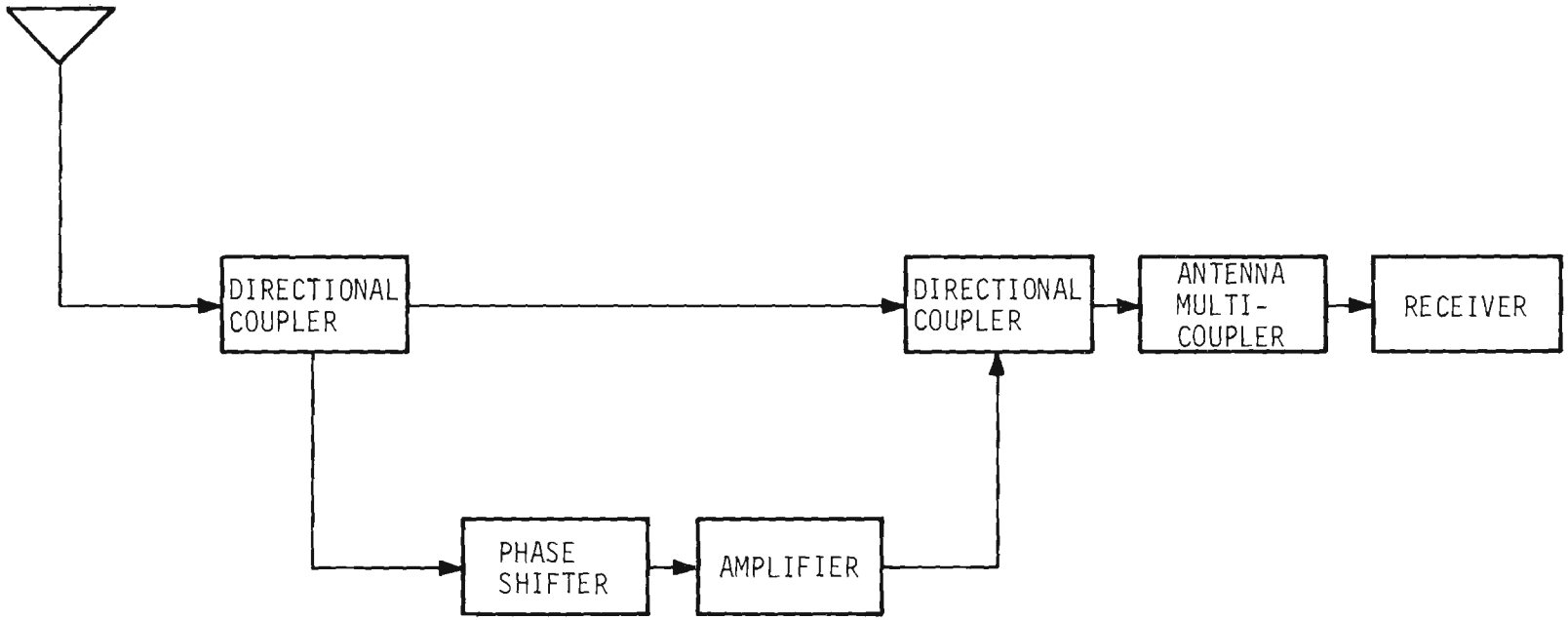

Figure 6. Simplified Block Diagram of the Feed Forward Cancellation Technique.

An increased output capability with improved linearity was obtained with a Nuvistor vacuum tube amplifier. This amplifier was constructed as a relatively narrow bandwidth tuned amplifier. A tuned amplifier is not a significant limitation to the use of the system since there are other elements in the system which are tunable.

Gain adjustments were performed with a current controlled attenuator. This type of attenuator is attractive in that it can be constructed in a small physical configuration and can be continuously varied over a wide range. A π network configuration of PIN diodes[2] produced the desired attenuation characteristic.

Prototype models of 10 dB directional couplers were constructed from published design data.[3] Directional couplers are used as signal samplers in preference to other techniques, such as resistive coupling, because the directivity of the couplers attenuates feedback components which tend to cause oscillations around the loop.

The suppression of a CW signal with the feed forward system is demonstrated in figure 7. Figure 7A shows the spectrum analyzer display of a 290 MHz signal through the system with the auxiliary path disconnected. Figure 7B shows that this signal can be suppressed greater than 60 dB with the system. The cancellation of AM signals is illustrated in figure 8. Figure 8B illustrates 55 dB of suppression of the AM signal shown in 8A.

Since this cancellation technique is primarily of interest as a possible solution to an adjacent channel interference problem, its ability to improve the reception of a weak signal in the presence of a strong undesired signal is important. Figure 9A depicts a situation where an undesired CW signal only 60 KHz away from a desired signal is 40 dB higher than the level of the desired signal. In figure 9B, the undesired signal is suppressed greater than 60 dB so that its level is approximately 15 dB less than the level of the desired signal. Although the desired signal is also attenuated by about 10 dB, relatively speaking, there is a 55 dB improvement in the ratio of the desired to undesired signal levels.

Figure 10 shows the relative suppression of an AM signal located only 60 KHz away from the desired signal. For these two signal tests, a cavity with a Q of 800 was used to permit the close spacing of 60 KHz without undue attenuation of the desired signal. The insertion loss of this cavity is about 6 dB. The cavity resonator used in the single signal tests had a lower Q of about 150 but its insertion loss was less than 1 dB. The greater insertion loss of the higher Q cavity created a higher gain requirement in the auxiliary loop than the Nuvistor amplifier was able to supply. A commercial power amplifier of higher gain was necessary for the two signal tests. The greater nonlinearities of this amplifier limited the degree of cancellation obtainable for an AM signal.

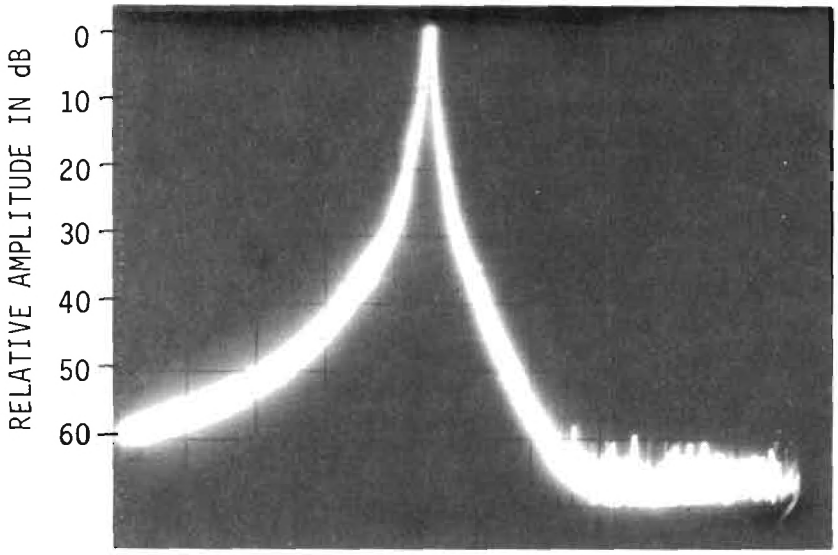

A. BEFORE CANCELLATION

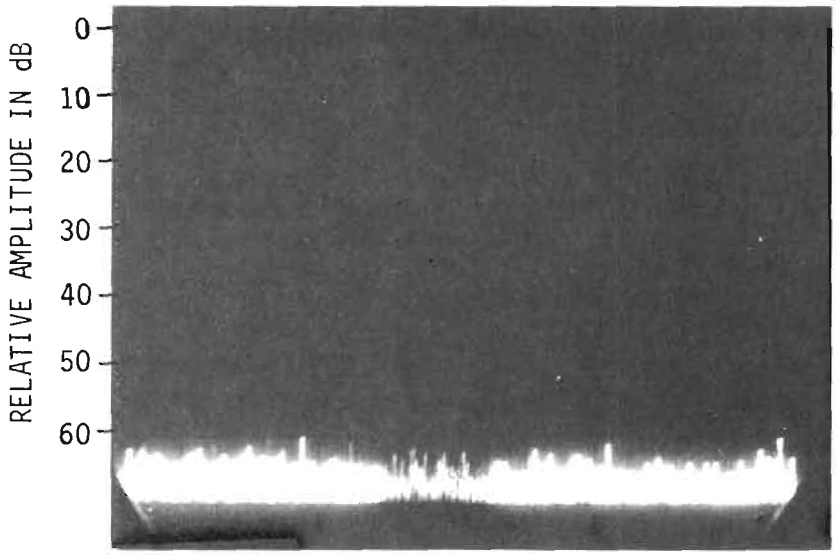

B. AFTER CANCELLATION

CENTER FREQUENCY: 290 MHz
SPECTRUM WIDTH: 30 KHz/cm

Figure 7. Cancellation of a CW Signal.

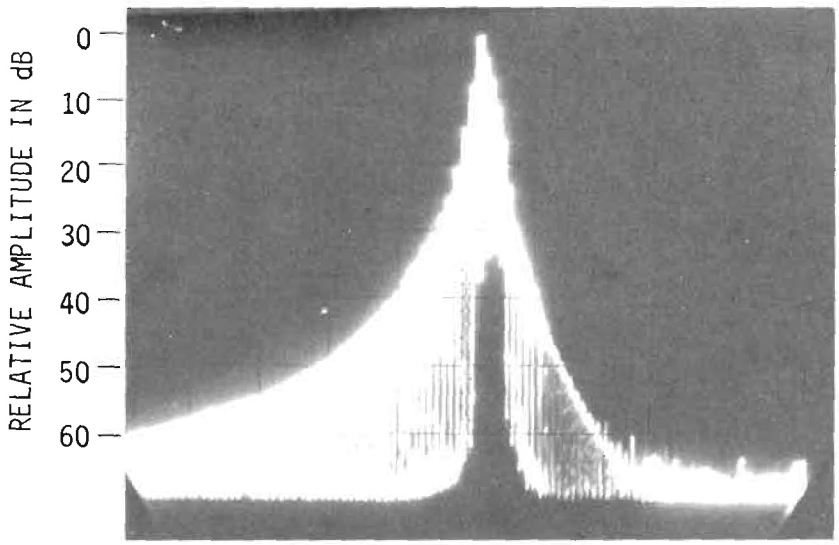

A. BEFORE CANCELLATION

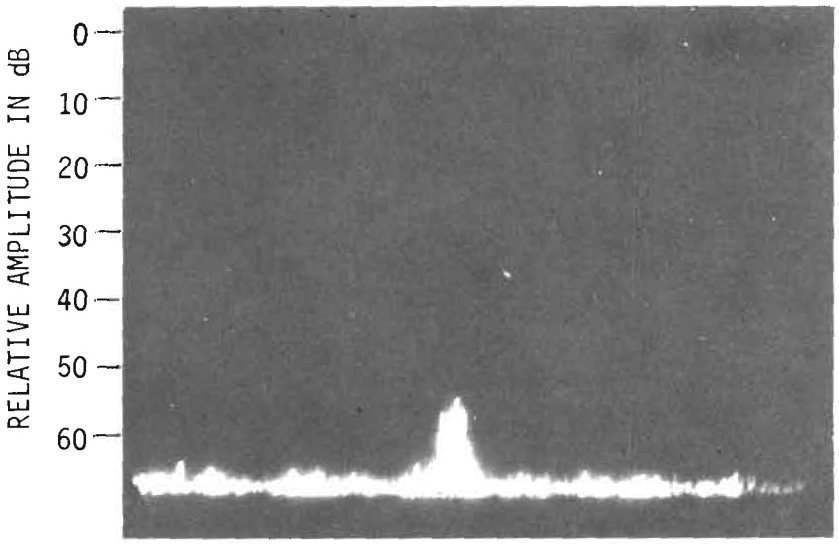

B. AFTER CANCELLATION

CENTER FREQUENCY: 290 MHz
SPECTRUM WIDTH: 30 KHz/cm

Figure 8. Cancellation of an AM Signal.

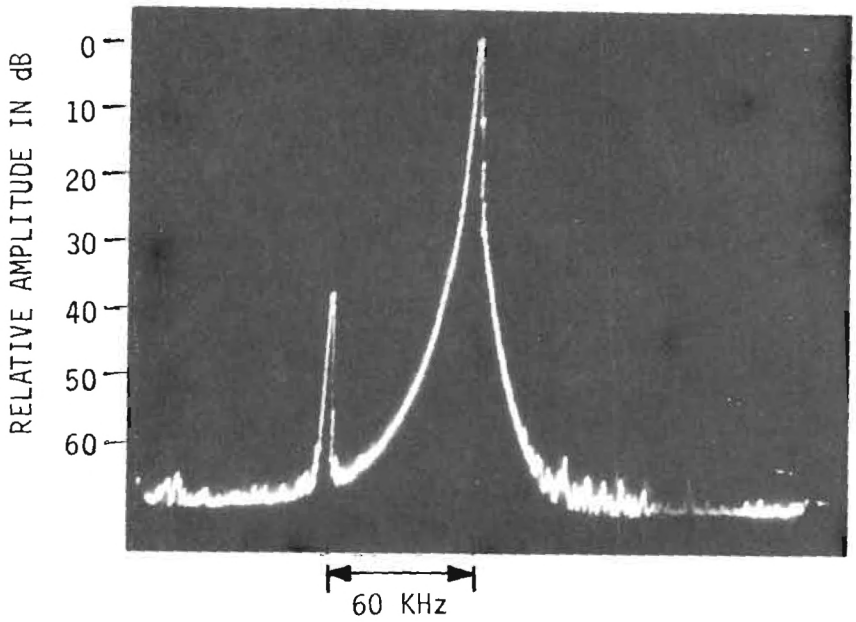

A. BEFORE CANCELLATION

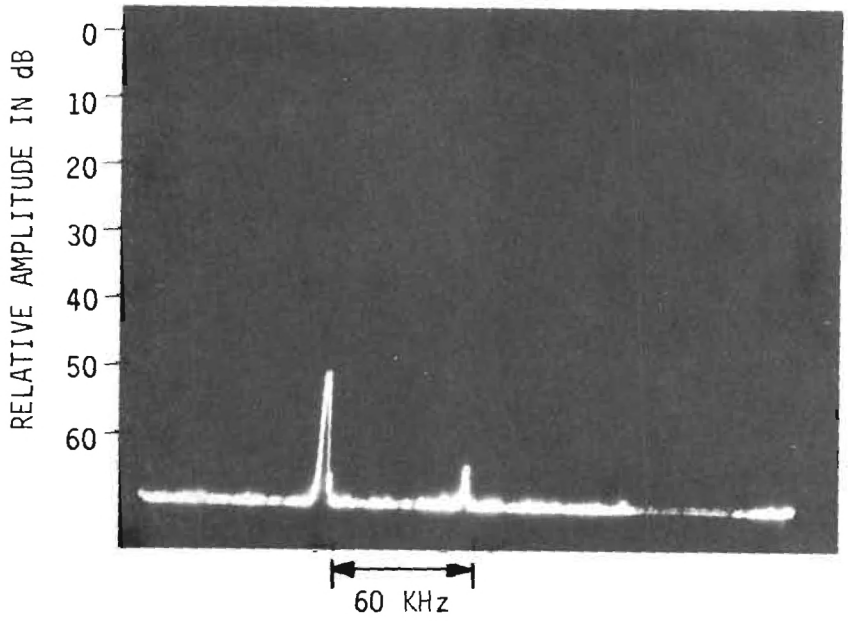

B. AFTER CANCELLATION

CENTER FREQUENCY: 290 MHz

Figure 9. Cancellation of a Closely Spaced CW Interfering Signal.

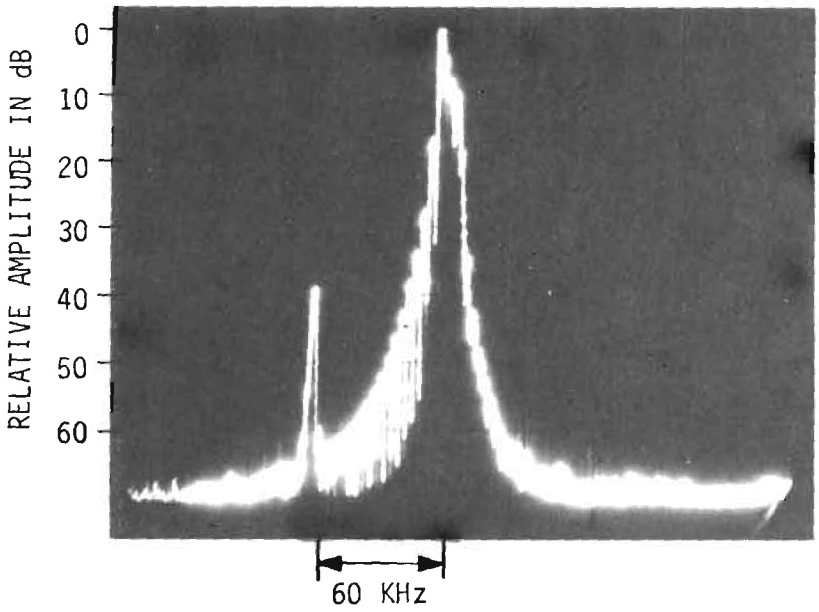

A. BEFORE CANCELLATION

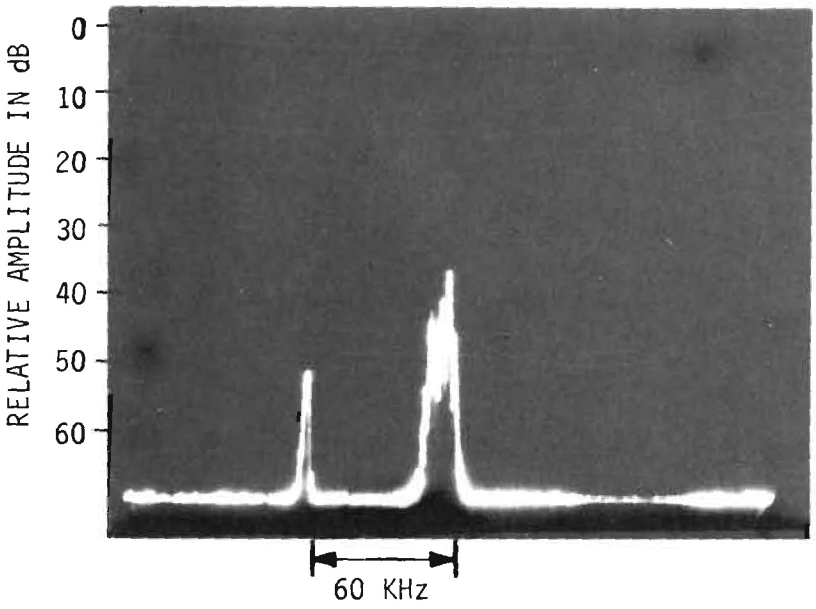

B. AFTER CANCELLATION

CENTER FREQUENCY: 290 MHz

Figure 10. Cancellation of a Closely Spaced AM Interfering Signal.

C. Dual Loop AM System

In both of the previous systems, no closed feedback loops for the adjustment of the amplitude of the cancellation signal are necessary because once initial adjustments are made and cancellation obtained any subsequent amplitude variations in the interfering signal source occur in the cancellation signal also. These systems are ultimately limited, however, either to some minimum frequency separation between the desired and undesired signals because of the finite phase slope obtainable with practical resonators or because an auxiliary signal can not be obtained from the source.

In the absence of a signal sample from the source, the cancellation technique shown in the block diagram of figure 11 permits closer spacing of the desired and undesired signals than is permitted by the feed forward system. The allowed frequency spacing between the desired and undesired signals is determined in this dual closed loop system only by the characteristics of the phase lock loop and the relative amplitudes of the two signals.

In the system of figure 11, a cancellation signal is generated by controlling the frequency, phase and amplitude characteristics of an auxiliary oscillator so that they match those of the interference signal. A sample of the interference signal is obtained from the output side of the summation junction to provide the reference for the dual closed loop system. The phase of the interference sample is compared in a phase lock loop with the phase of the cancellation signal. The error voltage which is proportional to the phase difference between the two signals is used to correct the phase of the cancellation oscillator. In addition to the phase lock loop, a closed amplitude correction loop detects the amplitude of the interference signal. The level of the detected audio signal controls a high level amplitude modulator which adjusts the output of the cancellation oscillator to match the level of the interference signal at the summation junction.

The AM cancellation filter consists of two 200-400 MHz double conversion receivers sharing a common local oscillator. From the directional coupler, the RF input signal is fed to a cascode Nuvistor preselector which supplies approximately 15 dB or RF gain and establishes the system noise figure. The amplified RF signal and the cancellation signal are heterodyned in balanced mixers with the first local oscillator to produce 31 MHz first IF signals. Two 31 MHz amplifiers provide a gain of 58 dB with a nominal bandwidth of 1 MHz.

The two 31 MHz signals are heterodyned with a 24 MHz, crystal controlled, second local oscillator to produce 7 MHz second IF signals. An additional gain of 50 dB is supplied by second IF amplifiers over a bandwidth of 100 KHz. A portion of one of the 7 MHz output signals is used to develop an AFC voltage for stabilizing the frequency of the first local oscillator. An AFC voltage for the cancellation oscillator is obtained from the other 7 MHz signal. This signal is applied to a discriminator to develop an error signal which aids in the acquisition of phase lock of the cancellation signal to the interfering signal. The outputs from the two 7 MHz IF amplifiers are phase compared and the resultant phase error voltage is added to the AFC voltage and both are applied to the cancellation oscillator.

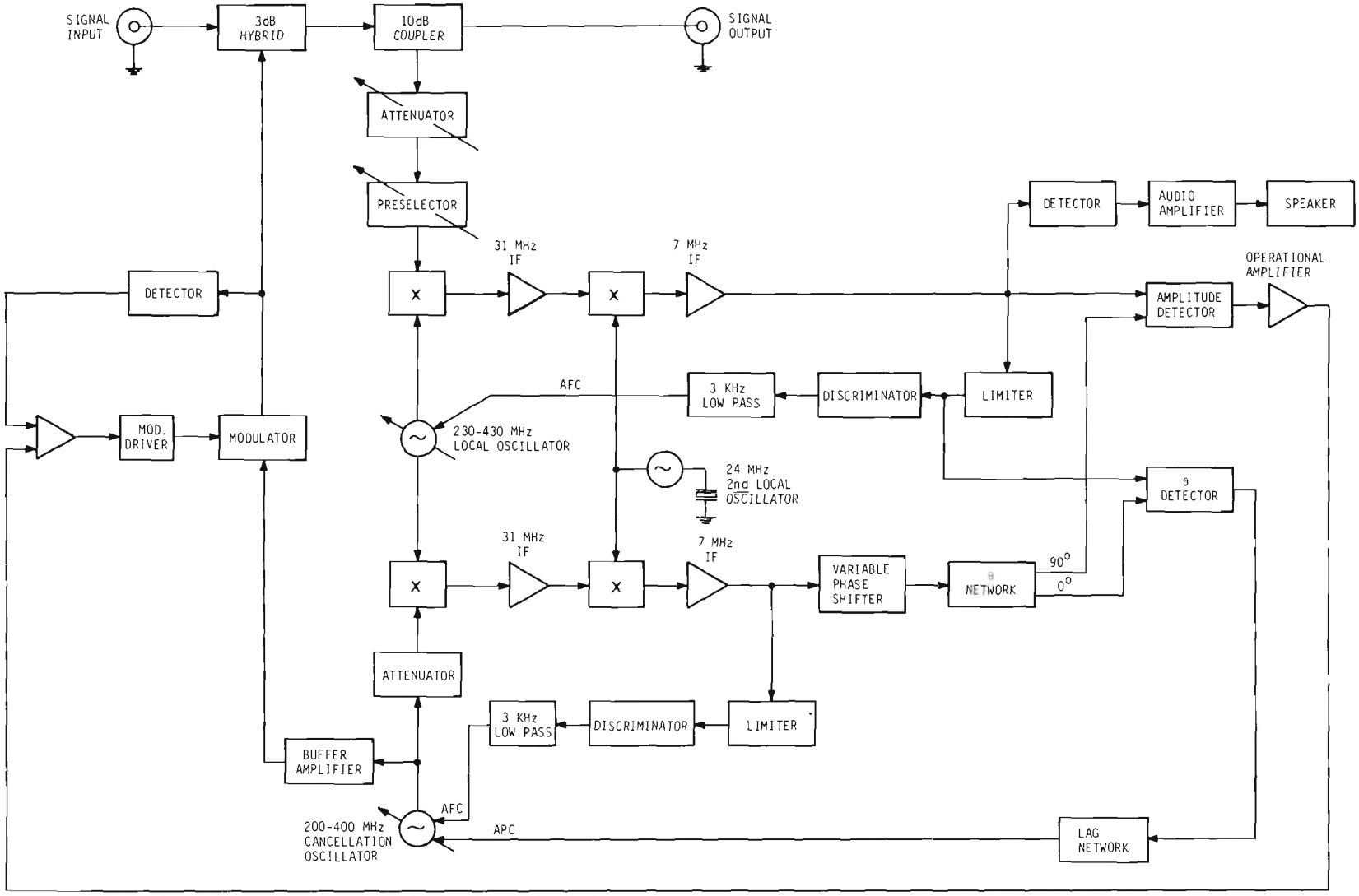

Figure 11. Block Diagram of the Dual Loop AM Cancellation System.

The adjustable phase shifter at the output of the 7 MHz IF amplifier in the cancellation oscillator loop has a range in excess of 360 degrees. Adjustment of the phase of the 7 MHz IF signal results in the phase of the cancellation oscillator being shifted by the same amount since the phase lock loop maintains a quadrature relationship between the two 7 MHz IF signals. The fixed 90 degree phase shift shown on the block diagram of figure 11 results in the 7 MHz inputs to the amplitude detector being in phase since the two phase detector signals are in quadrature.

The output of the amplitude detector is coupled to a DC amplifier which supplies the drive signal to the high level modulator in the output of the cancellation oscillator. The basic modulator consists of a balanced bridge configuration of HPA 3001 PIN diodes. The high on-off impedance ratio of these diodes permits greater than 98 per cent modulation of the cancellation signal. Since nonlinearities in the modulator generate unwanted components in the cancellation signal, a closed loop modulation system samples the output of the modulator and compares it with the characteristics of the audio signal which is derived from the interference sample. As a result, the level of the cancellation signal is made to follow the amplitude variations of the interfering signal.

To aid in the initial adjustment of the system, a detector and audio amplifier with speaker is used to monitor the level of the interference signal. A null in the audio output signal indicates when cancellation is achieved.

An attenuator is provided between the directional coupler and the preselector to prevent a very high level interfering signal from saturating the preselector. If the preselector saturates, the correct amplitude characteristics of the interfering signal can not be discerned. As suppression of the interfering signal is approached, the attenuation is decreased which permits a greater degree of cancellation to be obtained.

The operation of this cancellation filter in a breadboard configuration achieved approximately 50 dB suppression of an AM signal. During the performance of this test, a high degree of RF leakage from the cancellation oscillator into other parts of the system, particularly into the interference signal channel, was observed. A much higher degree of cancellation should be possible with a more adequately shielded configuration.

SECTION III

UHF Q MULTIPLICATION

Although signal rejection techniques such as active cancellation have proven effective in reducing adjacent channel interference, these techniques are most appropriate for situations involving a small number of interfering signals. As the number of interference sources increase, the complexity of the cancellation system must grow accordingly. For those situations which involve several interfering signals, a simpler approach is to provide a sufficiently narrow band pass filter at the front end of the receiver. In this way, the desired signal is passed and all other undesired signals are attenuated.

One major difficulty encountered in the construction of passive element filters having the sufficiently small percentage bandwidths necessary for the rejection of undesired adjacent channel signals is the limited Q factor available in passive devices. This Q limitation has been overcome, in some instances, by the application of an active device connected in such a manner as to supply the inherent circuit losses associated with the passive circuit elements. This technique in effect multiplies the Q of the resonant circuit and produces a high degree of selectivity in the filter.

Basically, the technique of Q multiplication involves the controlled application of positive feedback around a resonant circuit. The block diagram of figure 12 illustrates the operational principles of a method which proved feasible at UHF.

In the course of the developmental program, certain features were found to be desirable in the various components of the system. For example, to avoid unpredictable loading effects on the antenna which would cause the input voltage, e_i, to fluctuate with adjustments in the system, a high degree of isolation was required between e_i and the output voltage, e_1, of the summing junction and between e_i and the feedback voltage, e_4. An active hybrid as the summing junction supplied the required isolation and in addition, provided some gain to both e_i and e_4.

The basic resonant structure of figure 12 whose Q is to be multiplied is designated as A(s), a second order response function. To minimize the order of multiplication required to achieve a specific Q with a small sized structure and thus avoid the inherent instabilities associated with high degrees of multiplication, a coaxial cavity having a loaded Q of approximately 800 was constructed. This high Q was obtained at the expense of a 6 dB insertion loss through the cavity. Sufficient gain was provided in the remainder of the system to overcome this loss.

The sampling ratio, k, was selected as approximately 0.1 which represents a compromise between the need to avoid excessive attenuation of e_2, the voltage

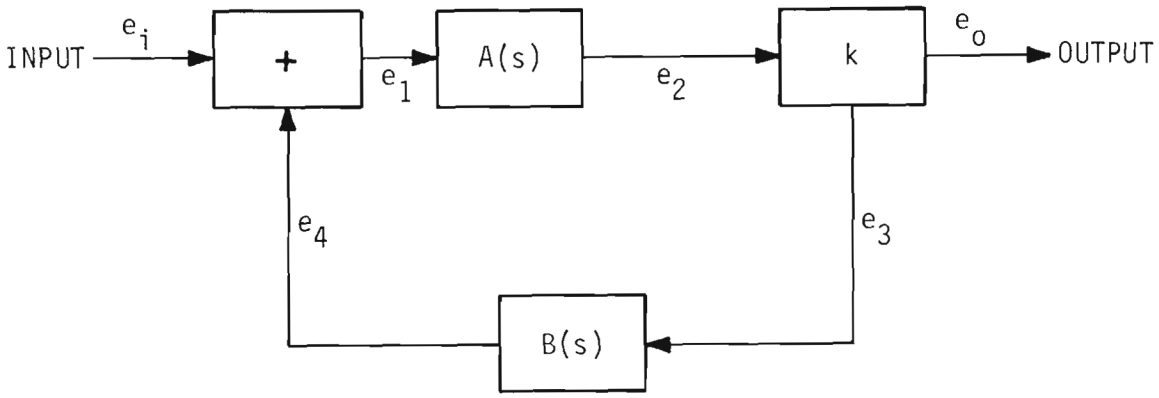

Figure 12. Block Diagram of UHF Q Multiplier.

output of A(s), and the need to provide an adequate voltage sample, e_3.

B(s) represents the variable gain and phase in the feedback path. The division of B(s) into essentially independent phase and gain functions resulted in greater ease in tuning. A voltage controlled phase shifter that exhibited very little gain variation with phase adjustments supplied the required phase characteristic. The independent gain adjustment was obtained with the use of a current controlled attenuator that exhibited a low phase shift versus current characteristic. Because of its independent gain and phase characteristics, B(s) can be considered as a gain function, G(s), and an independent phase function, $\Phi(s)$.

The behavior of the UHF Q multiplier is best explained in terms of its voltage transfer characteristic. To derive the voltage transfer characteristic of the system, first observe in figure 12 that

$$e_1 = a(e_i + e_4) \quad , \tag{1}$$

where a is the voltage gain between each junction input and its output; and further, that

$$e_2 = A(s)\, e_1 \quad , \tag{2}$$

$$e_3 = k\, e_2 \quad , \tag{3}$$

$$e_4 = B(s) e_3 \quad , \tag{4}$$

and, finally, that the output voltage

$$e_o = (1 - k) e_2 \quad . \tag{5}$$

Substituting the expression for e_2 from equation (2) into equation (5) gives

$$e_o = (1 - k)\, A(s) e_1 \quad . \tag{6}$$

From equation (1), obtain the expression for e_1 and substitute in (6):

$$e_o = (1 - k)\, A(s) \left[a\, (e_i + e_4) \right] \quad . \tag{7}$$

Expansion of equation (7) and subsequent substitutions from equations (4) and (3), respectively, result in

$$e_o = a(1 - k)\, A(s) e_i + ak(1 - k)\, A(s)\, B(s) e_2 \quad . \tag{8}$$

However, since

$$e_2 = \frac{1}{1 - k}\, e_o \tag{9}$$

from equation (5), equation (8) may be written as

$$e_o = a(1 - k)\, A(s) e_i + ak\, A(s)\, B(s) e_o \quad . \tag{10}$$

Rearrangement of the terms of (10) reveals that the voltage transfer, T(s), characteristic of the system is

$$T(s) = \frac{e_o}{e_i} = \frac{a(1 - k)\, A(s)}{1 - ak\, A(s)\, B(s)} \quad . \tag{11}$$

The transfer characteristic of a single cavity, coaxial resonator, tuned to $f_o = \frac{\omega_o}{2\pi}$ and characterized by $Q_U \gg Q_L$, where Q_U is the unloaded Q and Q_L is the loaded Q, is

$$A(s) = \frac{\frac{\omega_o}{Q_L}\, s}{s^2 + \frac{\omega_o}{Q_L}\, s + \omega_o^2} \quad . \tag{12}$$

Substituting this expression for A(s) into equation (11) gives

$$T(s) = a(1 - k) \quad \frac{\frac{\omega_o}{Q}\, s}{s^2 + \left[1 - ak\, B(s)\right] \frac{\omega_o}{Q}\, s + \omega_o^2} \quad , \tag{13}$$

which relates the overall transfer characteristic of the system to the basic characteristics of the resonator. For convenience, the loaded Q of the resonator is designated as simply "Q" in equation (13).

The multiplied Q of the response function of equation (13) can be defined as

$$Q' = \frac{Q}{1 - ak\ B(s)} \quad . \tag{14}$$

Defining the ratio of the multiplied Q to the natural Q as the multiplication factor, M_f, gives

$$M_f = \frac{Q'}{Q} = \frac{1}{1 - ak\ B(s)} \quad . \tag{15}$$

Since the behavior of the system is primarily of interest near the tuned frequency, $j\omega_o$ may be substituted for s in equation (15). Equation (15) then becomes

$$M_f = \frac{1}{1 - ak\ B(j\omega_o)} \quad . \tag{16}$$

For proper multiplication, the phase of $B(j\omega_o)$ is adjusted so that $B(j\omega_o) = + G(j\omega_o)$, where $G(j\omega_o)$ is the midband gain in the feedback loop. Figure 13 shows how the multiplication factor behaves as a function of the gain for selected values of the ak product. As would be expected, when the product ak $G(j\omega_o)$ approaches unity, the multiplication factor increases without bound or, in other words, the system approaches self sustained oscillations. Note that for a specific multiplication factor the slope of the curve is less at smaller ak values. Although more gain is required to produce a specific multiplication factor with smaller ak values, the system will be less sensitive to incremental gain variations in the less sloping regions of the curves.

Perhaps a more useful form for the multiplication factor is in terms of the change in bandwidth rather than in terms of Q. For example, suppose a cavity resonator with some natural Q is available. Then, the 3 dB bandwidth, Δf, at a particular frequency, f, is

$$\Delta f = \frac{f}{Q} \quad . \tag{17}$$

If the Q of the resonator is multiplied, the modified bandwidth is

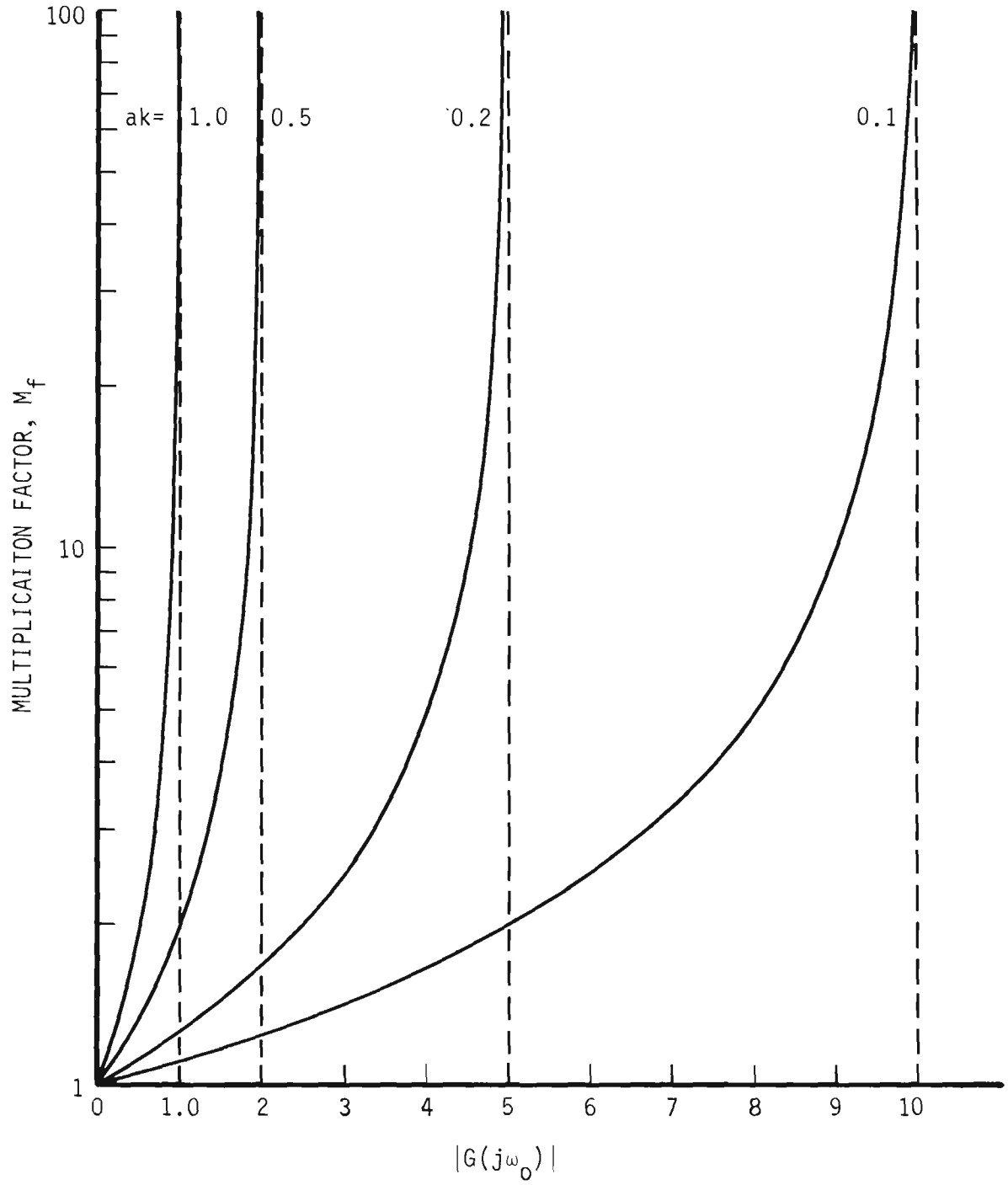

Figure 13. Multiplication Factor as a Function of the Midband Loop Gain.

$$\Delta f' = \frac{f}{M_f Q} \quad . \tag{18}$$

If a normalized bandwidth, $\overline{B}$, is defined such that

$$\overline{B} = \frac{\Delta f'}{\Delta f} \quad , \tag{19}$$

then it follows from (17) and (18) that

$$\overline{B} = \frac{1}{M_f} = 1 - ak\ B(j\omega_o) \quad . \tag{20}$$

The normalized bandwidth as a function of the gain, $G(j\omega_o)$, is shown in figure 14 for selected ak values. These curves again emphasize the greater system stability which results from lower ak values because bandwidth variations are less for specific gain changes at the lower values of the ak product.

In actual practice, incremental changes in system gain and phase can be expected which will cause bandwidth variations. In order to separate the effects of changes in the magnitude and phase of the loop gain on the normalized bandwidth, $\overline{B}$, equation (20) can be written in the form

$$\overline{B} = 1 - ak\ G(s)\ \Phi(s) \quad . \tag{21}$$

This division of the feedback characteristic into separate gain and phase functions is realistic since they are essentially independent in the actual system. The variation of the normalized bandwidth due to changes in gain or phase that may be caused by environmental factors such as temperature, humidity, and others can now be described by differentiating (21) to obtain an expression for the total differential, $d\overline{B}$. Since bandwidth fluctuations as a function of environmental factors are of greatest concern at a fixed frequency of operation, the frequency dependence of the gain and phase may be ignored. Then $G(s)$ and $\Phi(s)$ may be simply written as G and Φ, respectively. Under these circumstances, performing the necessary differentiation gives

$$d\overline{B} = - ak \left[G d\Phi + \Phi dG \right] \quad . \tag{22}$$

To illustrate the significance of (22), suppose the phase function is adjusted so that $\Phi = 1.0$ and suppose that $d\Phi = 0$. Changes in $\overline{B}$ because of changes in

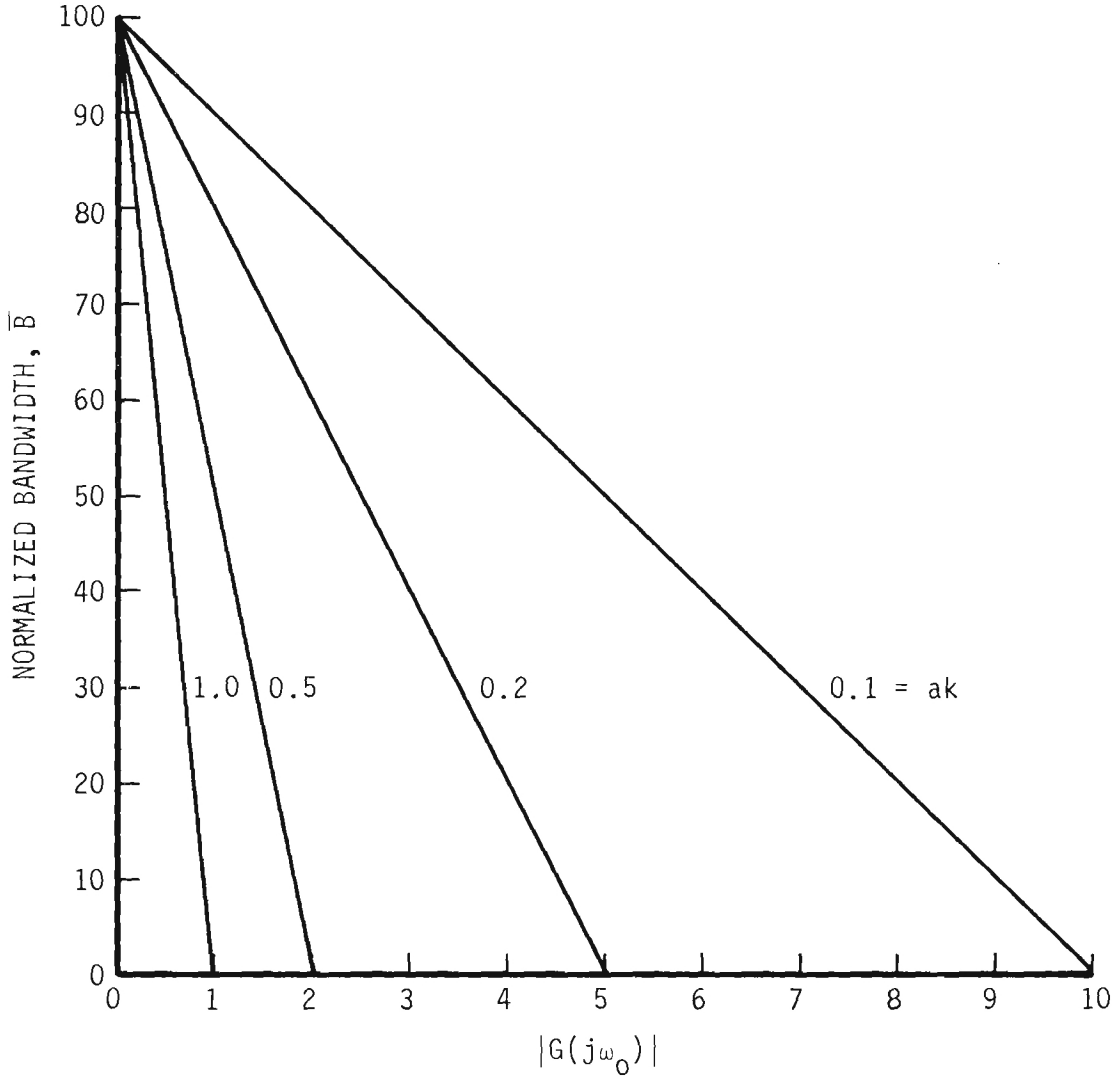

Figure 14. The Normalized Bandwidth of the Q Multiplier as a Function of the Midband Loop Gain.

gain, G, are then given by

$$d\bar{B} = - ak\, dG \quad . \tag{23}$$

The minus sign indicates that an increase in gain will decrease the bandwidth. Also observe that (23) is the equation that represents the curves of figure 14.

The net phase shift around the feedback loop will normally be adjusted so that $\Phi = 1.0$ at the center frequency. Since the maximum value of Φ is 1.0, any changes can only decrease Φ. Consequently, incremental phase shift changes in the system will increase the bandwidth.

The characteristics desired in the device which generates the $\Phi(s)$ function are those possessed by an ideal phase shifter. An ideal phase shift network permits the phase of the signal through the network to vary without affecting the amplitude of the signal. An example of an ideal phase shifter is the variable length of transmission line which is commonly used in the VHF and UHF regions. A principle limitation to the use of this type of shifter in the Q multiplication device is the long lengths of line required in the 200 to 400 MHz range. For example, at 300 MHz, a length variation of 50 centimeters is necessary to obtain at least 180 degrees of phase shift. Since one of the primary objectives in developing the Q multiplication technique is to realize large effective Q's in smaller physical systems, such long lengths of transmission lines are not desirable. Consequently, the development of a phase shifter more compatible with the overall Q multiplication concept was necessary.

A length of transmission line is an example of an all-pass network, that is, the amplitude of the transfer function is a non-varying function of frequency while the phase does vary as a function of frequency. The pole-zero (p-z) plot of an elementary all pass function is shown in figure 15. The transfer function represented by this p-z plot is

$$T(s) = \frac{s - z_1}{s - p_1} = \frac{s - \sigma_1}{s + \sigma_1} \quad . \tag{24}$$

Evaluating (24) at $s = j\omega_1$, point A, yields

$$T(j\omega_1) = \frac{j\omega_1 - \sigma_1}{j\omega_1 + \sigma_1} \quad . \tag{25}$$

The magnitude of the transfer function is

$$|T(j\omega_1)| = \frac{|j\omega_1 - \sigma_1|}{|j\omega_1 + \sigma_1|} = \frac{\sqrt{\omega_1^2 + \sigma_1^2}}{\sqrt{\omega_1^2 + \sigma_1^2}} = 1 \quad . \tag{26}$$

Note that as point A moves to a new frequency, $s = j\omega_2$, the value of $|T(j\omega)|$ remains unity.

The net phase shift, θ_T, through the network of the signal at frequency ω_1 is given by

$$\theta_T = \theta(z_1) - \theta(p_1) = \pi - \alpha - \alpha = \pi - 2\alpha = \pi - 2 \tan^{-1} \frac{\omega_1}{\sigma_1} \quad . \tag{27}$$

It can be seen from equation (27) that as the frequency of point A changes from ω_1 to another frequency ω_2 the phase shift through the network changes.

The objective of a phase shifter, however, is to vary the net phase between two points in a transmission path at a fixed frequency (point A not moving as above) with minimum perturbation to the amplitude. If instead of the fixed p-z pair of figure 15, suppose a pair of complex poles and zeros move on a line parallel to the $j\omega$ axis as shown in figure 16. The transfer function of this p-z function is

$$T(s) = \frac{(s - z_1)(s - z_1^*)}{(s - p_1)(s - p_1^*)} = \frac{(s - \sigma_1 - j\omega_2)(s - \sigma_1 + j\omega_2)}{(s + \sigma_1 - j\omega_2)(s + \sigma_1 + j\omega_2)} \quad . \tag{28}$$

The amplitude of $T(s)$ evaluated at $s = j\omega_1$ can be shown to be

$$|T(j\omega)| = \frac{\left(\sqrt{\sigma_1^2 + (\omega_1 + \omega_2)^2}\right)\left(\sqrt{\sigma_1^2 + (\omega_2 - \omega_1)^2}\right)}{\left(\sqrt{\sigma_1^2 + (\omega_1 + \omega_2)^2}\right)\left(\sqrt{\sigma_1^2 + (\omega_2 - \omega_1)^2}\right)} = 1 \quad . \tag{29}$$

Equation (29) shows that as the complex poles and zeros move up and down parallel to the $j\omega$ axis the amplitude is invariant.

The net phase shift at point A is

$$\theta_T = \theta(z_1) + \theta(z_1^*) - \theta(p_1) - \theta(p_1^*) \quad . \tag{30}$$

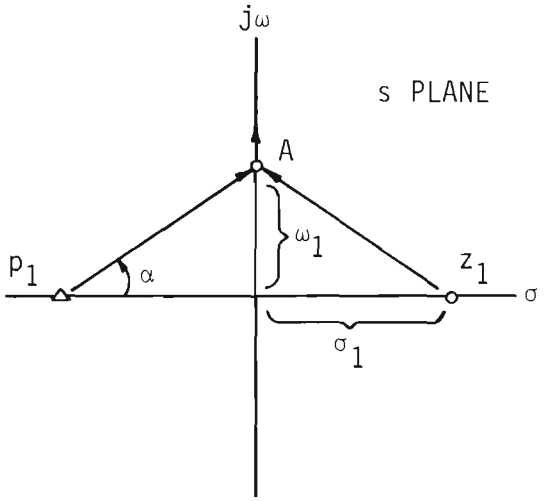

Figure 15. Pole-Zero Plot of a Simple All-Pass Network Function

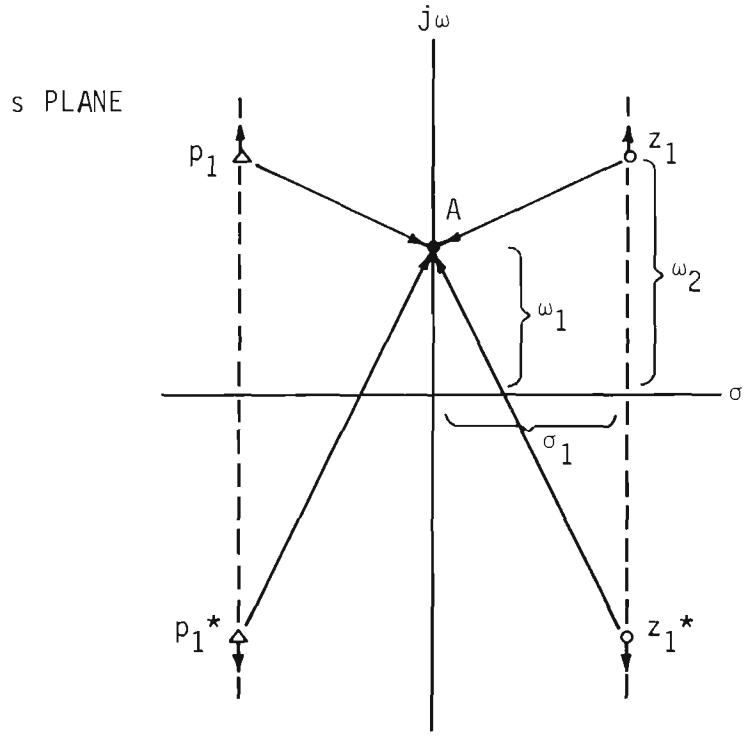

Figure 16. Pole-Zero Plot of An Ideal Phase Shifter.

From equation (28) the expression for the total phase shift can be written as

$$\theta_T = \tan^{-1}\left(-\frac{\omega_1 - \omega_2}{\sigma_1}\right) + \tan^{-1}\left(-\frac{\omega_1 + \omega_2}{\sigma_1}\right) - \tan^{-1}\left(\frac{\omega_1 - \omega_2}{\sigma_1}\right) - \tan^{-1}\left(\frac{\omega_1 + \omega_2}{\sigma_1}\right) \quad . \tag{31}$$

Equations (29) and (31) show that the p-z configuration of figure 16 represents the network function of an ideal phase shifter since the phase angle but not the amplitude of the transfer function is a function of requency.

Another way of expressing equation (28) is

$$T(s) = \frac{s^2 - \frac{\omega_o}{Q}s + \omega_o^2}{s^2 + \frac{\omega_o}{Q}s + \omega_o^2} \quad . \tag{32}$$

Being an improper fraction, T(s) may be written as one plus a proper fraction:

$$T(s) = 1 + \frac{P(s)}{N(s)} \quad , \tag{33}$$

or

$$T(s) - 1 = \frac{P(s)}{N(s)} \quad . \tag{34}$$

Performing operation (34):

$$\frac{P(s)}{N(s)} = \frac{s^2 - \frac{\omega_o}{Q}s + \omega_o^2}{s^2 + \frac{\omega_o}{Q}s + \omega_o^2} - 1 = \frac{-2\frac{\omega_o}{Q}s}{s^2 + \frac{\omega_o}{Q} + \omega_o^2} \quad . \tag{35}$$

The form of the expression (35) for P(s)/N(s) is immediately recognized as the second order response such as that obtained with a conventional LC circuit. Consequently, this analysis indicates that a practical phase shifter should

be obtainable with a proper combination of relatively simple networks such as that shown in figure 17.

Figure 18 is a detailed block diagram of a voltage controlled phase shifter which was constructed for the frequency range of 300 to 350 MHz. The input signal is divided into two paths of equal amplitude with the power divider. Channel one consists of a wideband amplifier with appropriate resistive padding to provide constant gain over the desired frequency range. Channel two contains a voltage controlled, single tuned amplifier with appropriate buffers to stabilize the input and output impedance of the channel as the tuning is varied. From equation (35) the net gain at resonance through the tuned amplifier channel must be twice that of the other channel and the net phase difference between the two must be 180 degrees. Consequently, the net gain of channel two is adjusted to be twice the gain of channel one. To insure that 180 degrees of phase difference is maintained at the summing junction over the desired frequency range, a short piece of transmission line is incorporated in channel one to equalize the time delay through both channels. Figure 19 shows that this system permits greater than 180 degrees of phase adjustment over the frequency range from 275 to 350 MHz.

An expanded block diagram of the UHF Q multiplier is shown in figure 20.

The completed device is shown in the photograph of figure 21.

Figure 22 shows the response curve of an unmodified resonator with a natural Q of approximately 700 at 325 MHz. The response curve of the cavity with Q multiplication is also shown in figure 22. The 3 dB bandwidth of approximately 50 KHz represents an effective Q of 6500 or a multiplication of approximately 9.3. These curves show that the system not only narrows the bandwidth but also relatively increases the skirt attenuation to signals which are essentially out of band.

The attenuation as a function of bandwidth is demonstrated in figure 23 for four resonator combinations. The transmission characteristics of the cascaded combination of a Collins UHF Filter, Model 56C-2, and the Q multiplied cavity shows the narrower passband with improved skirt rejection that is obtained over just the Collins Filter alone.

The ability of the Q multiplier to effectively discriminate against one signal while allowing another closely spaced signal to pass is illustrated in figure 24. When the two equal amplitude signals shown in figure 24A are passed through the Q multiplier and the UHF filter, their relative amplitudes are as shown in figure 24B. One of the signals is attenuated approximately 40 dB while the other is not affected.

Figure 25A depicts a situation where an undesired signal, spaced 1.5 MHz away, is more than 40 dB stronger than the desired signal. Note that the desired signal can not be discerned from the spectrum analyzer noise. When the signals are passed through the UHF filter and the Q multiplier, the desired signal is amplified and the undesired signal is attenuated. As evident in figure 25B, the resulting desired signal level is 20 dB greater than the

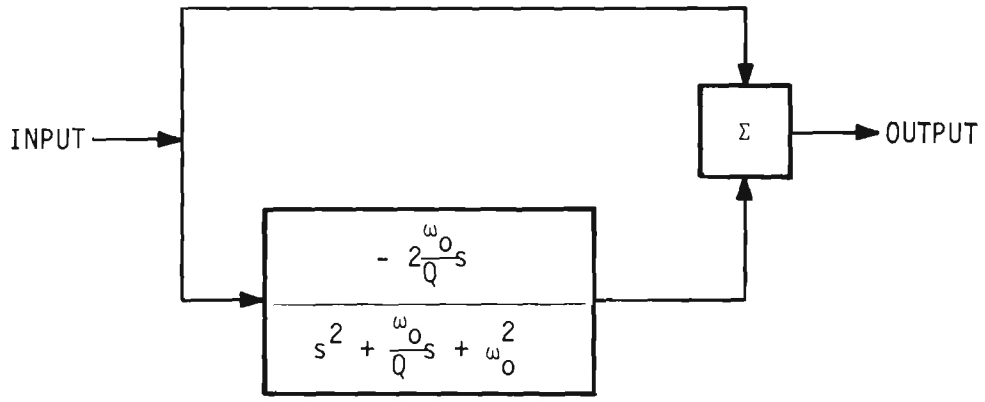

Figure 17. Block Diagram of An Ideal Phase Shifter.

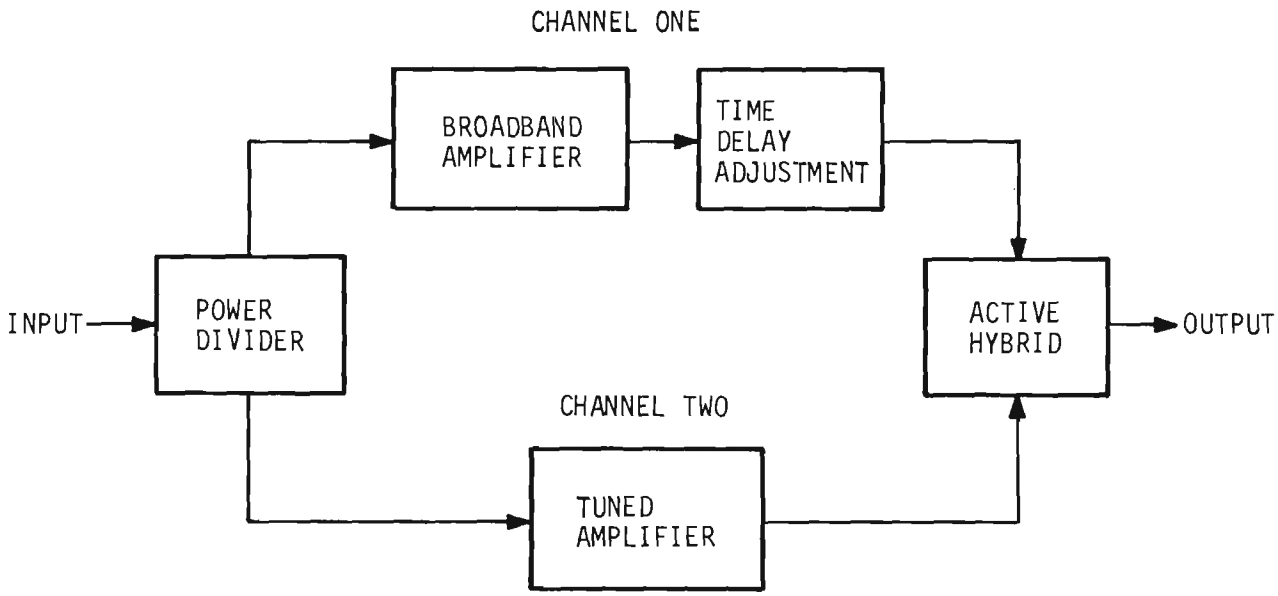

Figure 18. Block Diagram of Voltage Controlled Phase Shifter.

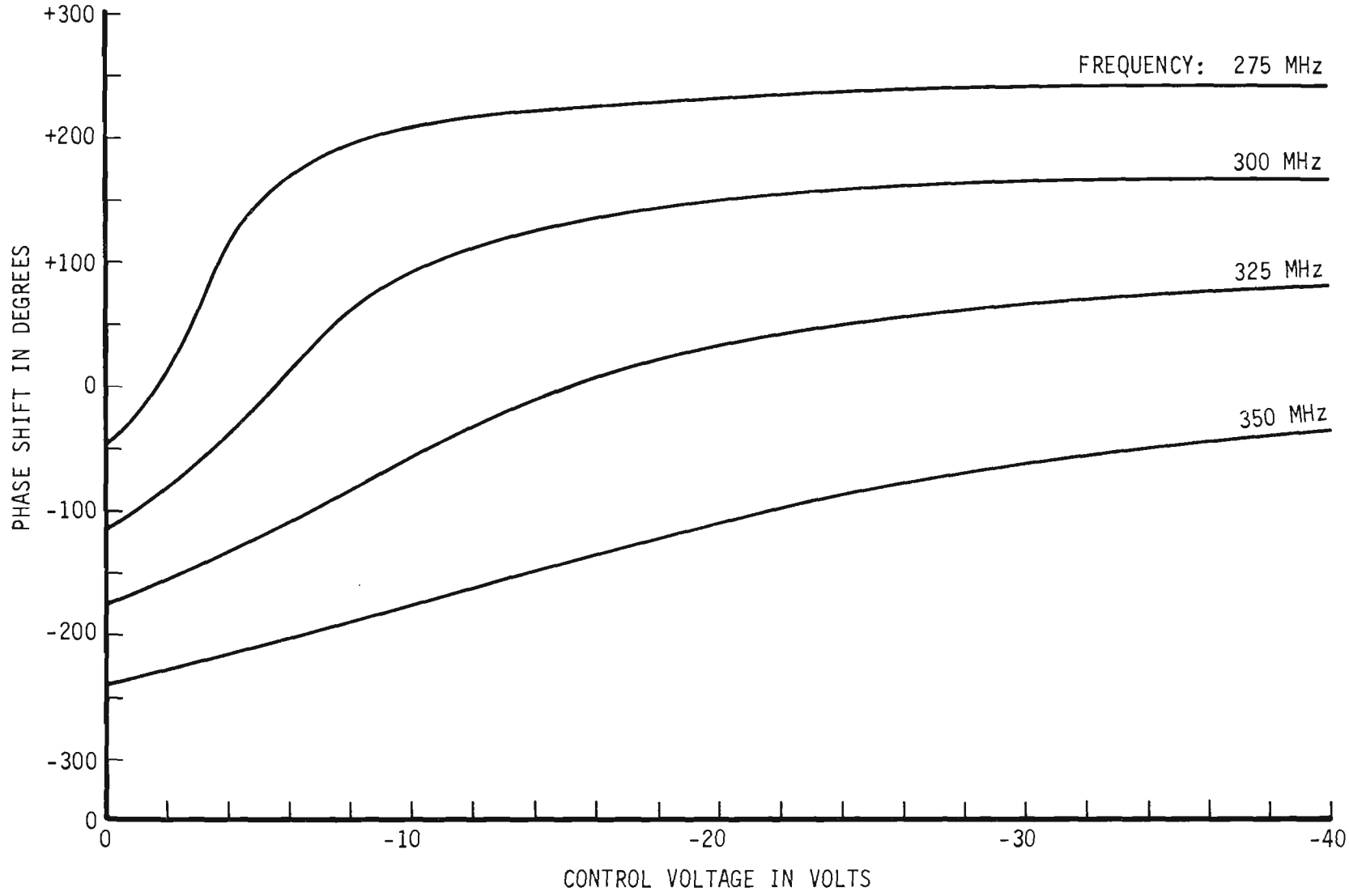

Figure 19. Phase Shift Versus Control Voltage at Selected Frequencies Between 275 and 350 MHz.

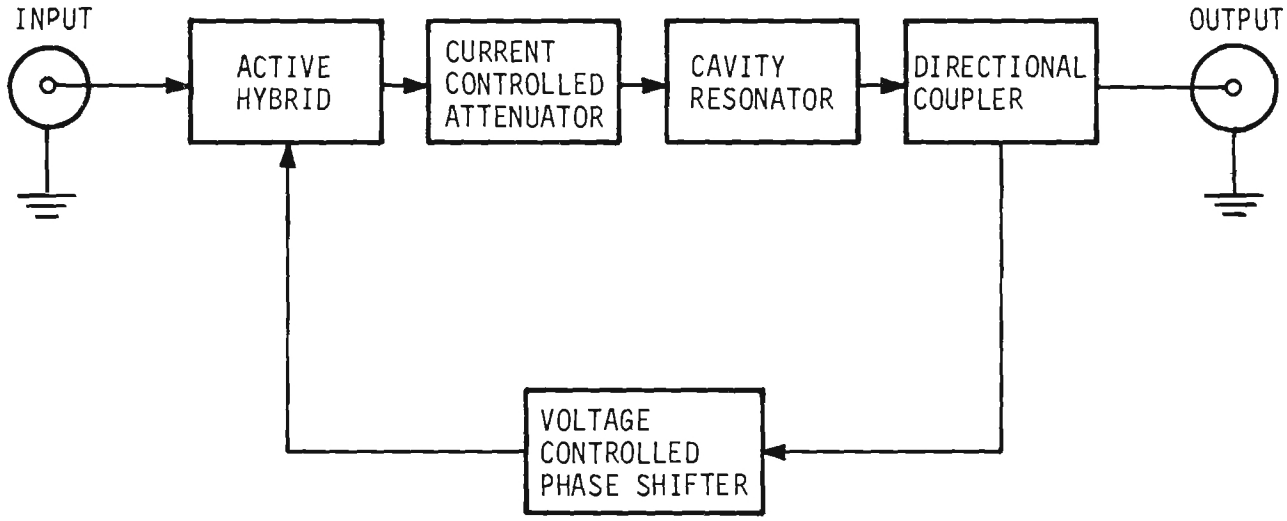

Figure 20. Expanded Block Diagram of the UHF Q Multiplier.

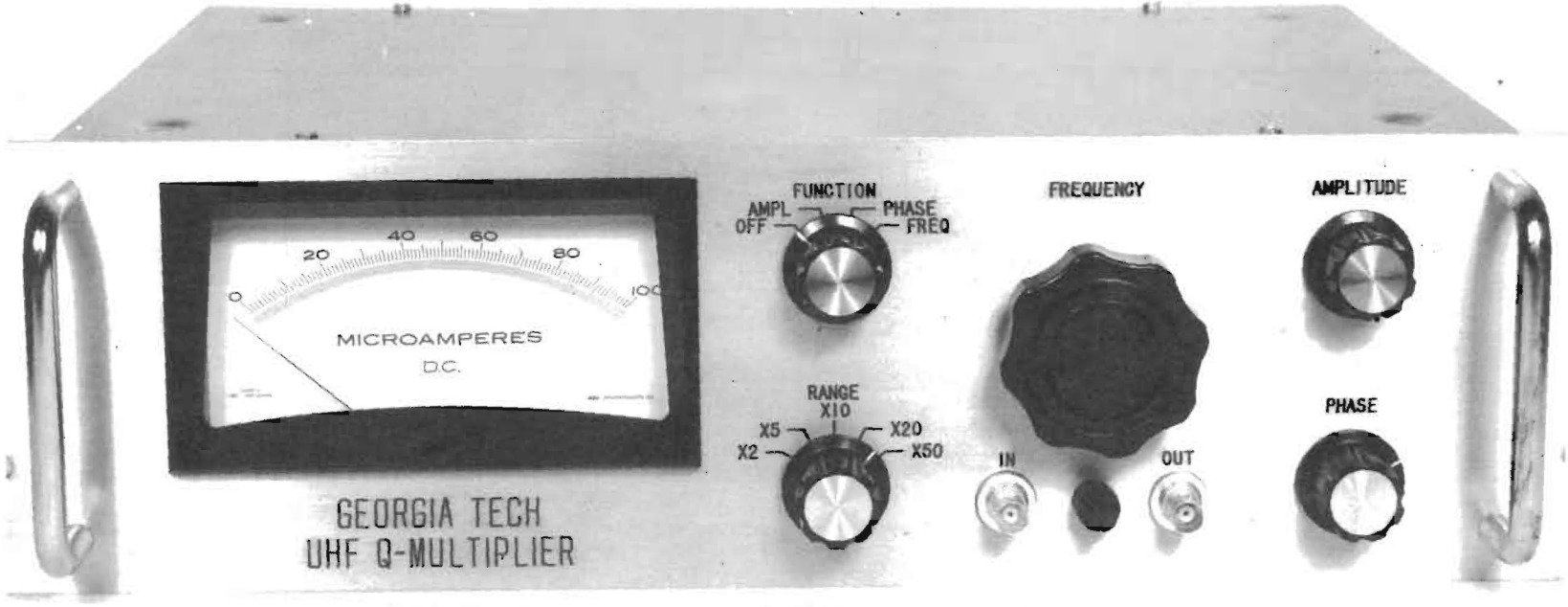

Figure 21. Photograph of the UHF Q Multiplier.

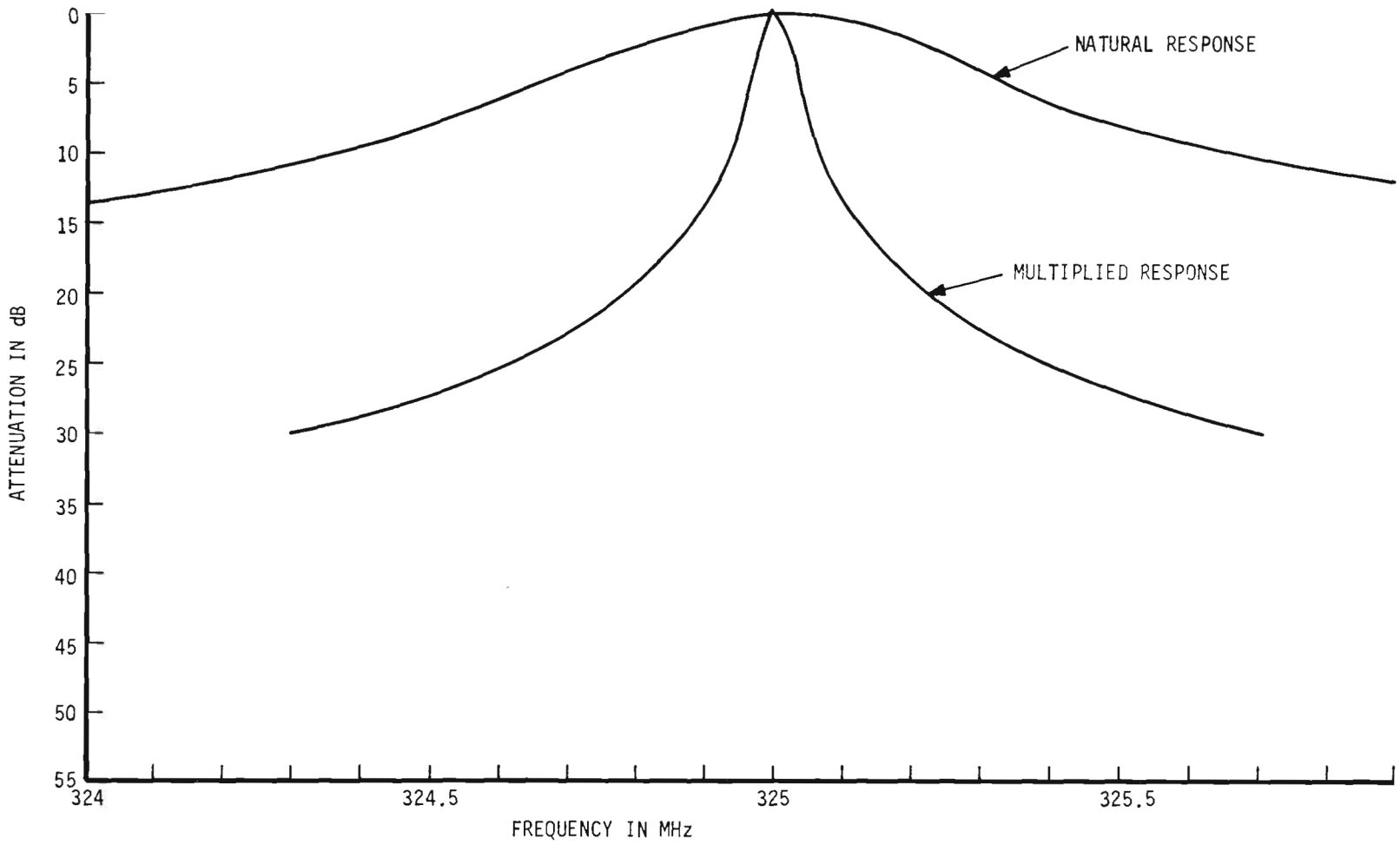

Figure 22. Response Characteristics of a Coaxial Cavity With and Without Q Multiplication.

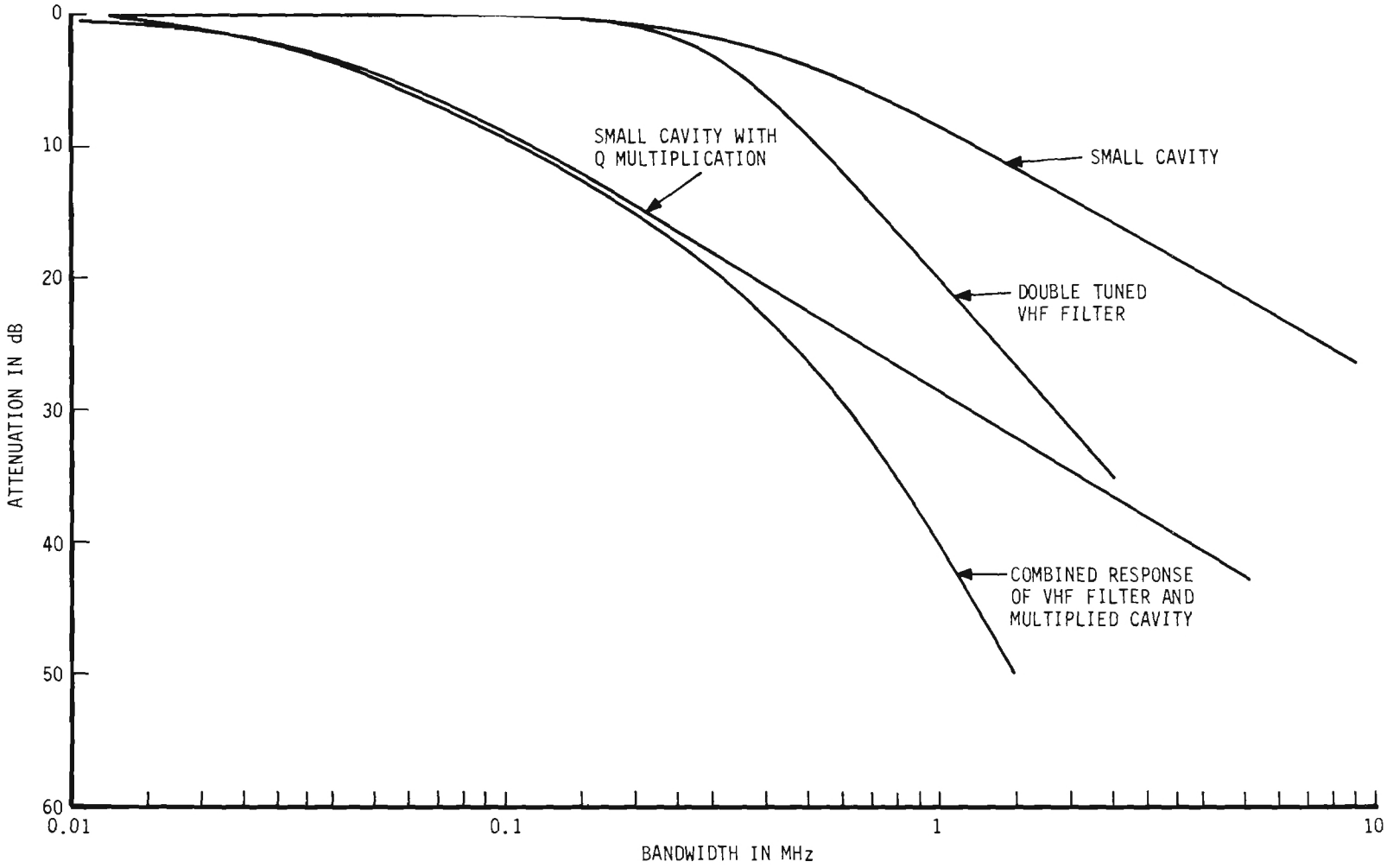

Figure 23. Transmission Characteristics of the Combination of a High Q UHF Filter and a Small Cavity of Multiplied Q.

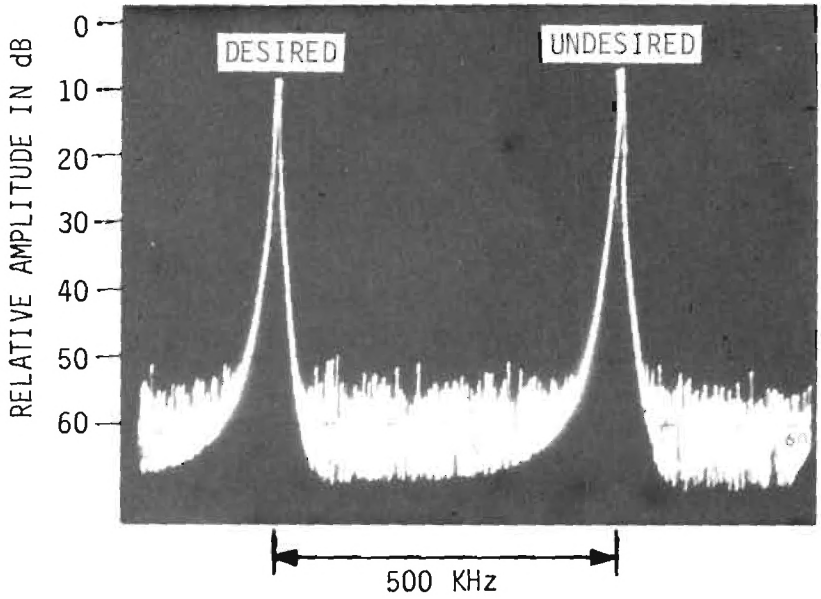

A. BEFORE FILTERING

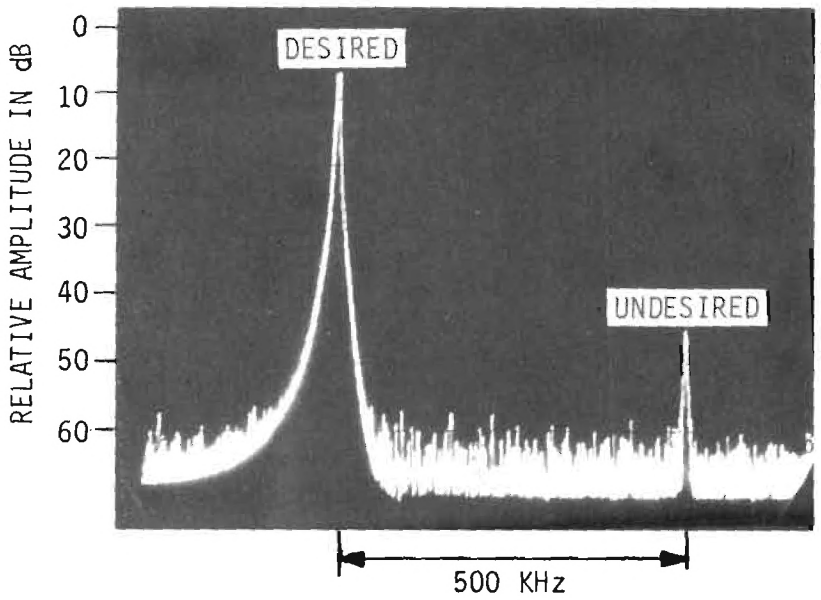

B. AFTER FILTERING

Figure 24. Comparative Levels of Two Closely Spaced Signals at 325 MHz Before and After Filtering With the Combined UHF Filter and Q Multiplier.

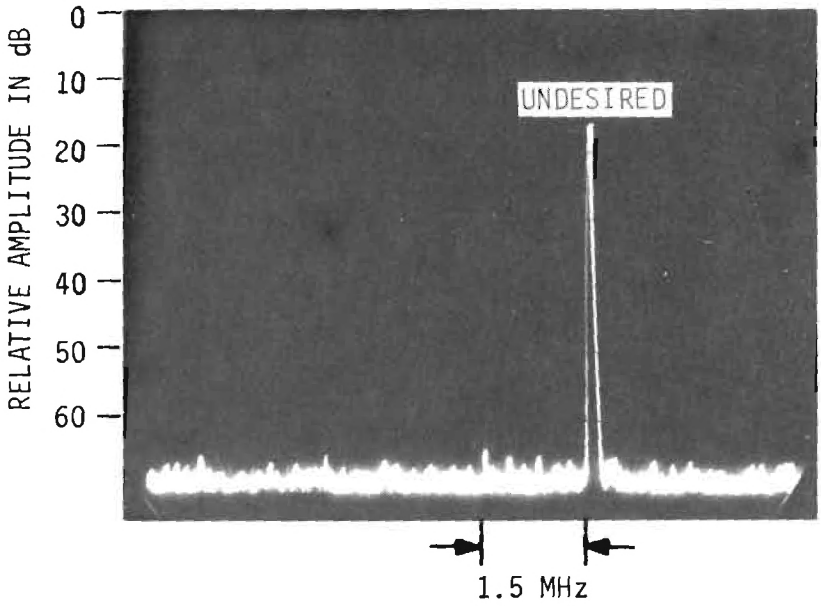

A. BEFORE FILTERING

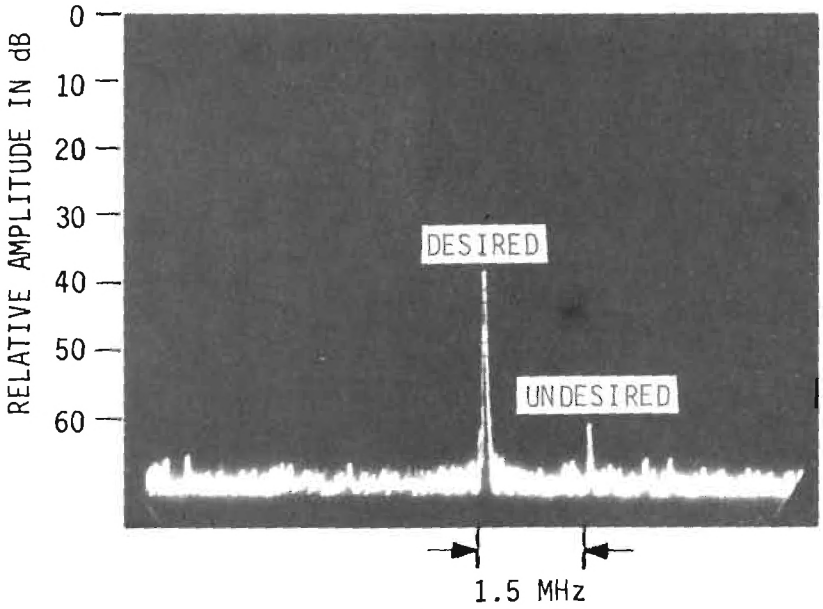

B. AFTER FILTERING

Figure 25. Relative Suppression of An Undesired Signal Spaced 1.5 MHz from the Desired Signal at 325 MHz.

undesired signal level.

Being an active device, the Q multiplier might be expected to generate unwanted responses which could become a source of interference in themselves. Of particular concern are the third order intermodulation products between the desired and undesired signals which might be generated in the active hybrid summing junction. Intuitively, any third order intermodulation products should, at most, be no higher than the level of the interfering signal itself out of the multiplier because the multiplier's response characteristics should discriminate against the unwanted products as effectively as against the undesired signal. In fact, the typical level of intermodulation products generated in the system are as shown in figure 26 which shows that, for 160 KHz spacing between the two input signals, the third order product is better than 50 dB below the desired signal level.

Figure 27 permits an evaluation of the relative cross modulation properties of the system to be made. Figure 27A is a spectral display of the audio components in the output of a highly selective receiver (Singer Metrics, NF 105) when two signals with 250 KHz spacing at 325 MHz are applied to the receiver's input. The desired signal is amplitude modulated at 400 Hz and the undesired is modulated at 1000 Hz. The other audio components are generated by cross modulation within the receiver. With the UHF Filter tuned to the desired signal (400 Hz modulation) some attenuation of the 1000 Hz component is evident as shown in figure 27B. Some reduction in the level of the harmonics of 400 Hz also occur along with a decrease in the level of the cross modulation components. Figure 27C shows that filtering the desired signal through the Q multiplier effectively removes the undesired signal. Equally important, this display shows no evidence of cross modulation in the Q multiplication device.

Although no particular effort was applied to developing a low noise device, an input signal level of -85 dBm is sufficient to develop a 10 dB signal-to-noise ratio at the output of the Q multiplier.

These performance results verify that the technique of Q multiplication for the realization of narrow passband filters is feasible at UHF. The resulting device represents a practical approach to the reduction of adjacent channel interference in the 200 to 400 MHz range.

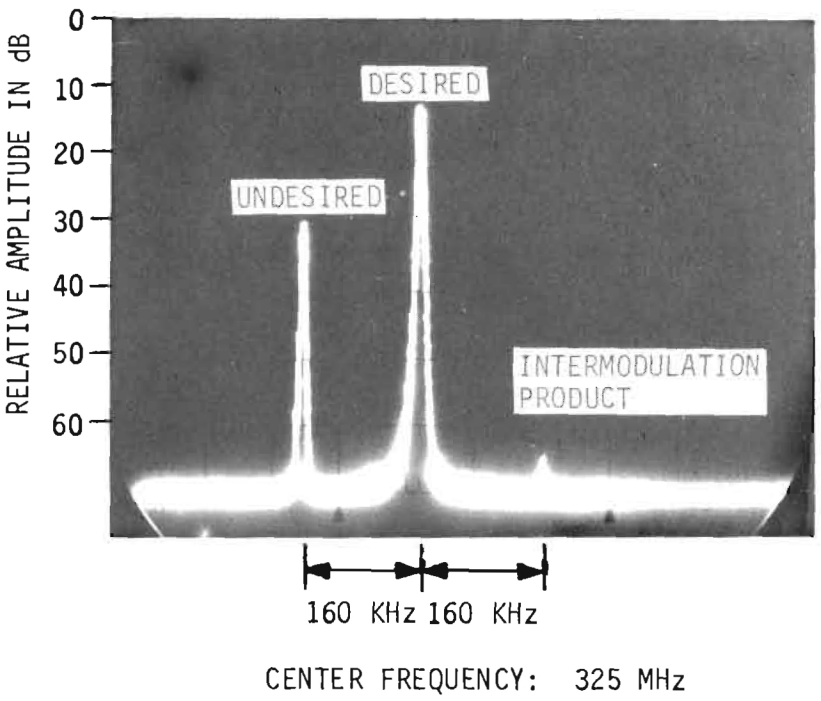

Figure 26. Typical Intermodulation Generation in the Q Multiplier.

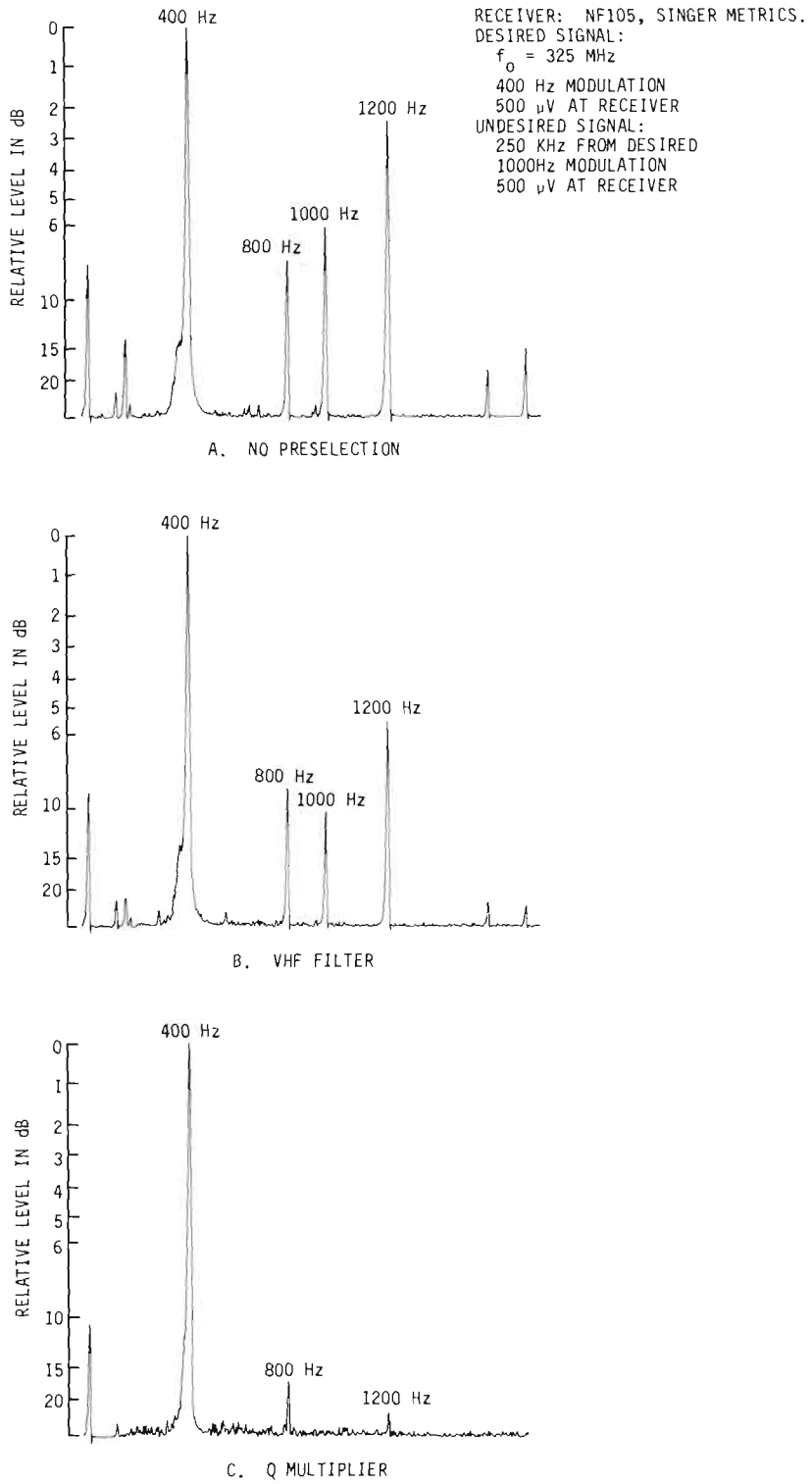

Figure 27. Audio Output Spectral Displays which Show the Effectiveness of the Q Multiplier in Reducing Cross Modulation.

SECTION IV

CRYSTAL INTERFERENCE FILTERS

Quartz crystal resonators are a class of passive devices having extremely narrow transmission bandwidths. The exceptionally high Q values exhibited by quartz crystals suggest the application of these devices to the solution of adjacent channel interference problems. However, crystal resonators suffer certain limitations which restrict their direct application to interference situations. For example, a single resonator can not be used to cover a wide frequency range of situations because of the fixed frequency nature of the overtone responses. Further more, only limited use can be made of a single quartz resonator in a bandpass configuration because the extremely narrow passband may cause appreciable distortion when the desired signal drifts slightly in frequency. Normally, several resonators must be used to produce a filter with sufficient bandwidth to prevent distortion. In this regard, considerable success has been achieved in constructing multi-element bandpass filters in crystal lattice configurations below about 120 MHz.[4] Unfortunately, these devices are not currently available in the 225 to 400 MHz frequency range.

While quartz resonators have only limited applications as bandpass filters at VHF, they may be used with fewer limitations in a band stop configuration. When used as a band reject filter to attenuate an interfering signal, small variations in the attenuation over the band occupied by the interfering signal or a slight drift in the interfering signal frequency are unimportant so long as the attenuation always exceeds the amount required to produce interference free reception of the desired signal. In many instances, the required rejection can be supplied with a single resonator. With this advantage and the fact that a single resonator in a band reject configuration may be effectively operated at higher overtone frequencies (approaching the UHF region), the band reject configuration is more desirable than the bandpass configuration.

The schematic diagram of a simple bandpass filter which has a sharp rejection notch at the peak of the bandpass response is shown in figure 28. The rejection characteristics of this crystal notch filter at 100 MHz are also shown. While the peak of the response occurs at the parallel resonant frequency of L and $(C + C_o)$, where C_o is the crystal parasitic capacitance, the sharp notch occurs at the series resonant frequency of the crystal. The depth of the notch depends directly on the ratio of the series resonant resistance of the crystal to the parallel resonant impedance of L and $(C + C_o)$. A primary limitation of this filter configuration is the large number of undesirable spurious responses. If the desired signal falls within the region of these spurious responses, it may be subject to severe distortion and attenuation. Therefore, a crystal free of spurious responses or a circuit configuration capable of suppressing the spurious responses is needed. Since the development of crystals free of spurious responses was outside the realm of of this study, efforts were directed toward the development of circuit

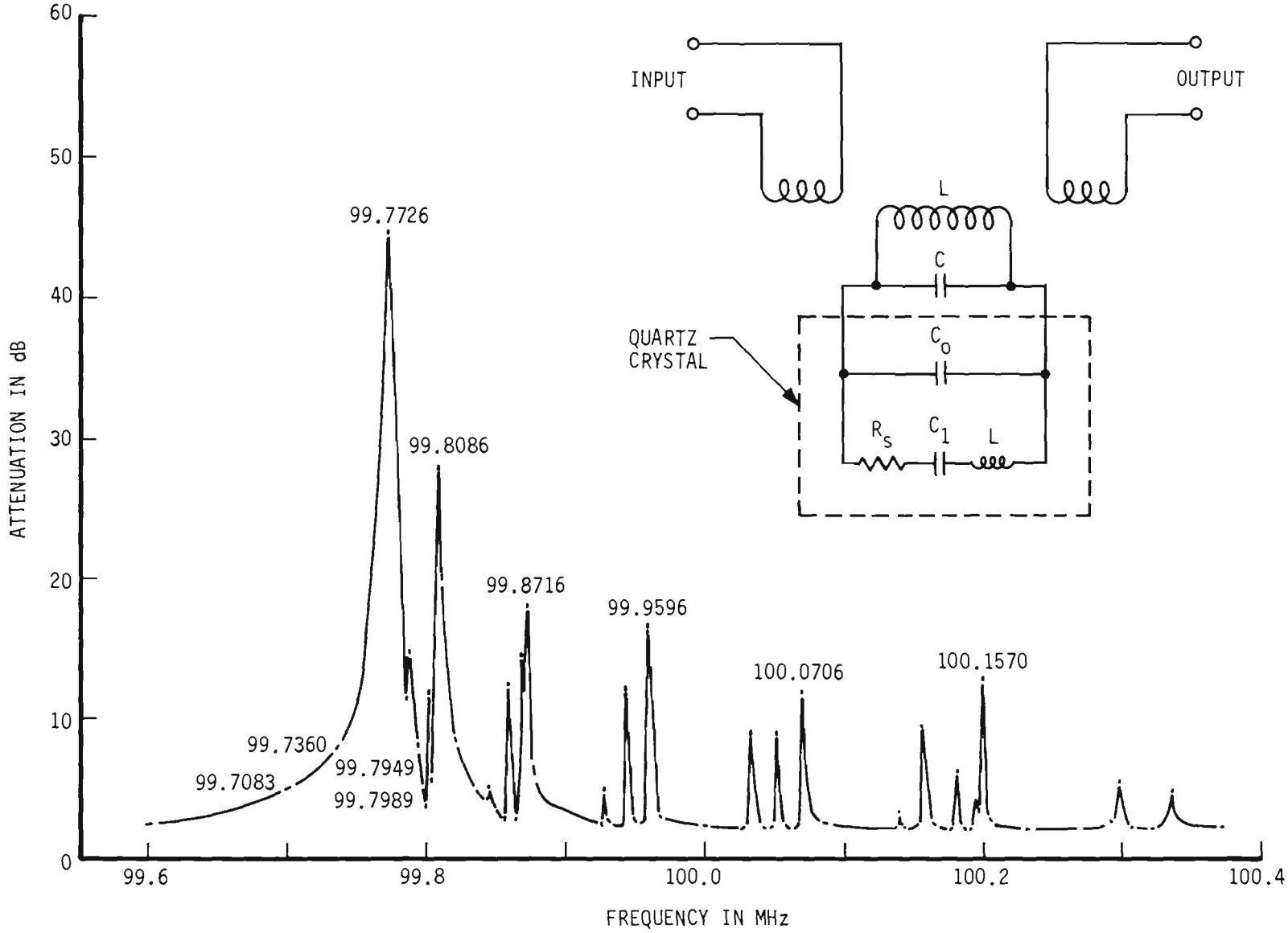

Figure 28. Rejection Characteristics of Simple Notch Filter.

configurations which suppress spurious responses.

One configuration found to be quite effective in suppressing the undesired spurious responses is the balanced bridge. This configuration takes advantage of the fact that normally the series resistance at a spurious response is higher than the resistance at the main response. By balancing the bridge at the resistance of the main response, the effectiveness of the main response is enhanced and the effects of the spurious responses are degraded. The response characteristics of the bridge type notch filter which are shown in figure 29 reveal a significant reduction in the number and magnitude of the spurious responses as compared to those of the simple notch filter. An additional advantage is gained by the use of the bridge configuration in that the depth of the notch depends directly on the precision of the bridge balance rather than on the ratio of the crystal resistance to the parallel resonant impedance of the tuned circuit.

Figure 30 illustrates the performance of a balanced bridge filter near 220 MHz. The maximum response ripple in the passband, 3 kHz above and below the notch, is less than 2 dB. In this region, a desired signal would be subject to little attenuation from the notch filter. The passband insertion loss with this configuration at 220 MHz is on the order of 10 dB compared to 2 dB at 100 MHz. Unfortunately, the insertion loss of this filter further increased at the higher overtone frequencies as shown in Table I.

Table I

CHARACTERISTICS OF AN OUTPHASING BRIDGE BALANCED AT SEVERAL OVERTONE FREQUENCIES OF 20 MHz QUARTZ CRYSTAL

Crystal Overtone	Frequency (MHz)	Insertion Loss (dB)	Rejection Level (dB)	Approximate 3 dB Bandwidth (kHz)	Approximate Q
3rd	59.8583	2.8	48	8.8	6,800
5th	99.7747	2.0	46	9.6	10,400
7th	139.6858	3.0	44	8.8	15,900
9th	179.5951	5.2	42	11.0	16,300
11th	219.5019	9.0	41	14.9	14,700
13th	259.4062	14.0	37	16.3	15,900
15th	299.3070	20.0	30	26.3	11,400
17th	339.2261	26.0	> 25	44.4	7,700
19th	379.1300	28.0	> 23	57.6	6,600

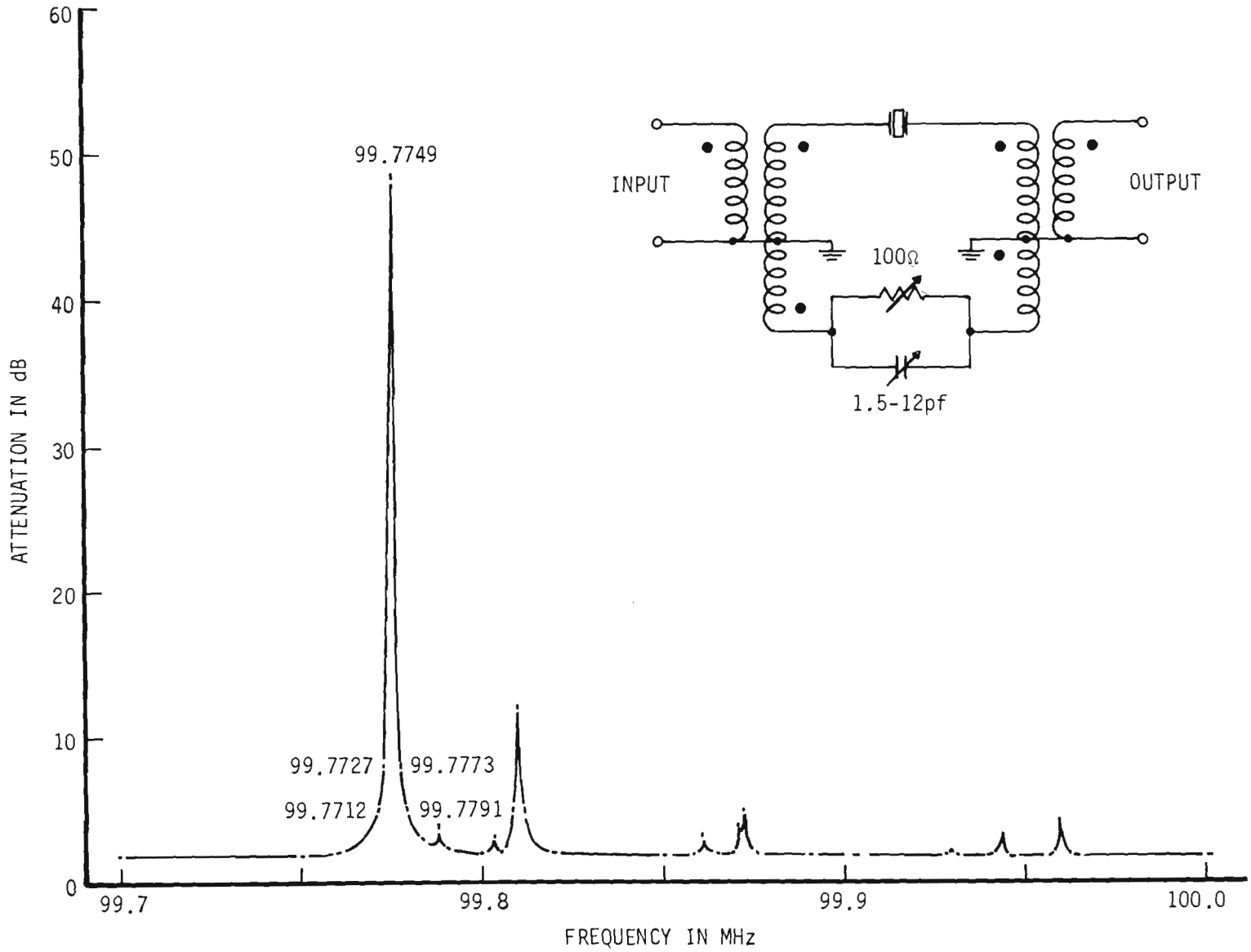

Figure 29. Rejection Characteristics of a 100 MHz Bridge Notch Filter.

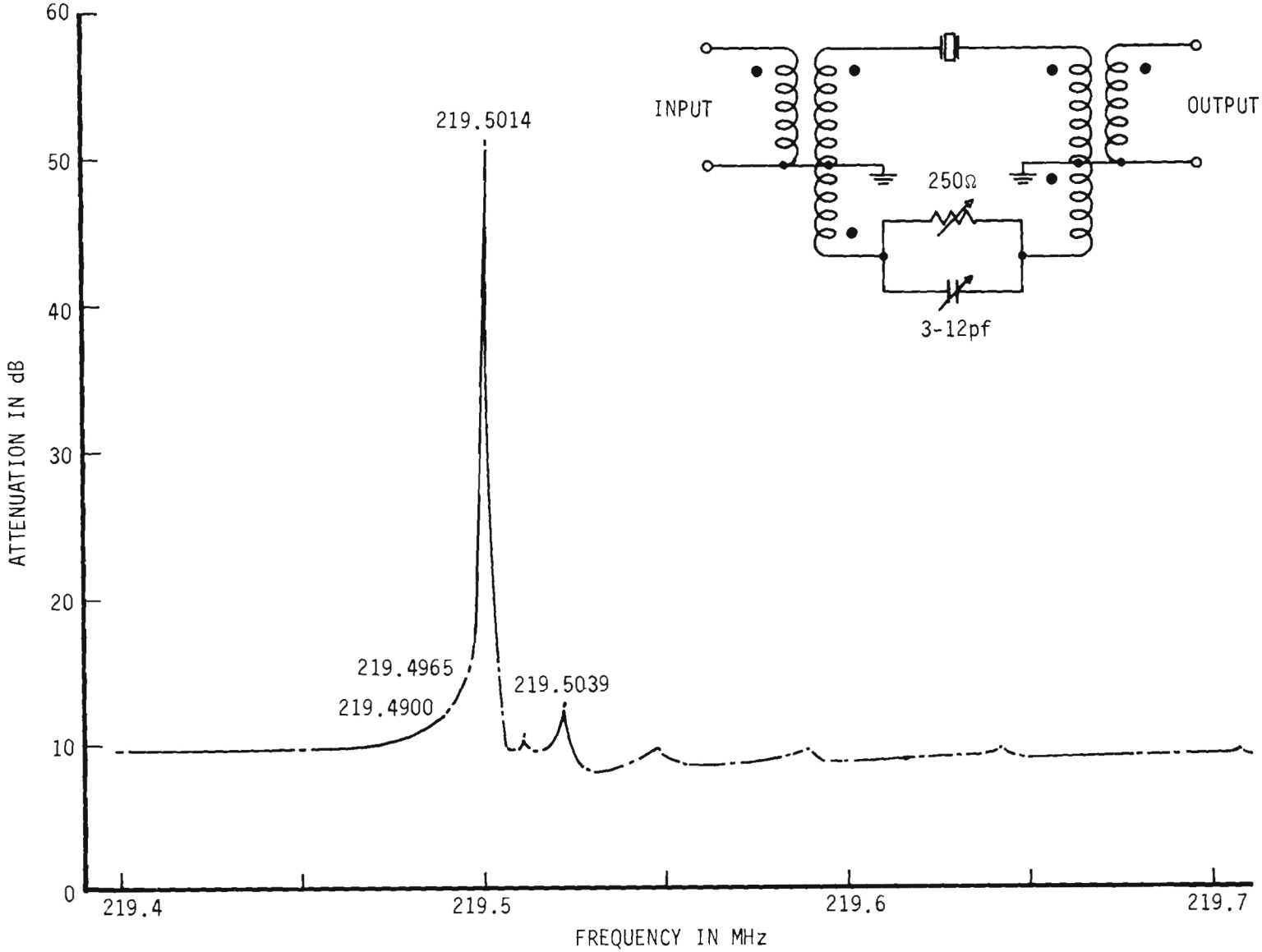

Figure 30. Rejection Characteristics of a 220 MHz Bridge Notch Filter.

While part of the increase in insertion loss may be attributed to the larger resonant resistance of the crystal at the overtone frequencies, a large part of the insertion loss was believed to be due to the increase in core loss and decrease in transformer coupling which occurs at the higher frequencies. A filter insertion loss of 18.5 dB at 380 MHz with the bridge unbalanced indicated that the transformers were contributing a large part of the loss. However, an insertion loss of 19.5 dB at 260 MHz with the original transformers replaced with low loss UHF transformers[5] indicated that additional factors were responsible for the high value of loss.

Further study of the bridge configuration revealed that the insertion loss was related to the series resonant impedance of the crystal at the overtone response frequency. With a crystal in one arm of the bridge and an impedance in the other arm matched to the series resonant impedance of the crystal and the shunt capacity of the holder, cancellation of the signal in the frequency range of crystal resonance produces an effective notch filter. Off resonance, the crystal becomes a high impedance which unbalances the bridge. However, the resistance and capacitance necessary for balancing the crystal resonant impedance remain in series with the signal path and determine the passband insertion loss of the filter. In general, at the higher overtone responses, the series resonant impedance of the crystal increases and the result is that the overall insertion loss of the filter rises. Consequently, low insertion loss with the balanced bridge configuration depends upon low series impedance at the overtone responses. Crystal resonators with a sufficiently low series impedance at overtone responses up to 400 MHz were not available to permit any significant reduction in the passband insertion loss of this filter configuration.

Since broadband hybrid junctions were available that had lower loss characteristics in the VHF region than conventional transformers, a crystal notch filter was developed which employed a hybrid junction in the manner shown in figure 31. In the hybrid junction, a signal applied to the summing port is split between the two side arm ports. Any impedance mismatch at the side arms reflect the signals to the output difference port. With one side arm containing the crystal and the other side arm containing an impedance matched to the series resonant impedance of the crystal and the shunt capacity of the holder, cancellation of the signal at the crystal series resonant frequency produces a notch characteristic as shown by the response curve of figure 31. Off resonance, the high impedance of the crystal unbalances the hybrid and the amount of unbalance determines the insertion loss of the filter. Typically, this filter configuration exhibited a 3 dB lower insertion loss than the simple balanced bridge.

The depth of the notch obtainable with the balanced hybrid filter depends upon the precision of match between the side arm impedances. The passband insertion loss, however, depends upon the degree of mismatch between these impedances. Minimum insertion loss with maximum rejection at the notch frequency will, consequently, be obtained with a crystal unit of lowest series resonant impedance. The low balancing impedance required to produce the notch characteristic at crystal resonance then exhibits a large mismatch to the crystal off-resonance impedance which results in a lower insertion loss.

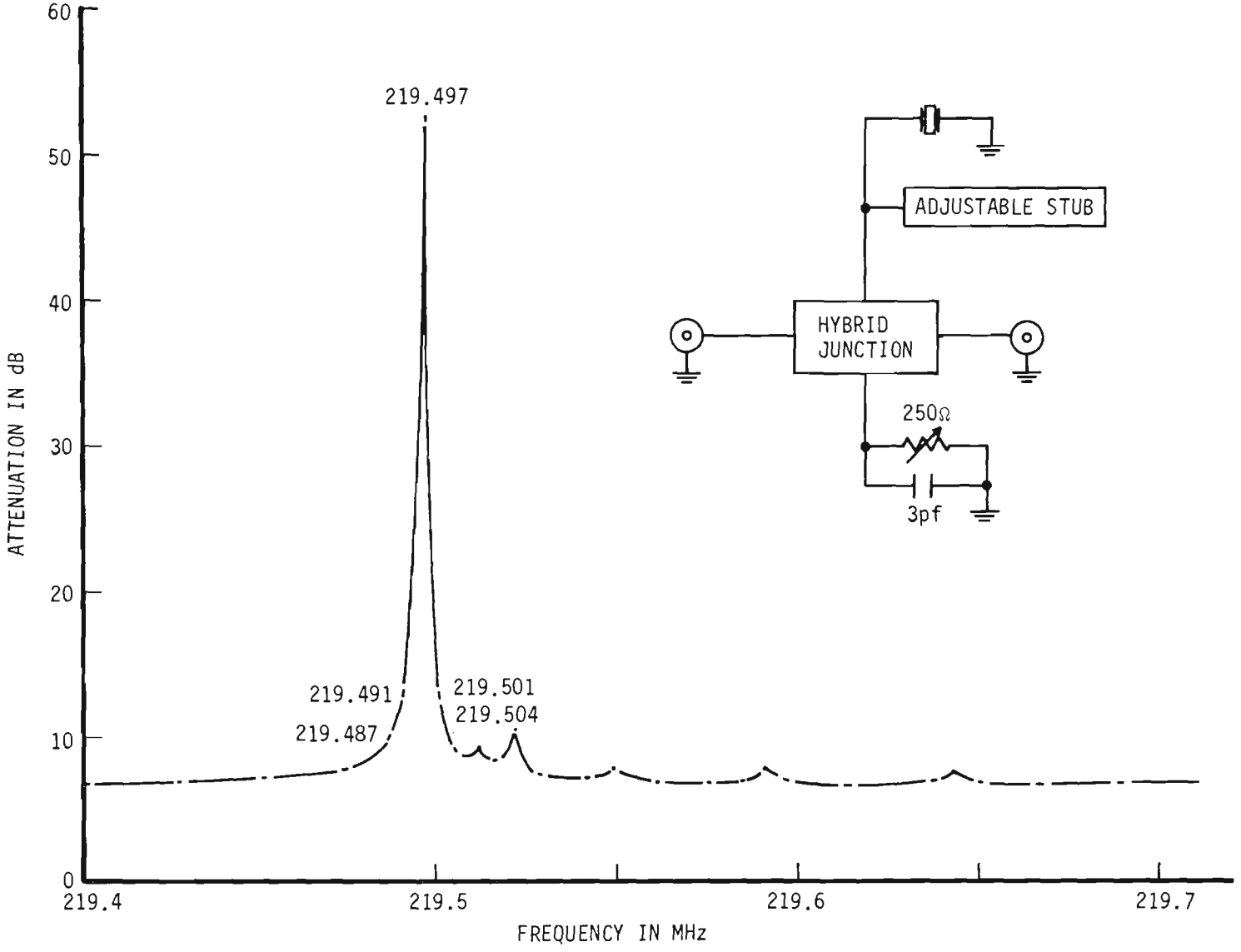

Figure 31. Rejection Characteristics of Hybrid Notch Filter.

By decreasing the potentiometer setting to minimum resistance, the passband insertion loss was reduced to 3.5 dB at the 220 MHz measurement frequency. Naturally, this procedure unbalanced the bridge and degraded the notch rejection value but it verified that a lower value of crystal resonant impedance is necessary to reduce the passband insertion loss of the notch filter configuration.

One limitation of crystal interference filters is the lack of flexibility because of their fixed tuned characteristics. A way of circumventing this limitation is to have available a large number of crystals with response frequencies appropriate to the interference environment. For maximum flexibility in meeting changes in the environment, the crystal elements should be interchangeable with minimum perturbation to the overall performance of the filter. The bridge configuration is limited in this regard as it must be balanced at each frequency of operation. Increased flexibility can be obtained by incorporating some of the crystal parameters into the integral design of a broadband filter configuration such as a high-pass or low-pass. For example, the shunt capacity, C_o, is primarily a function of the holder and can be integrated into the filter design. Then, as crystals of this holder group are interchanged to obtain responses at different frequencies, the overall bandpass response will not be materially changed.

Figure 32 illustrates the behavior of a low-pass filter which was designed to incorporate the crystal holder capacity. The crystal resonant impedance provides a shunt path across the transmission line at the series resonant frequency. The amount of attenuation provided by this shunt path depends upon the ratio of the characteristic impedance of the filter to the series resonant impedance of the crystal. Consequently, the impedance level of the filter should be at the maximum practical value and the series impedance of the crystals should be as low as possible. To provide maximum attenuation at crystal resonance, the low-pass filter was designed for a 200 ohm impedance level. The decrease in the attenuation, which is evident at the higher overtone response frequencies, is caused by the higher shunting impedance at the crystal overtone responses.

A crystal resonator is characterized by a number of parallel resonant frequencies which alternate between the conventional overtone and spurious response frequencies. The impedance level at parallel resonance is high compared to the series impedance. This high impedance can be used to obtain narrow bands of high insertion loss in the passband of a high-pass filter such as the one shown in figure 33. Although rejection ratios of greater than 20 dB are evident at 100 MHz, the rejection ratio rapidly deteriorates to a negligible value at 200 MHz indicating a limited applicability of this technique at UHF.

Two quartz crystals having the same fundamental response will not, in general, exhibit the same pattern of spurious responses. If the spurious response frequencies are not the same, at the particular frequency where one crystal has a low impedance path, the other crystal should exhibit a high impedance path. It might be expected, then, that a filter containing two

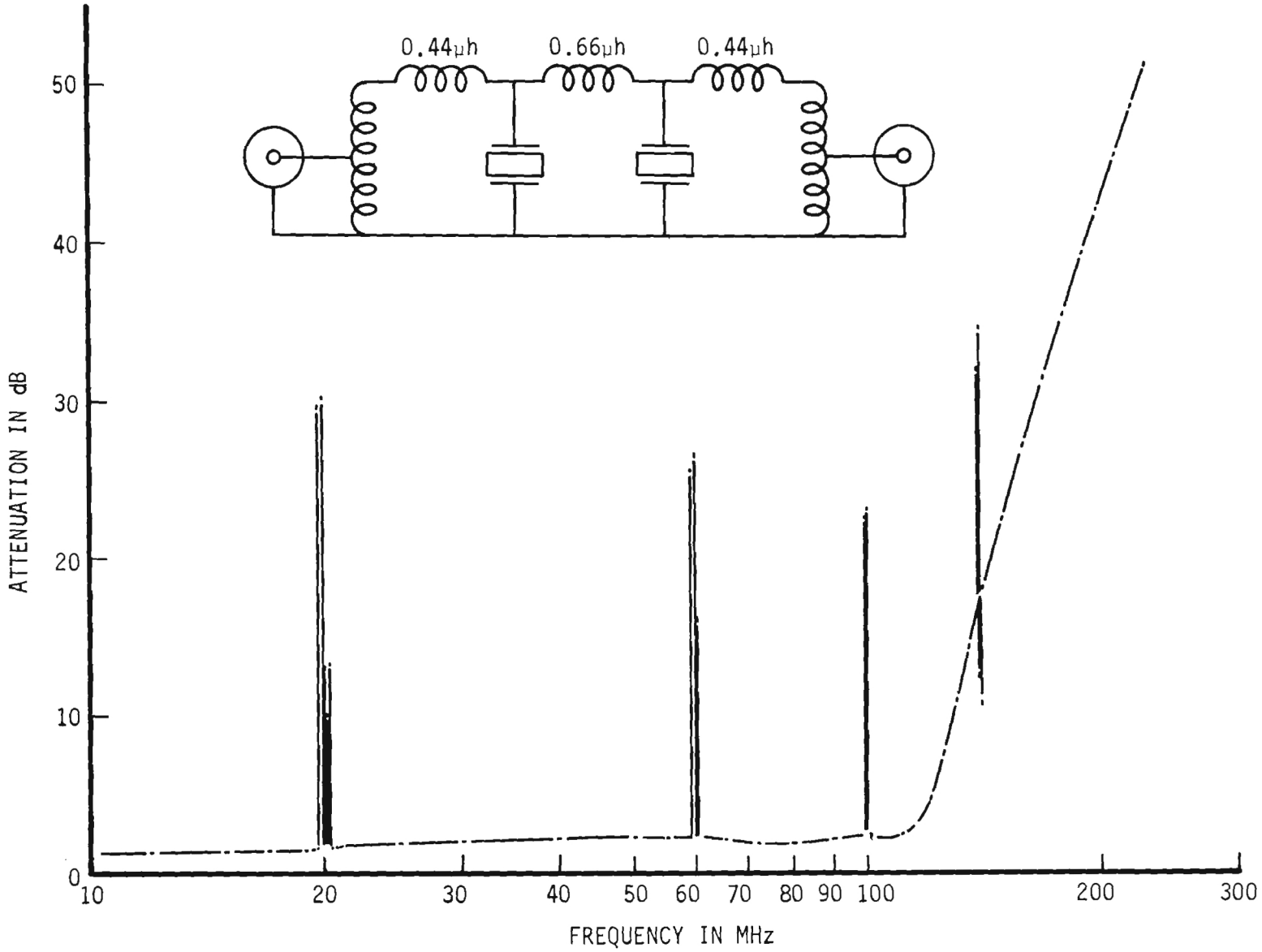

Figure 32. Rejection Characteristics of Low Pass Filter.

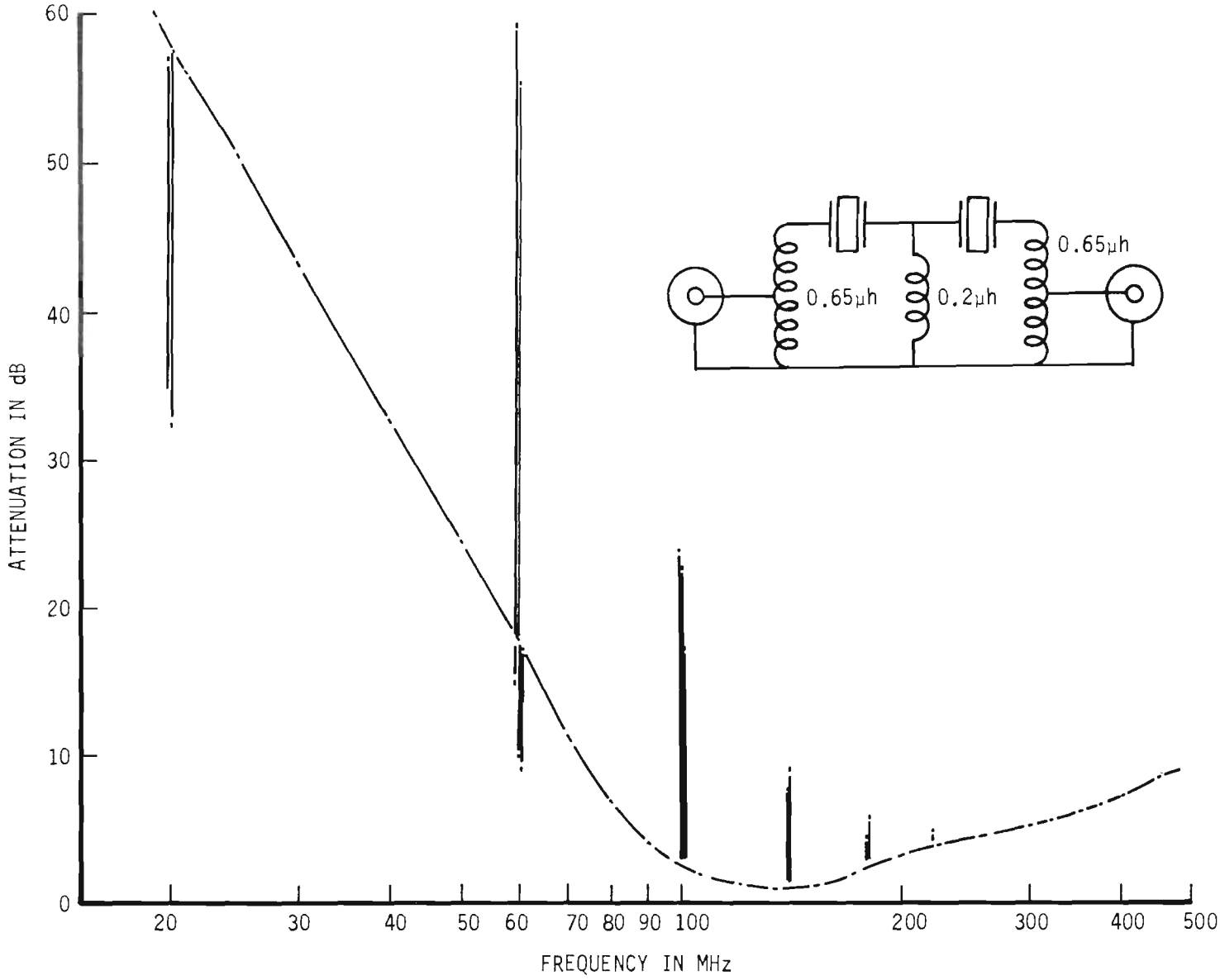

Figure 33. Rejection Characteristics High Pass Filter.

series crystal elements having the same fundamental response frequency would have fewer spurious responses than a single crystal filter. The transmission characteristics of a bandpass filter designed to include two crystal elements in series are shown in figure 34. Also shown for comparison purposes are the transmission characteristics of the filter with each crystal individually in the filter. Rather than having fewer spurious responses, this filter with two crystals in series displayed a number of spurious responses approximately equal to the sum of the responses with each crystal separately in the filter. It is possible that these two crystals were cut from the same blank and were plated by identical processes. If this is true, the spurious response of the two units would tend to coincide and both units would exhibit low impedance paths at the same frequencies. However, this test would indicate that the cascading of two crystal elements of the same fundamental frequency is not a very promising technique for reducing the number of spurious responses.

The achievement of crystal interference filters having high attenuation in the stop band and low attenuation in the passband is limited by the high series impedance of typical quartz resonators in the 200 to 400 MHz region. A reduction of this impedance is necessary for a low insertion loss in the bridge type filters and a high rejection ratio in such filters as the integrated low-pass. One way to reduce the effective series impedance is to supply some of the energy loss with an active device. By connecting the active device into the circuit in such a manner as to generate a negative resistance, the net impedance at crystal resonance can be reduced.

The diagram of figure 35 illustrates a network arrangement which can exhibit negative resistance properties. The net impedance, R, at the input terminals of the circuit can be determined by first assuming an input voltage, V, then calculating the input current, I_1, and finally obtaining the ratio,

$$R = \frac{V}{I_1} \quad . \tag{36}$$

Suppose R_1 defines the amplifier input impedance as reflected through the 1:1 transformer, and R_2 designates the terminating impedance of the phase shifter. Further assume that the output impedance of the phase shifter is 50 ohms, and that G is equal to the net closed loop gain. The circuit loop equations can now be written as:

$$(R_1 + R_2)\, I_1 - R_2\, I_2 = V \tag{37}$$

$$- R_2\, I_1 + (R_2 + 50)\, I_2 = G(I_1\, R_1) \quad . \tag{38}$$

The current I_2 is the second loop current as illustrated in figure 35. After solving equations (37) and (38) for I_1 and substituting into equation (36),

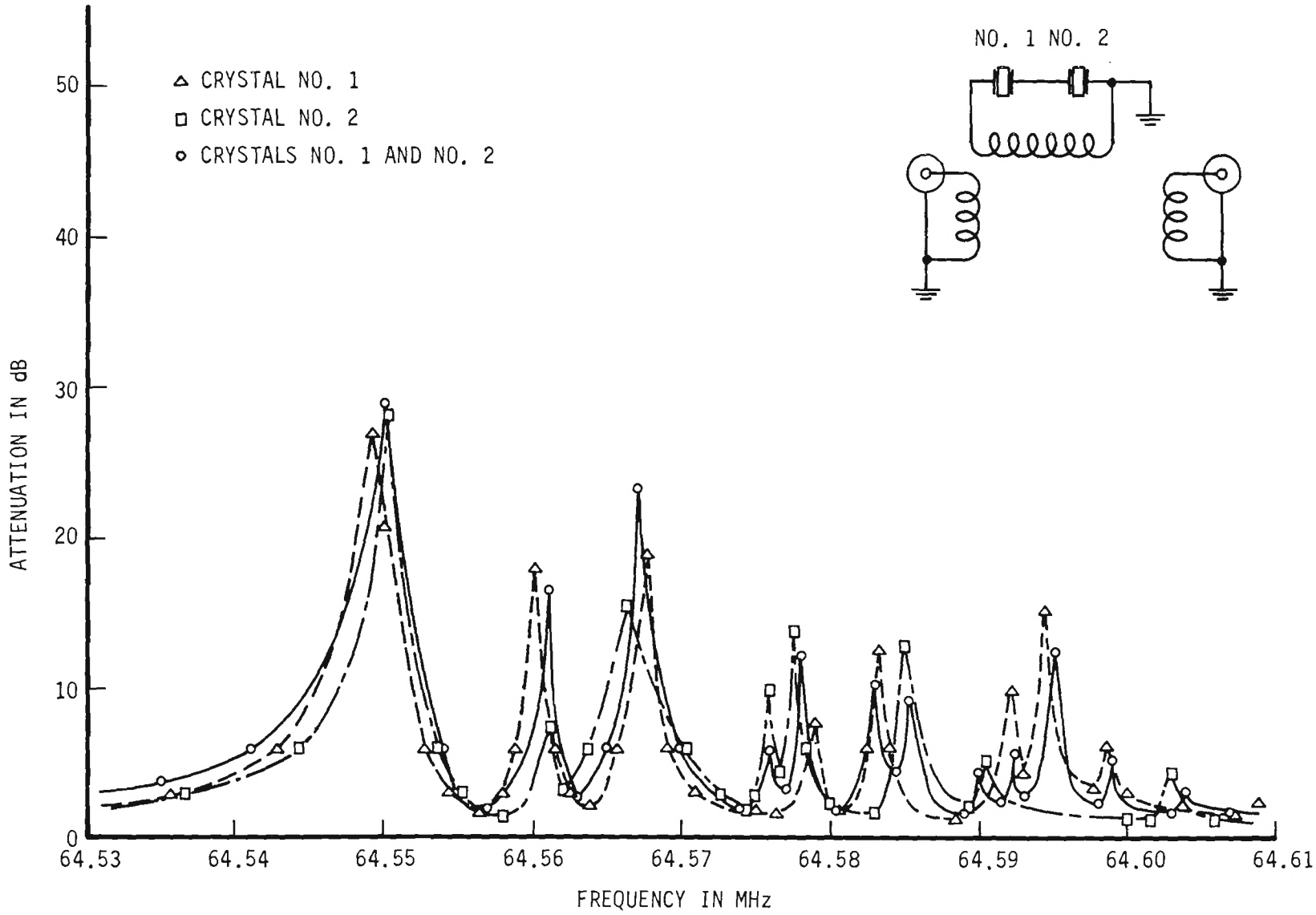

Figure 34. Rejection Characteristics of Two Cyrstals in a Simple Notch Filter.

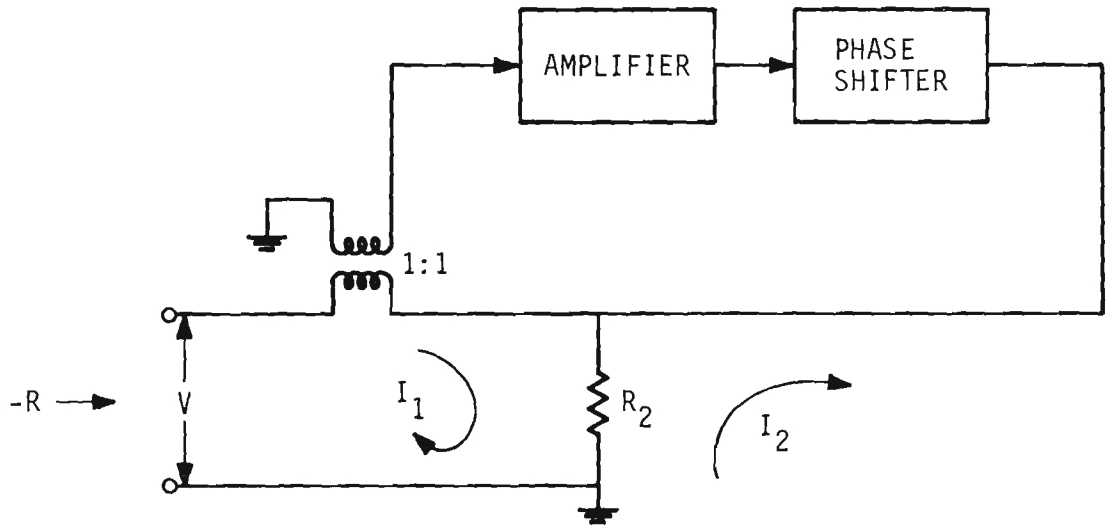

Figure 35. Block Diagram of Negative Resistance Circuit.

the input impedance is found to be

$$R = \frac{50\,(R_1 + R_2) + (1 - G)\,R_1\,R_2}{R_2 + 50} \quad . \tag{39}$$

If $R_1 = R_2 = 50$ ohms, equation (39) becomes

$$R = 25\,(3 - G) \quad . \tag{40}$$

Equation (40) indicates that for $G > 3$, the circuit input impedance is negative which represents an unstable condition. However, when this negative resistance is connected in series with a crystal element, stability is assured so long as the magnitude of R remains less than the resonant impedance of the crystal.

The effectiveness of the negative resistance circuit in the improvement of the rejection ratio of a crystal band reject filter is illustrated in figure 36. An increase of more than 35 dB in the rejection of this simple filter configuration is evident in this figure. Although not apparent in figure 36, a second response was observed at 221 MHz. This response probably resulted from the series resonance of the crystal holder capacitance with an inductive component of the negative resistance circuit. Two attractive features of the series combination of the crystal and negative resistance are its inherent suppression of spurious responses and its relative freedom from intermodulation products. Because the series impedances at the spurious responses are much higher than at the main response, the negative impedance will effectively cancel only the main response impedance. The effect is similiar to that described earlier in connection with the balanced bridge configuration in that the filter's response is enhanced at the main overtone response but the response at the spurious resonances is not affected. The crystal element itself helps to prevent the generation of undesirable intermodulation products in the active portion of the circuit. Since the crystal is in series with the active device, two signals with a frequency separation greater than the crystal's bandwidth are greatly attenuated prior to the active device and thus do not produce intermodulation products.

Another way to overcome the losses caused by the crystal series impedance and, at the same time, reduce the effect of the crystal's spurious responses is to incorporate the crystal in a Q multiplier configuration. Figure 37 illustrates the effect of Q multiplication on a crystal bandpass filter. The curves represent a Q multiplication of approximately 6.5 and show a suppression of spurious response levels by 12 to 16 dB.

The diagram of figure 38 illustrates a technique for generating a frequency sensitive impedance. The input impedance, R(s), of the coupler is 50 ohms at all frequencies except those within the crystal bandwidth. When the

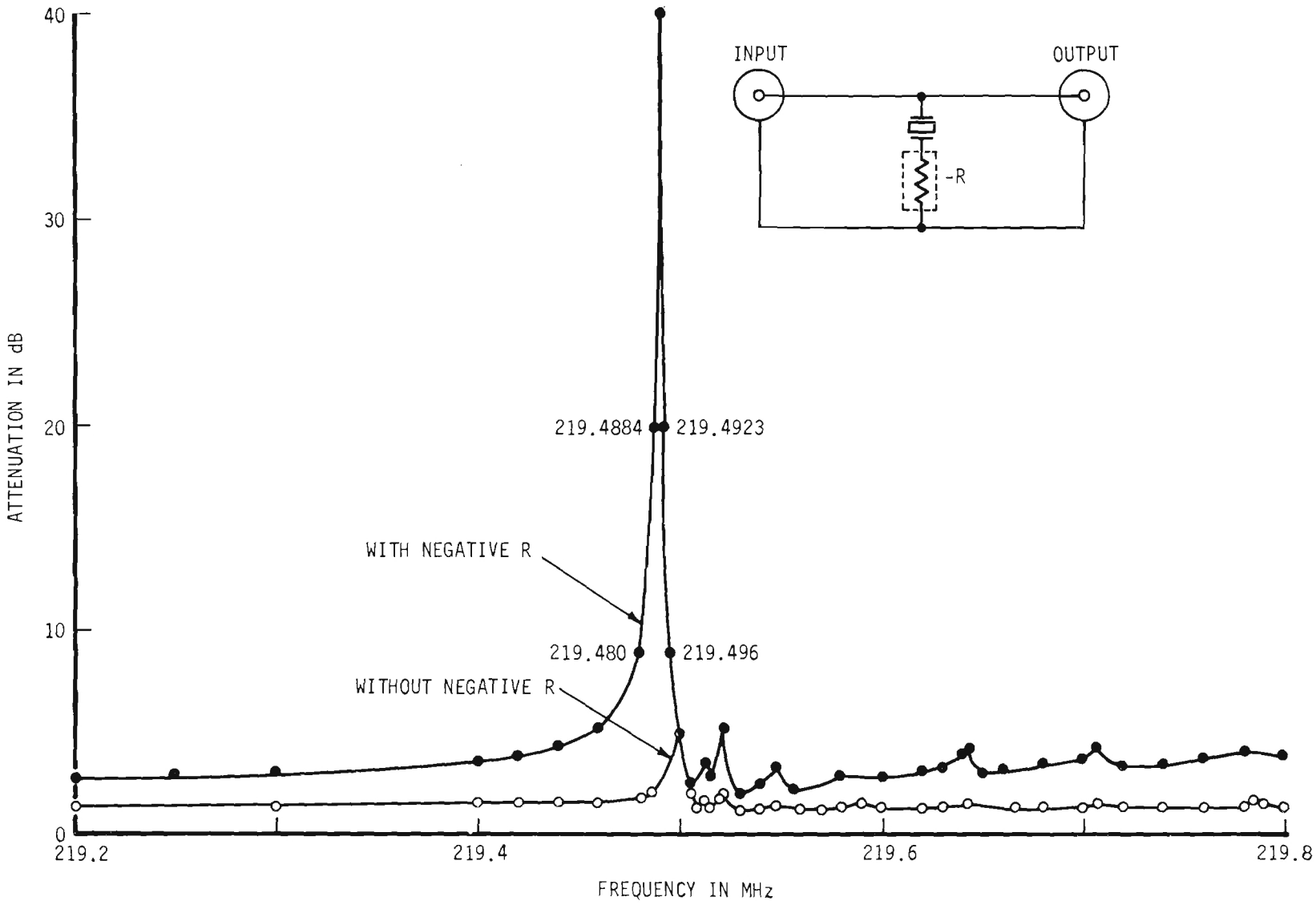

Figure 36. Effects of Negative Resistance on a Crystal Notch Filter Response.

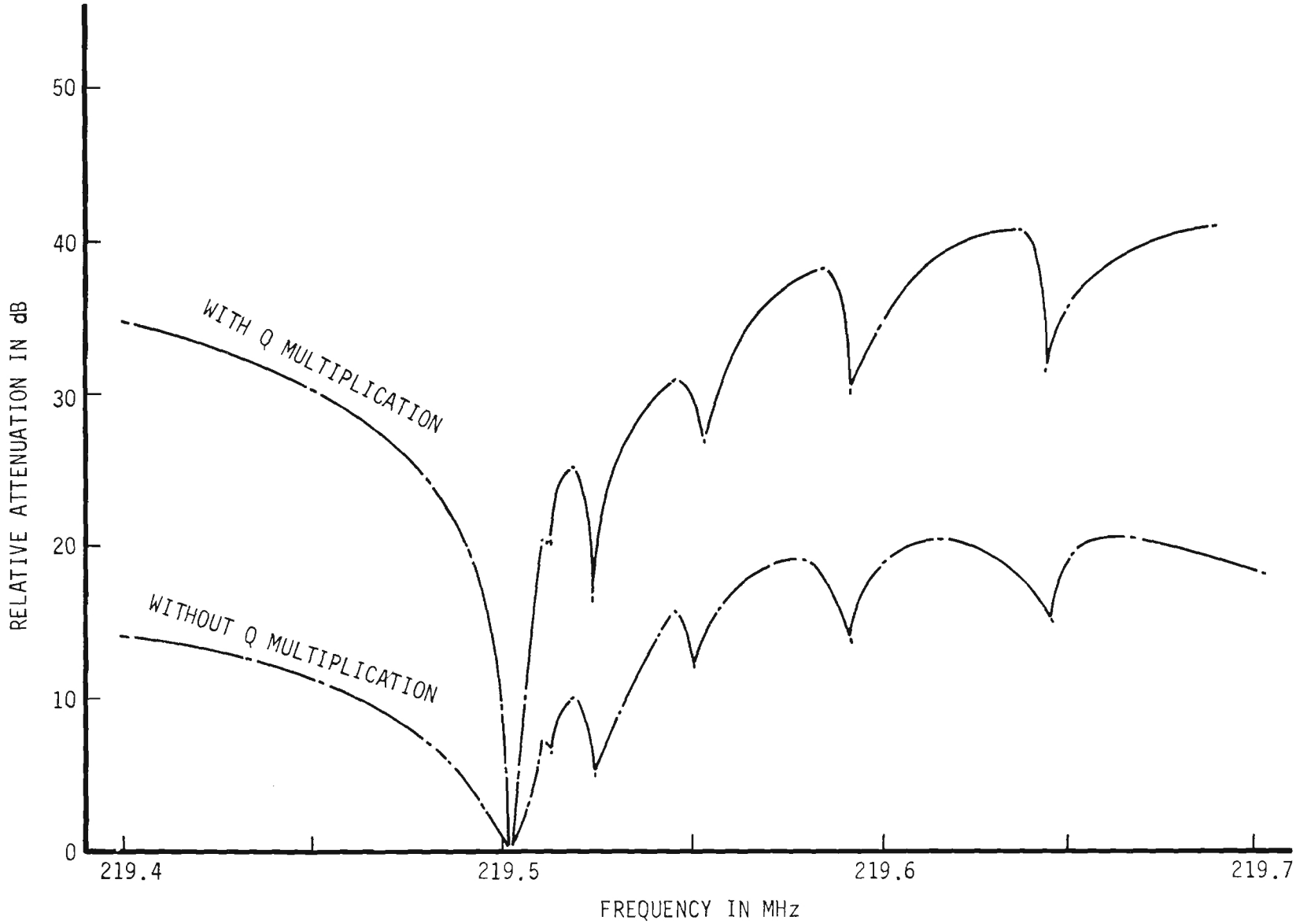

Figure 37. Q Multiplication of a Crystal Response.

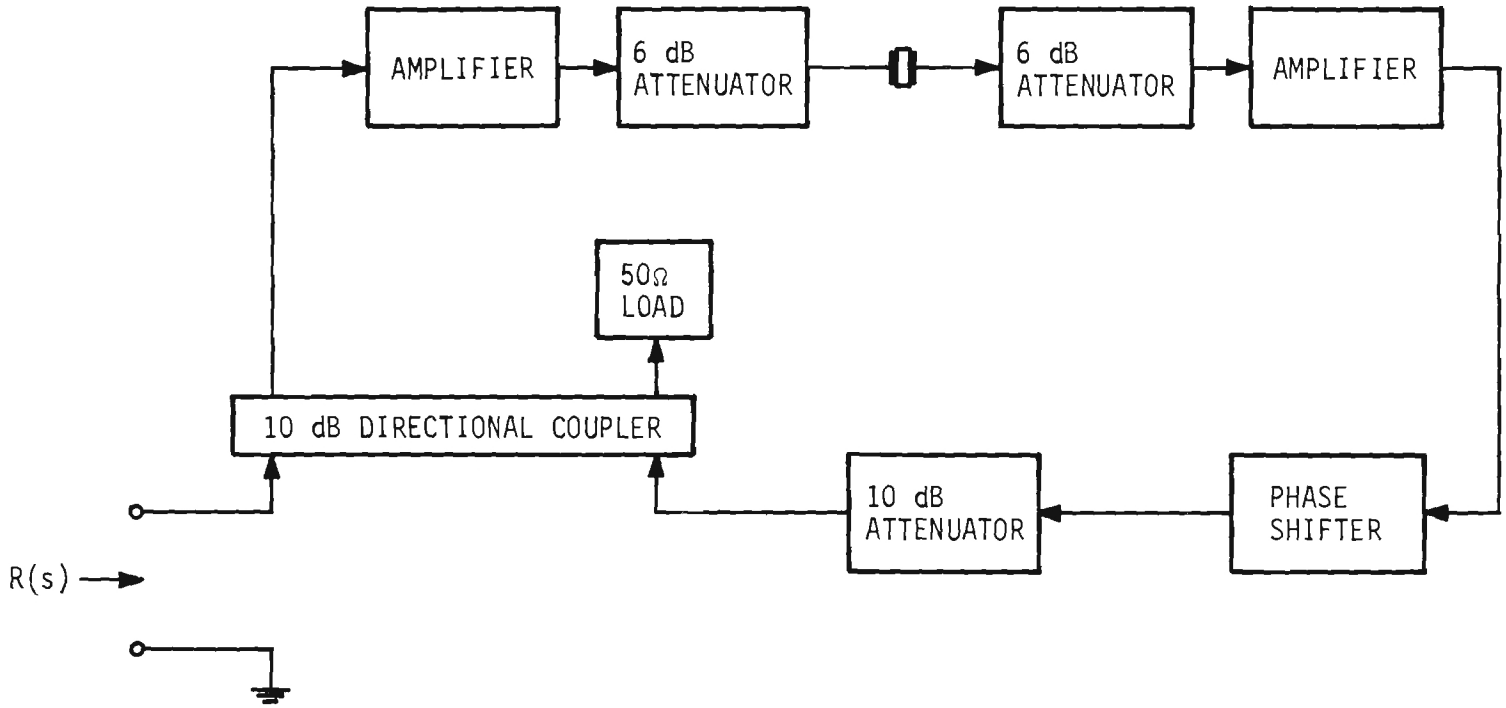

Figure 38. Block Diagram of a Crystal Controlled Impedance.

loop is adjusted such that the loop gain is real with a magnitude of unity at the crystal resonant frequency, the input impedance becomes very high. Off crystal resonance, the loop gain is much less than unity and R(s) then becomes approximately equal to 50 ohms.

This frequency sensitive impedance can be employed in conjunction with a hybrid junction to develop an improved, narrow bandpass filter. The basic filter configuration is shown in figure 39 along with its transmission characteristics. The off resonance attenuation of the filter results from the hybrid junction being balanced at all ports because R(s) is approximately equal to 50 ohms. At crystal resonance, however, the high value of R(s) unbalances the hybrid and maximum transmission through the filter occurs. This filter provides greater off resonance attenuation than does simply a crystal element in series with the transmission line. In addition, the effects of the crystal spurious responses are suppressed.

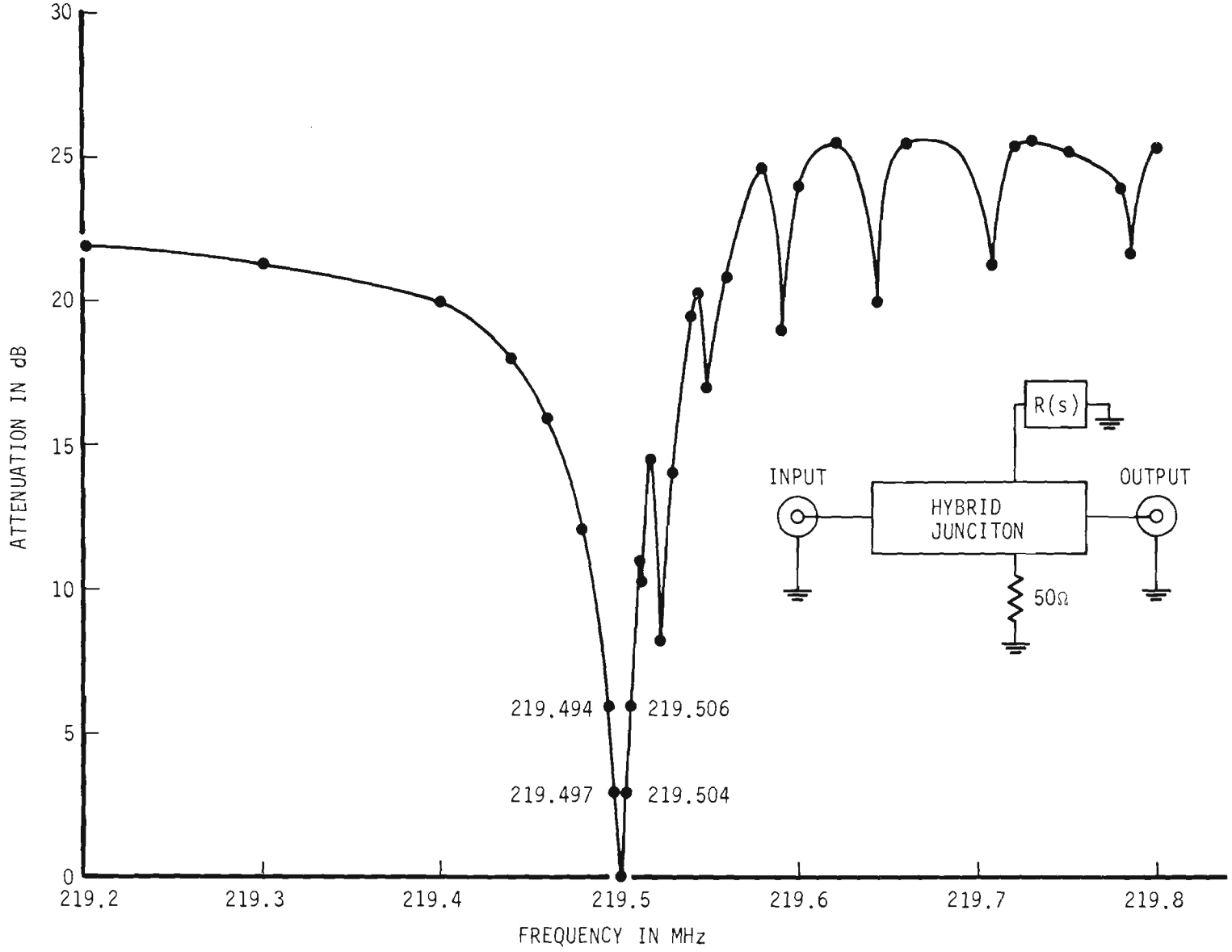

Figure 39. Response of a Hybrid Filter With a Crystal Controlled Impedance.

SECTION V

CONCLUSIONS

Active cancellation techniques may be effectively employed to reduce adjacent channel and co-channel interference. The three techniques developed during this study are applicable to a wide variety of operational situations. When the interfering source is sufficiently close by to obtain a sample of the interfering signal, the automatic phase lock of the first system can effectively maintain the degree of suppression of the undesired signal. If a sample can not be obtained from the source, as is generally the case, the second or feed forward system may be used to suppress the interference. A suppression capability of greater than 60 dB for CW signals and greater than 50 dB for AM signals was demonstrated with this system. However, when the frequency spacing between the interfering signal and the desired signal is less than 50 kHz, the feed forward system attenuates the desired signal excessively. For those situations involving very closely spaced signals, the third or dual loop cancellation system is suggested. As long as the phase and amplitude characteristics of the interfering signal can be discerned from those of the desired signal, this system typically provides 50 dB of suppression to the interference.

In their present state of development, the active cancellation systems can effectively handle interfering signal levels up to 100 milliwatts. In view of the high power level of some interfering signals, the operating power level of these systems should be increased through such techniques as power division and distributed amplification.

The degree of suppression of the interference is limited to approximately 60 dB by the nonlinearities of the active components in the systems. Further work should be directed to increasing this degree of suppression by the application of techniques such as negative feedback to the development of more linear active components.

The technique of Q multiplication was successfully applied in the UHF region. With this technique, filter characteristics exhibiting very narrow bandwidths were realized using relatively small passive resonators. Q values approaching 7,000 were obtained in a relatively compact device. In the present state of development, this device can only handle power levels on the order of -25 dBm. In view of the promising results obtained with the device, further efforts should be directed to improving its power handling capabilities.

The overtone responses of quartz crystals may be used to produce very narrow bandpass and band reject responses in the VHF region. Balanced bridge and hybrid configurations are capable of rejection levels as great as 50 dB. Both configurations are effective in reducing the number and level of the crystal spurious responses. However, these filters exhibit insertion losses of 7 to 10 dB at 200 MHz and exhibit even greater insertion losses at higher

frequencies. The major portion of this insertion loss is due to the high resonant impedance of the crystal. Active techniques can reduce the effect of this high impedance. A negative resistance configuration achieved a band reject response with only 3 dB insertion loss in the passband. The technique of Q multiplication when applied to a bandpass configuration of a crystal filter increased the skirt rejection by approximately 20 dB. Both active techniques enhance the suppression of spurious responses. Unfortunately, they both produce an undesirable narrowing of the already very narrow crystal response. Further study should be made of methods for increasing the crystal response width while maintaining a low filter insertion loss and a high rejection ratio.

SECTION VI

REFERENCES

1. J. A. Hart, Jr., "UHF Active Cancellation Filter," RADC-TR-66-10, AD 486 927, Rome Air Development Center, Griffiss Air Force Base, New York, May 1966.

2. "An Attenuator Design Using PIN Diodes," Application Note 912, Hewlett-Packard Company, Palo Alto, California.

3. G. L. Matthaei, et al, Microwave Filters, Impedance-Matching Networks and Coupling Structures, McGraw-Hill, New York, 1964.

4. J. M. Giannotto and E. J. Chabak, "Suppression of Spurious Responses in VHF Crystal Filters," Proceedings of the IEEE, vol. 53, no. 6, June 1965.

5. C. L. Ruthroff, "Some Broadband Transformers," Proceedings of the IRE, vol. 47, no. 8, August 1959.

SECTION VII

SCHEMATIC DIAGRMAS

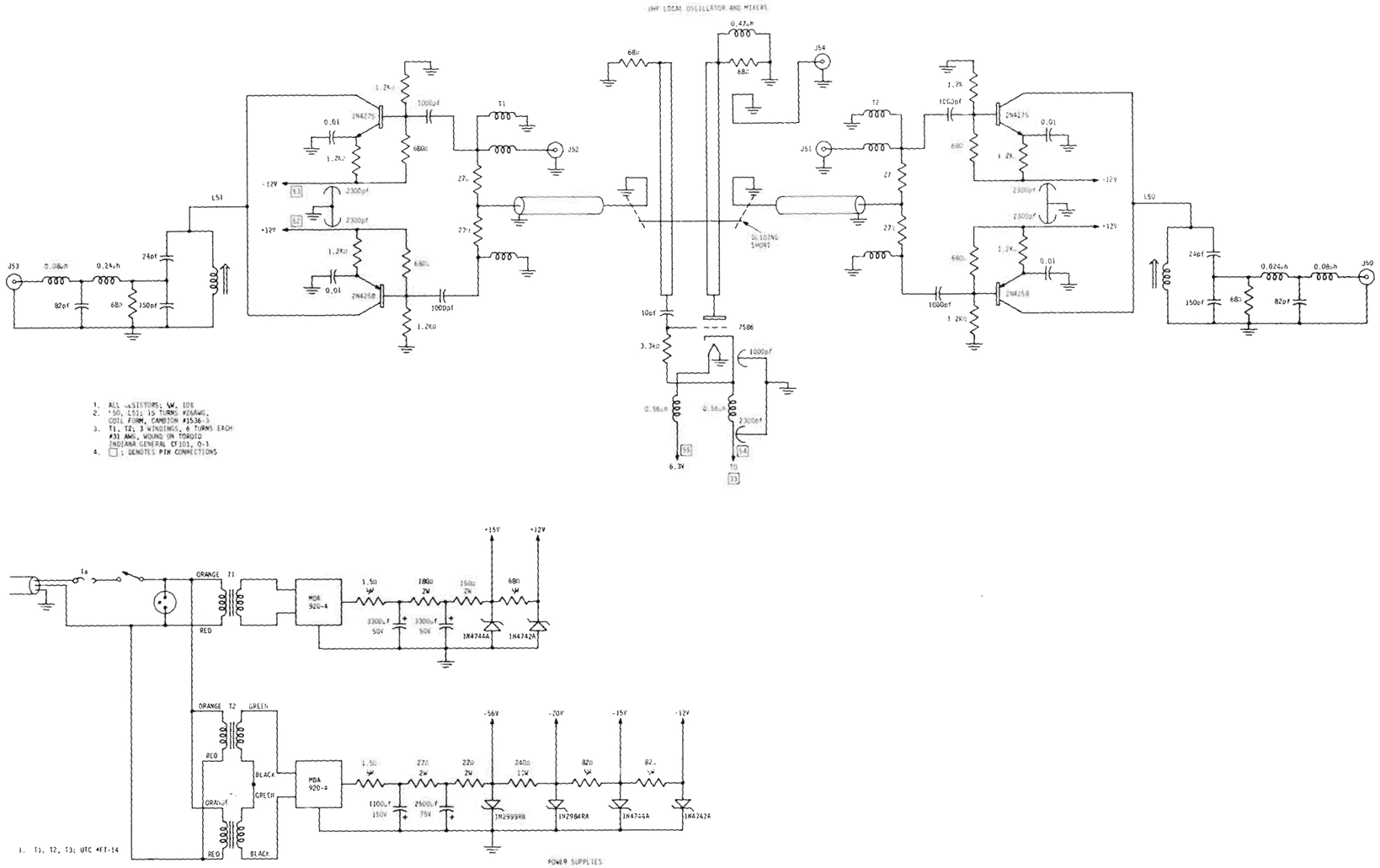

Diagram 1. UHF Local Oscillator, Mixers and Power Supply For Automatic Phase Control System.

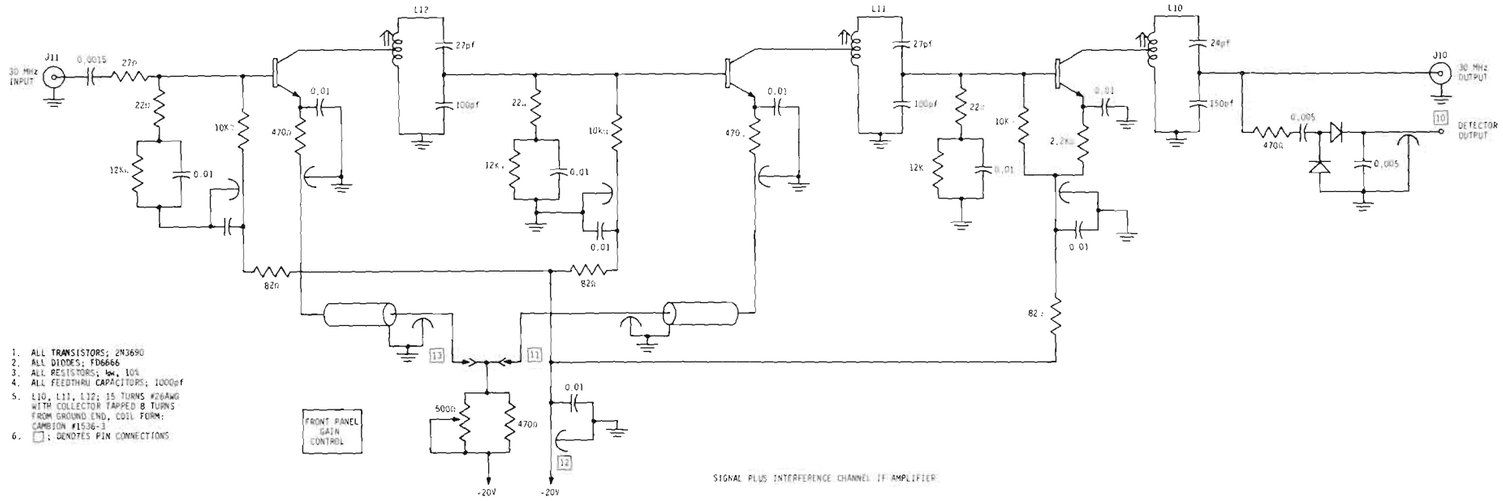

SIGNAL PLUS INTERFERENCE CHANNEL IF AMPLIFIER

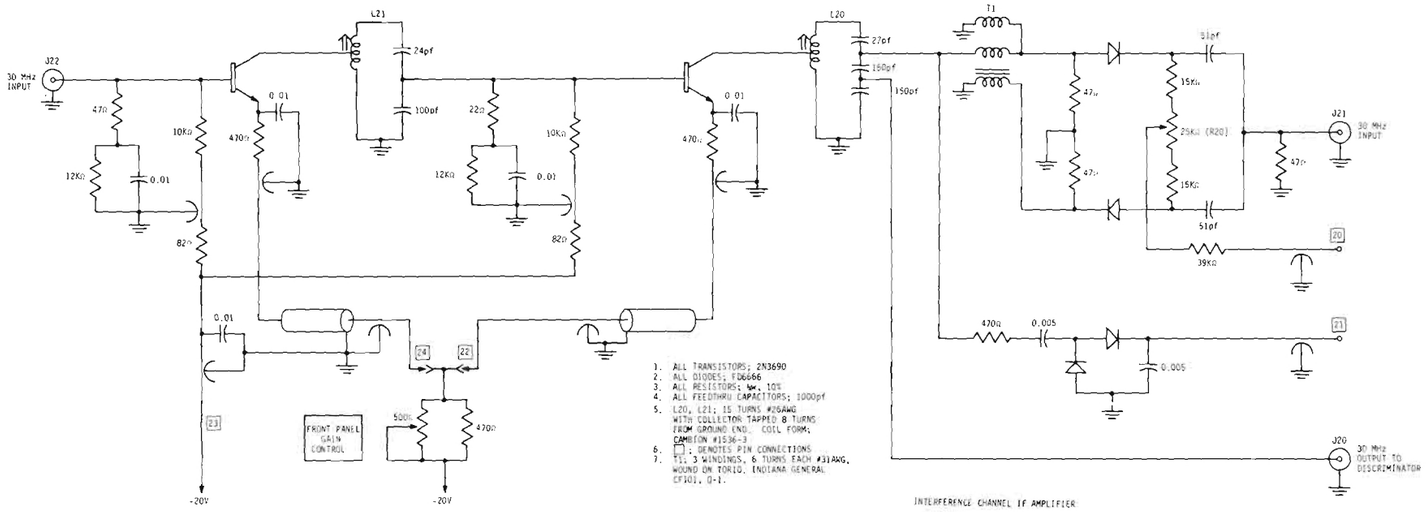

INTERFERENCE CHANNEL IF AMPLIFIER

Diagram 2. IF Amplifiers For Automatic Phase Control System.

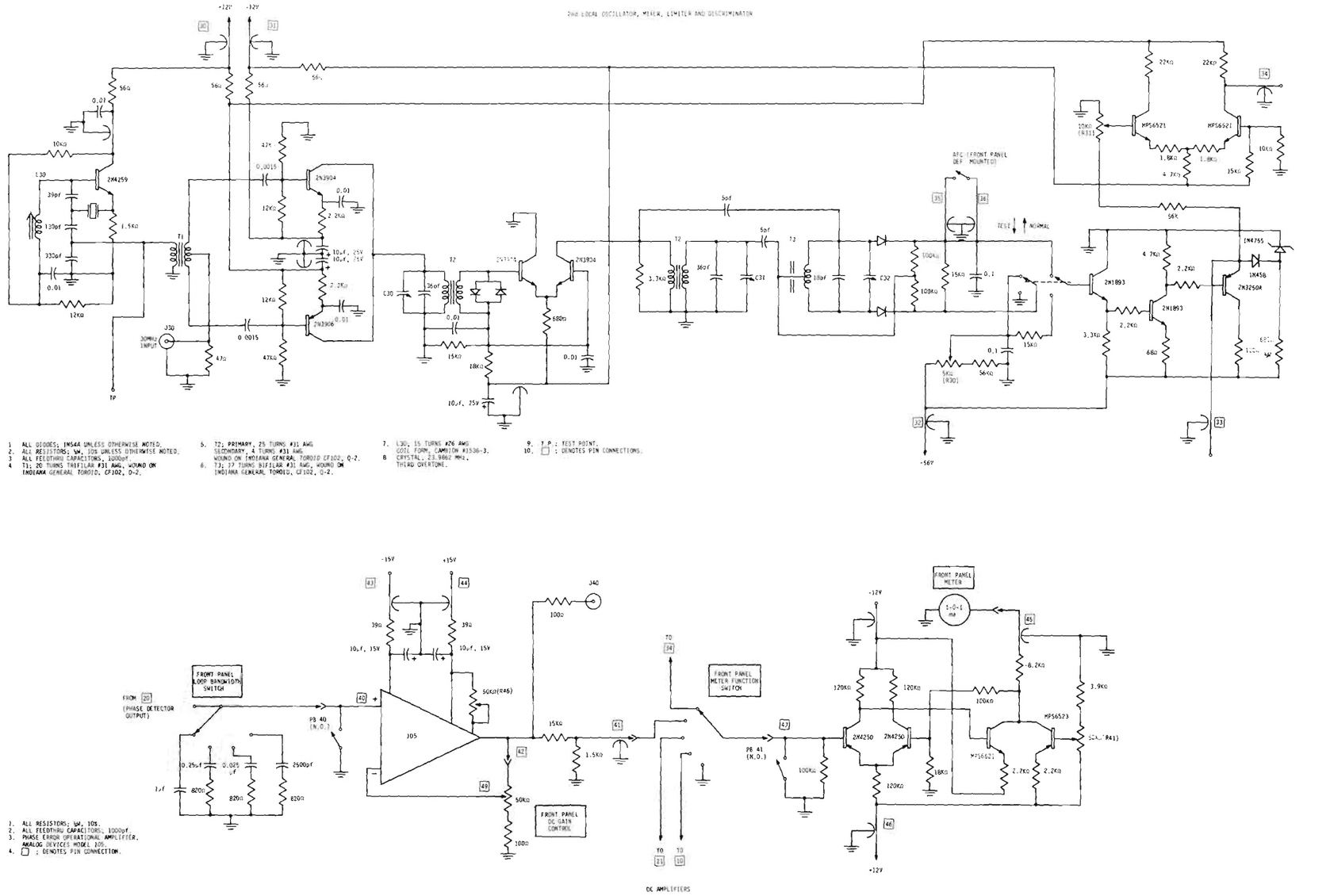

Diagram 3. Second Local Oscillator, Mixer, Limiter, Discriminator and DC Amplifiers For Automatic Phase Control System.

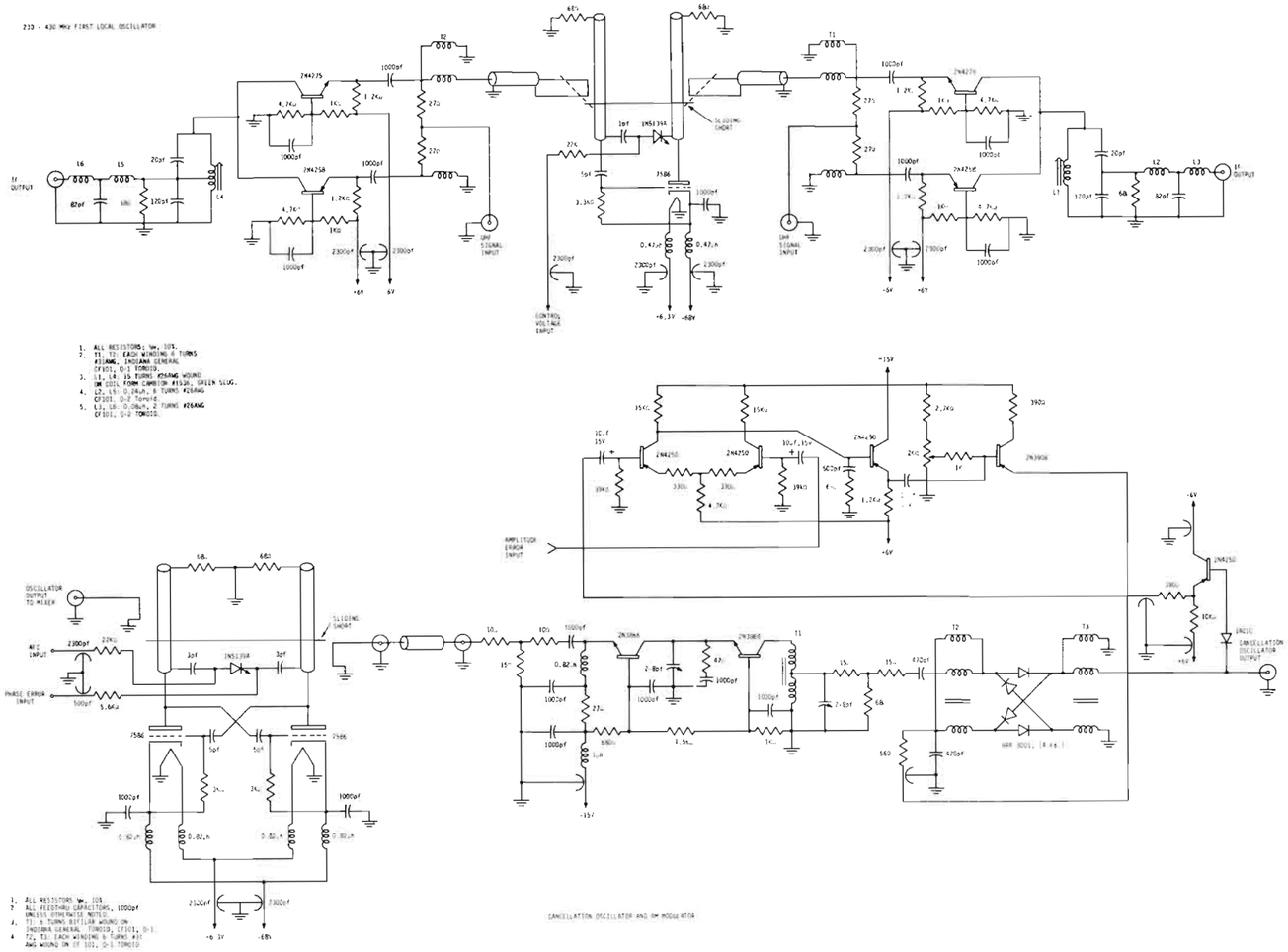

Diagram 4. First Local Oscillator, Cancellation Oscillator, Buffer Amplifier and AM Modulator For AM Cancellation Filter

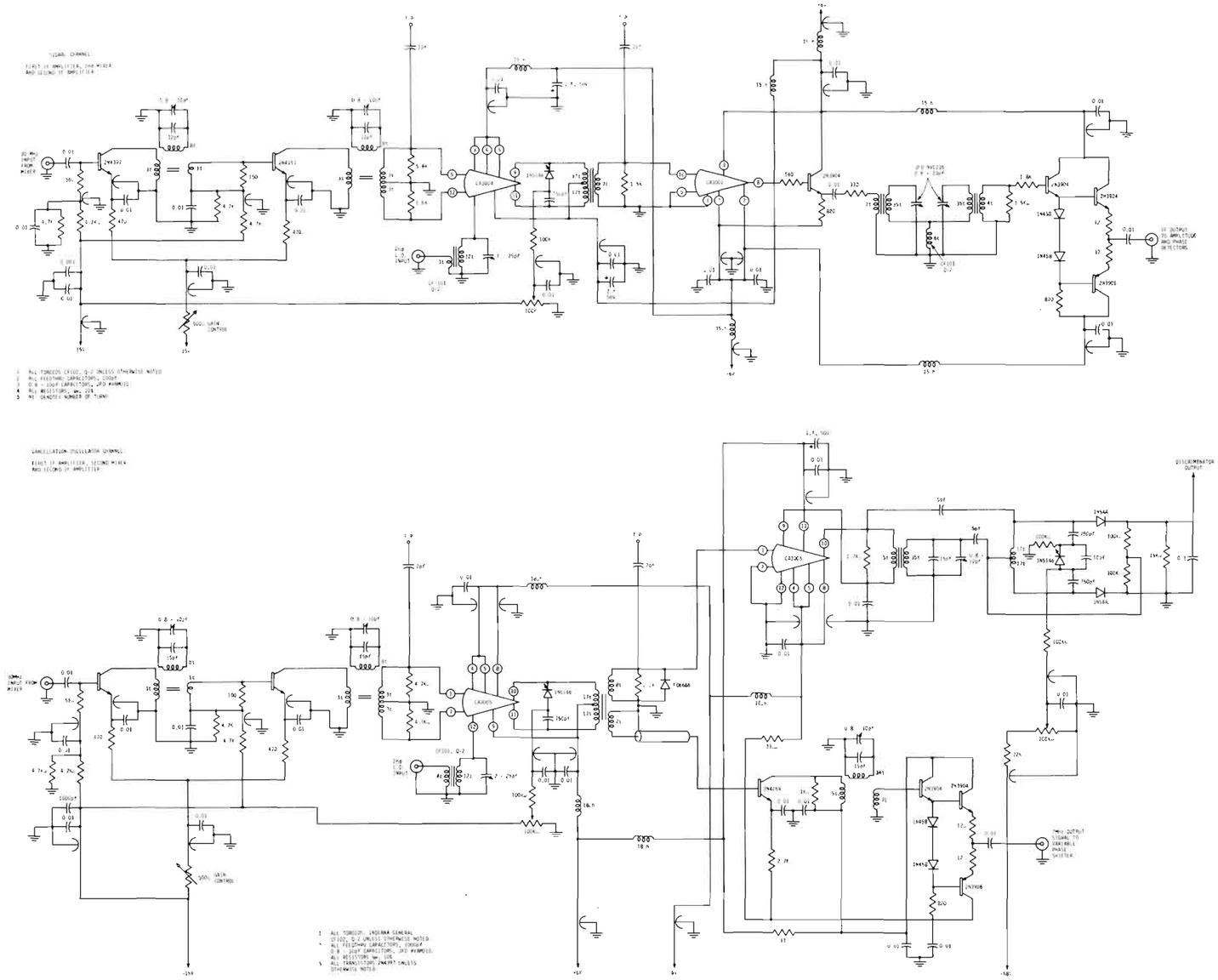

Diagram 5. First and Second IF Amplifiers For AM Cancellation Filter.

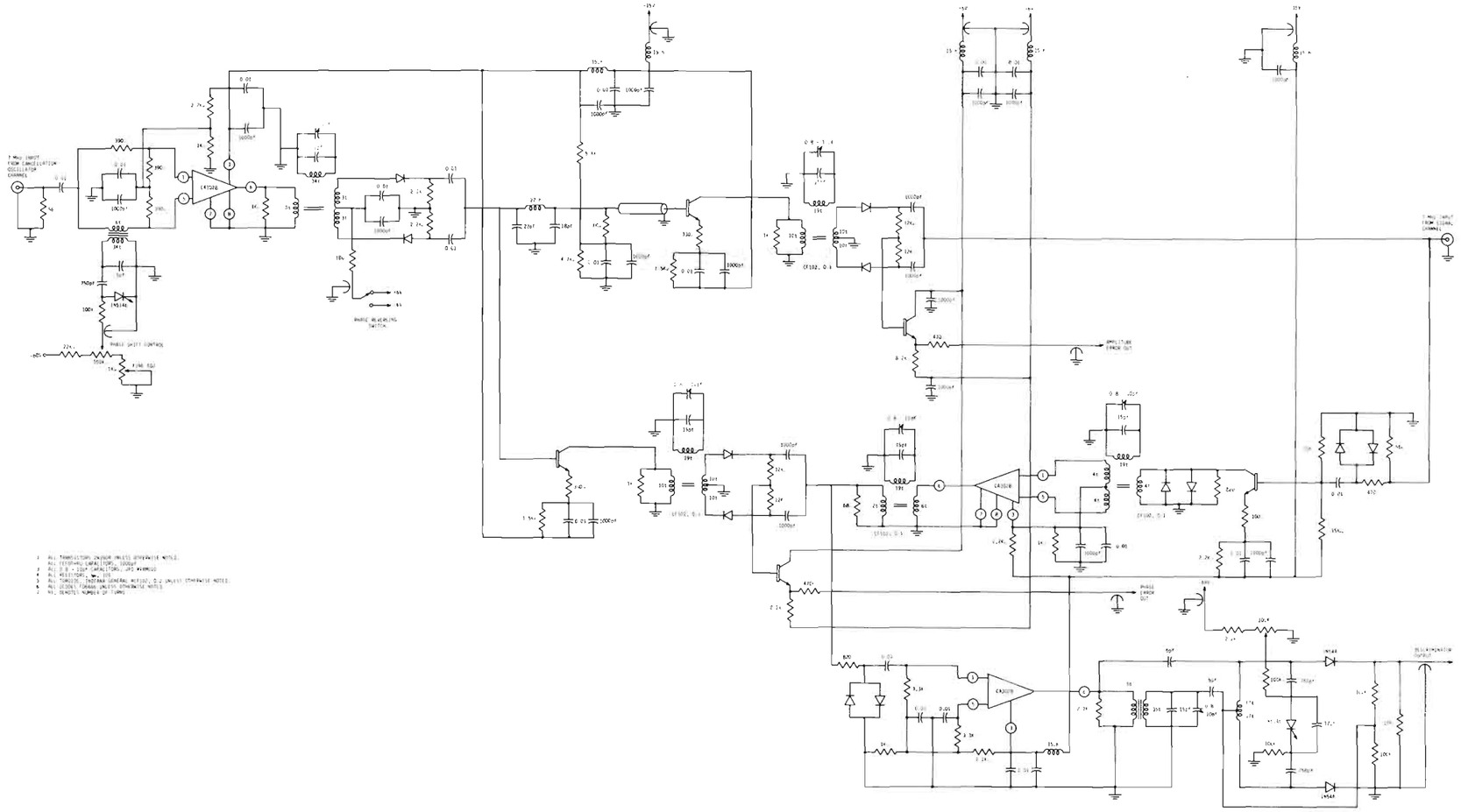

Diagram 6. Variable Phase Shifter, Phase and Amplitude Detectors and Signal Channel Limiter For AM Cancellation Filters.

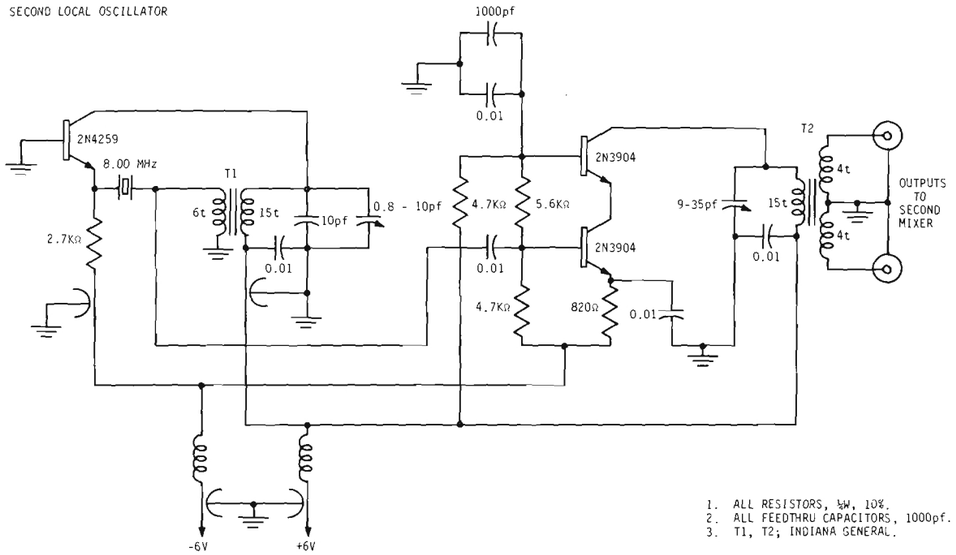

1. ALL RESISTORS, ¼W, 10%.
2. ALL FEEDTHRU CAPACITORS, 1000pf.
3. T1, T2; INDIANA GENERAL.

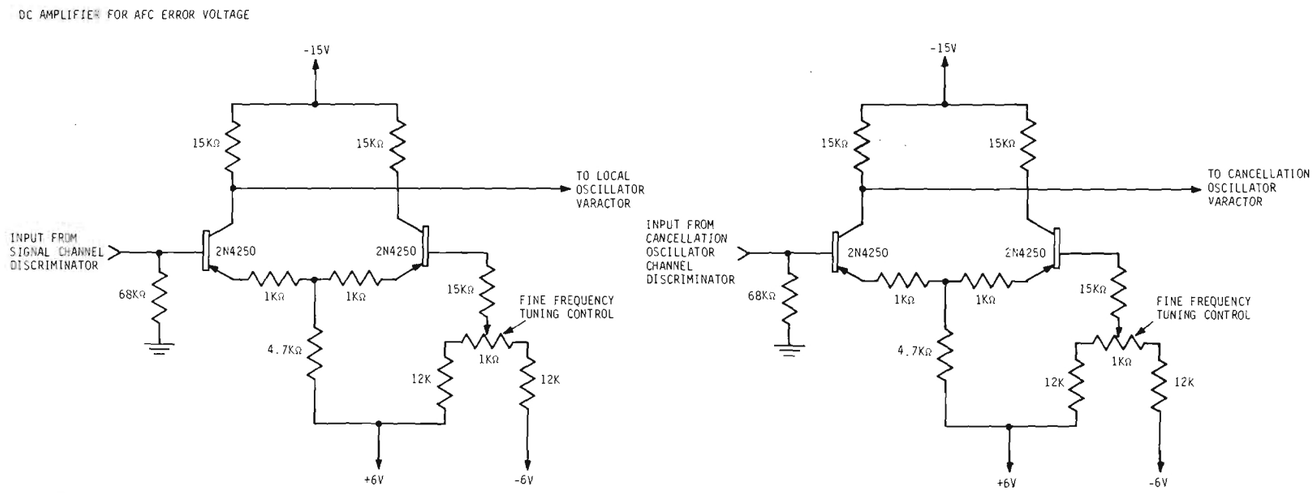

1. ALL RESISTORS, ¼W, 10%.

Diagram 7. Second Local Oscillator and AFC Loop Amplifiers For AM Cancellation Filters

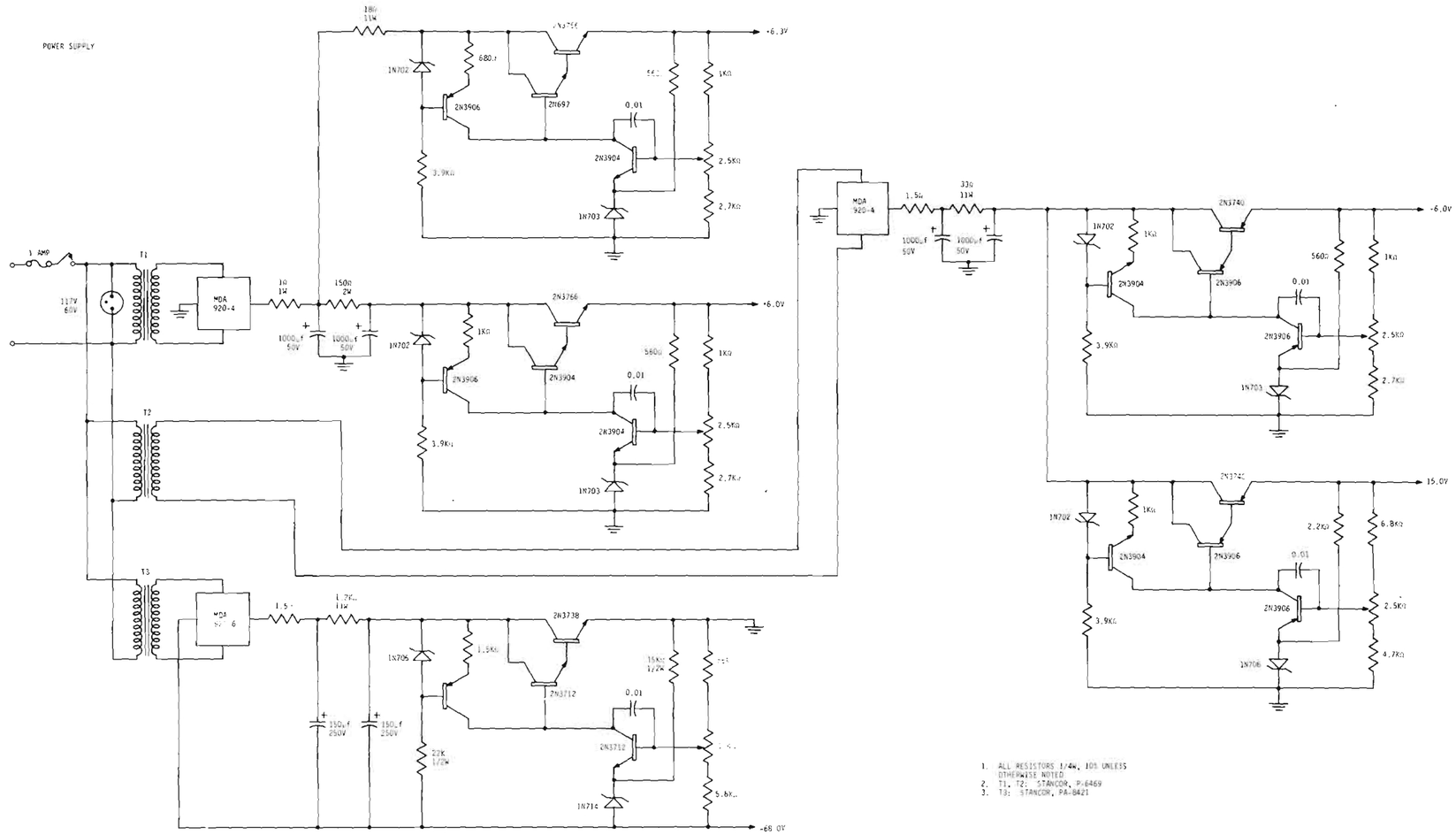

1. ALL RESISTORS 1/4W, 10% UNLESS OTHERWISE NOTED
2. T1, T2: STANCOR, P-6469
3. T3: STANCOR, PA-8421

Diagram 8. Power Supply For AM Cancellation Filter.

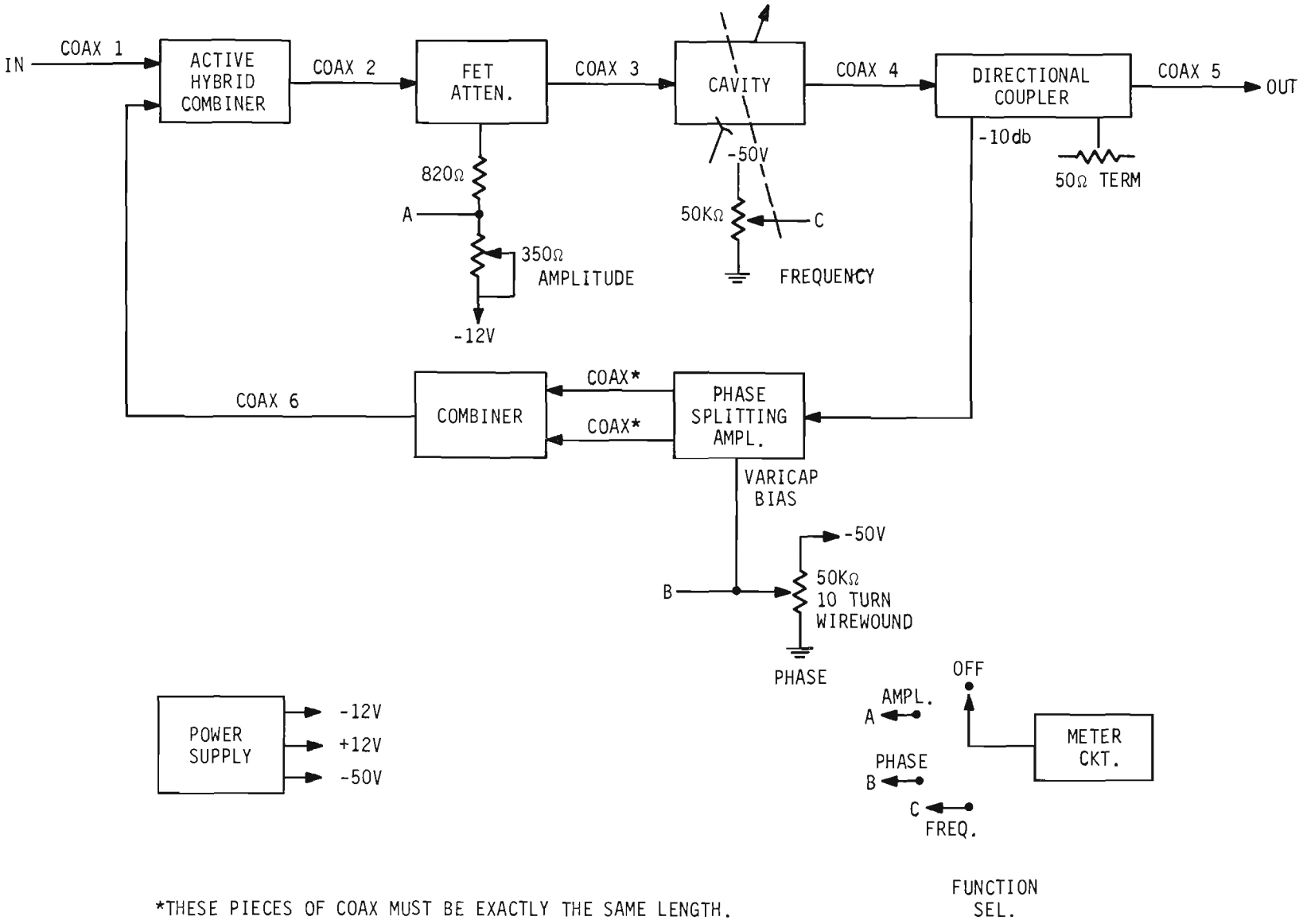

Diagram 9. System Control Functions of Q Multiplier.

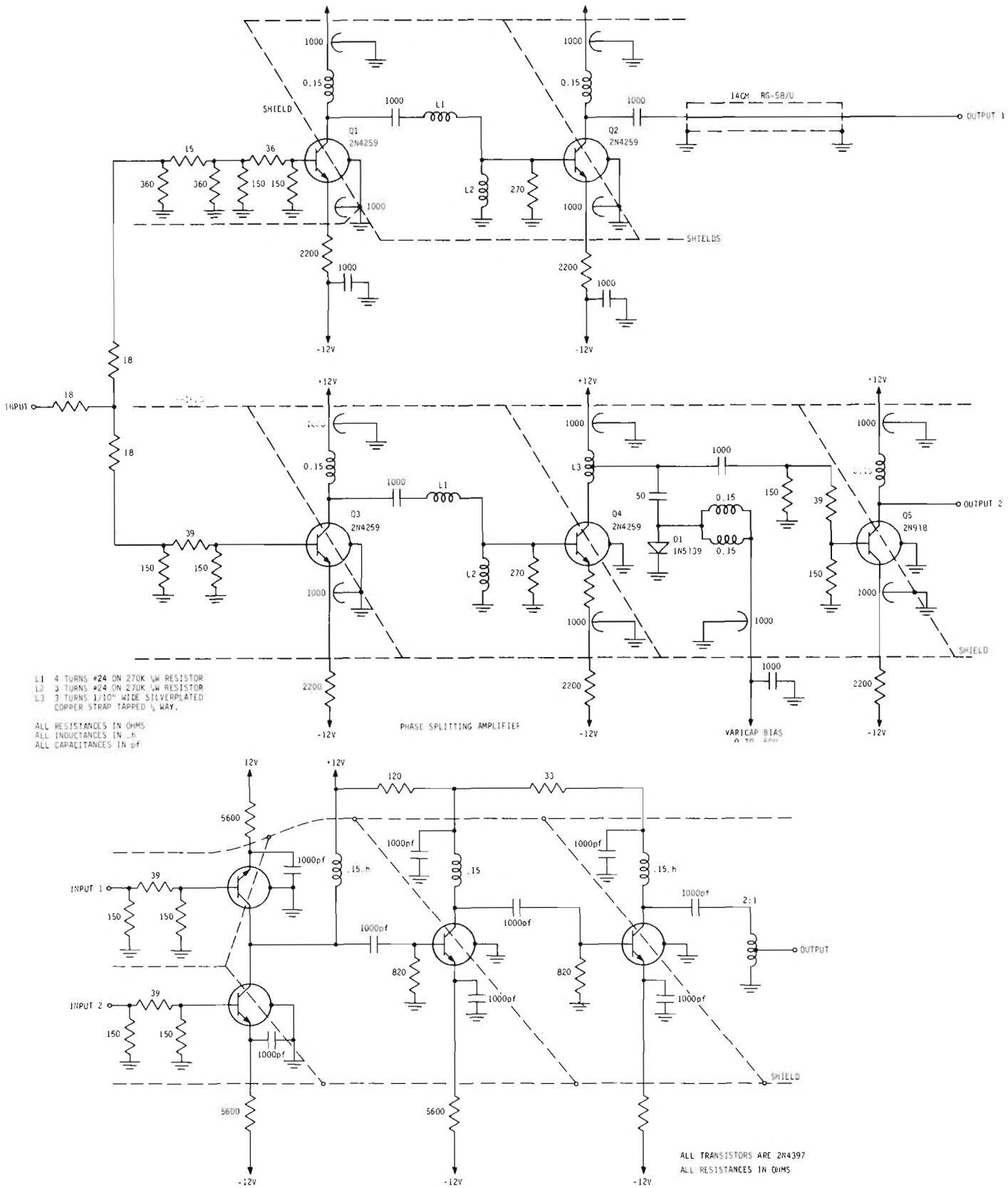

Diagram 10. Voltage Controlled Phase Shifter.

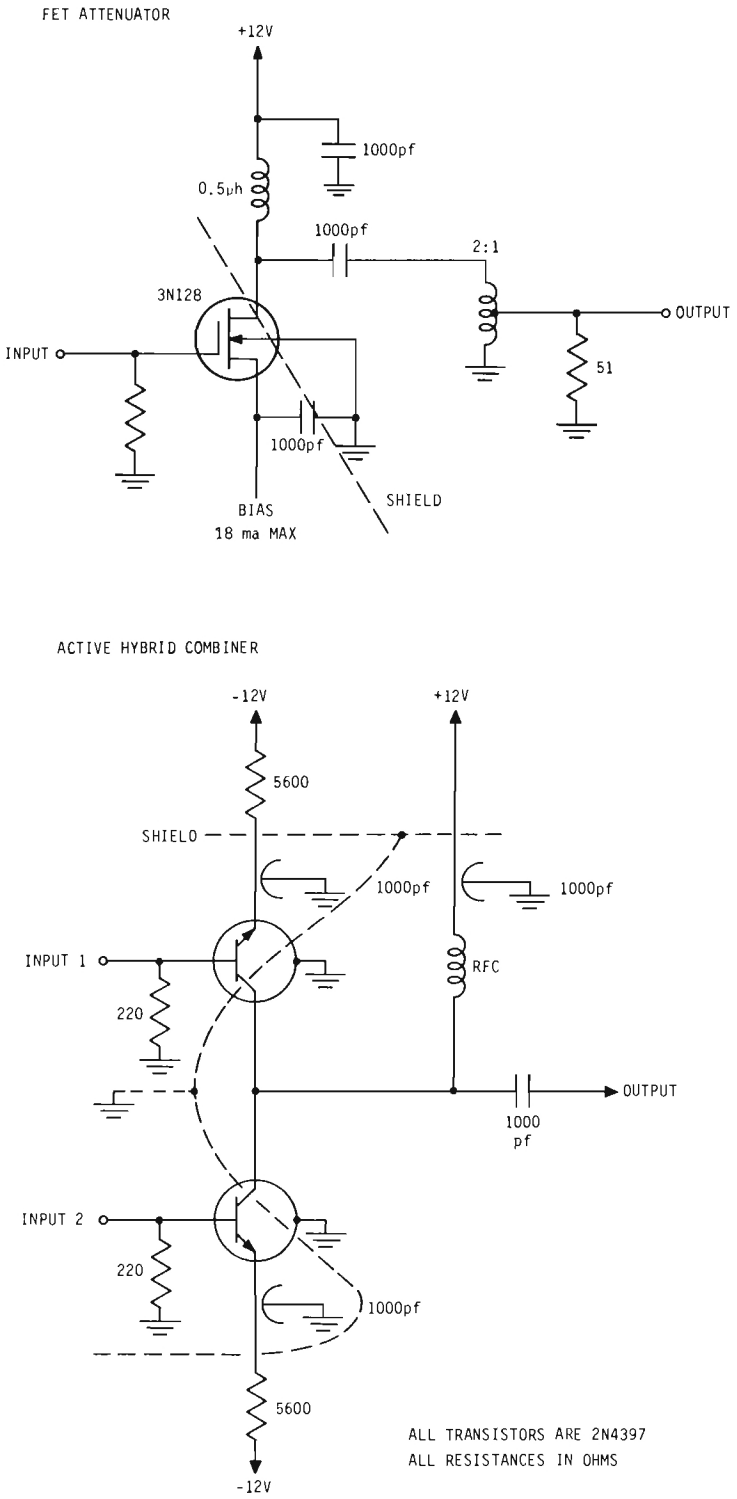

Diagram 11. FET Attenuator and Active Hybrid Combiner.

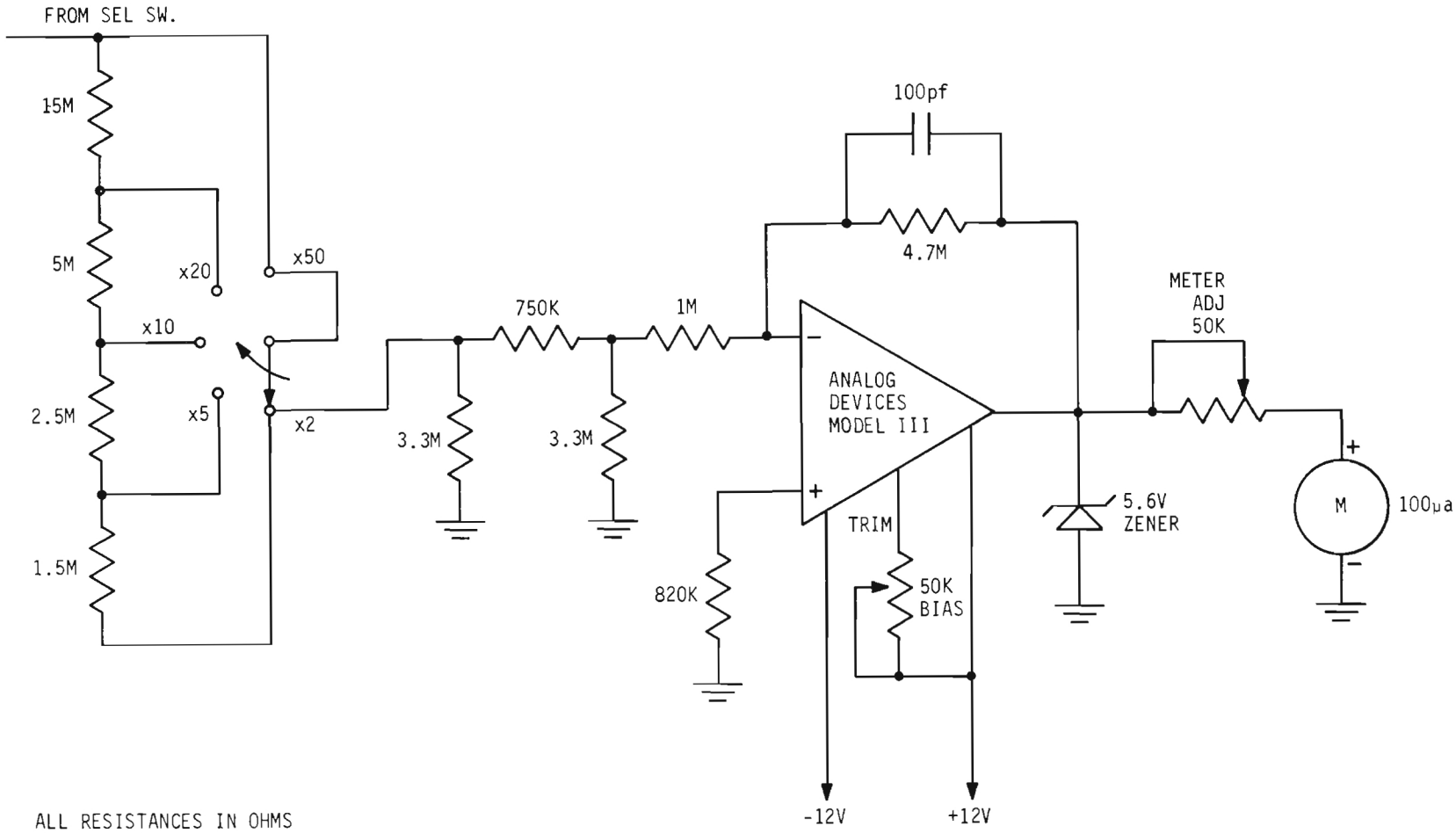

Diagram 12. Metering Circuit of Q Multiplier.

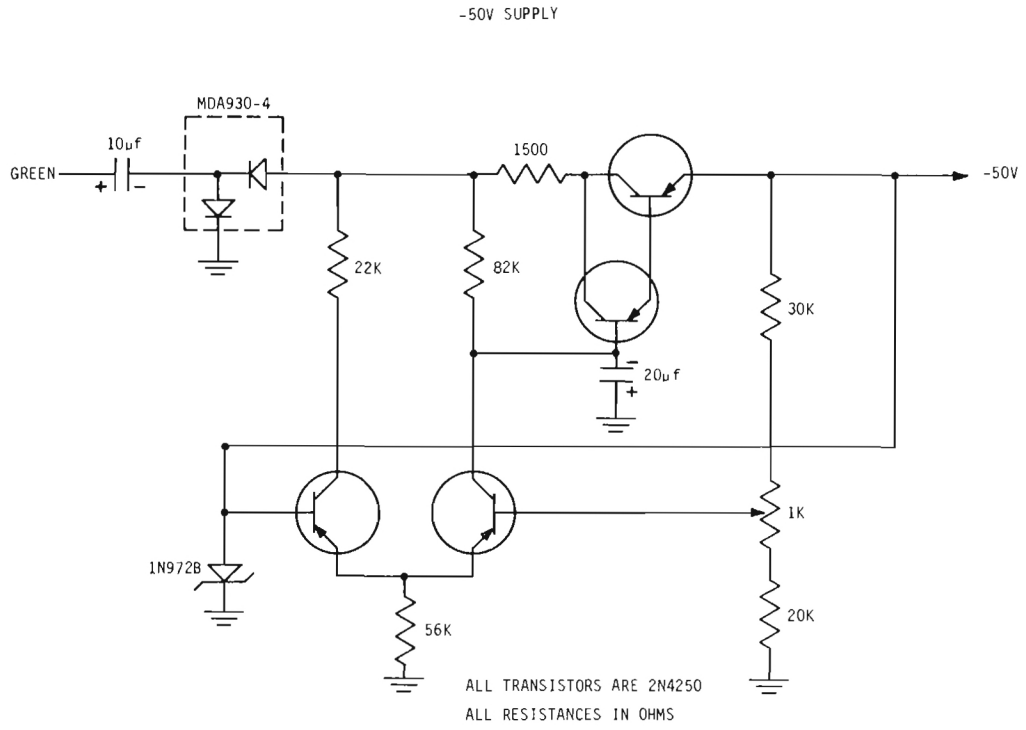

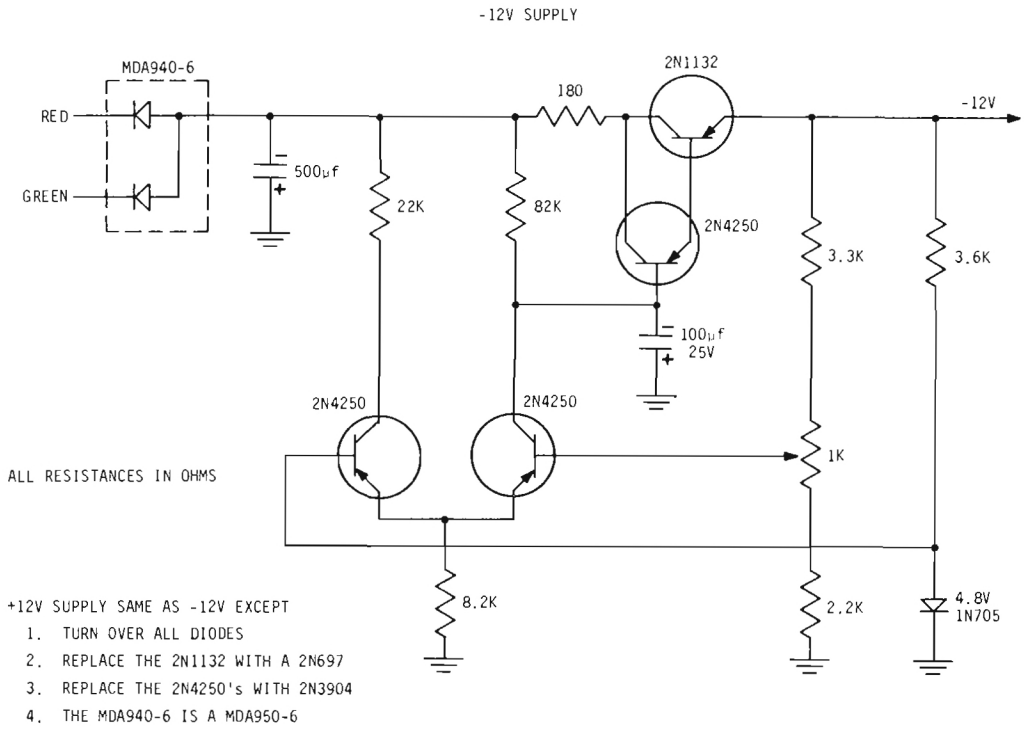

Diagram 13. Power Supplies for Q Multiplier.

UNCLASSIFIED

Security Classification

DOCUMENT CONTROL DATA - R & D

(Security classification of title, body of abstract and indexing annotation must be entered when the overall report is classified)

1. ORIGINATING ACTIVITY (Corporate author)	2a. REPORT SECURITY CLASSIFICATION
Georgia Institute of Technology	UNCLASSIFIED
	2b. GROUP

3. REPORT TITLE

Interference Reduction Techniques Employing Active Devices

4. DESCRIPTIVE NOTES (Type of report and inclusive dates)

Final Technical Report (1 December 1966 - 30 November 1967)

5. AUTHOR(S) (First name, middle initial, last name)

Hugh W. Denny Charles S. Wilson
Robert A. Byers
Carl R. Driskell

6. REPORT DATE	7a. TOTAL NO. OF PAGES	7b. NO. OF REFS
February 1968	106	5

8a. CONTRACT OR GRANT NO.	9a. ORIGINATOR'S REPORT NUMBER(S)
F30602-67-C-0066	
b. PROJECT NO. 4540	
c. Task No. 454003	9b. OTHER REPORT NO(S) (Any other numbers that may be assigned this report)
d.	RADC-TR-68-8

10. DISTRIBUTION STATEMENT

This document has been approved for public release and sale; its distribution is unlimited.

11. SUPPLEMENTARY NOTES	12. SPONSORING MILITARY ACTIVITY
	Rome Air Development Center (EMCVI-2) Griffiss AFB New York 13440

13. ABSTRACT

This report discusses the development and performance of several techniques employing active devices for the reduction of adjacent and co-channel interference in receivers. For operational situations where the interfering source is co-sited with the receiver, an automatic phase control system is described which detects the differential phase shift between the interference path and the direct path from the source and supplies a phase corrected signal for cancellation of the interfering signal. For the more general situation where the interference is not a cosite source, a feed forward system and a dual loop, phase locked system were developed. For 60 kHz spaced signals at 300 MHz, the feed forward system typically provides 55 dB suppression to CW interference and 40 dB suppression to AM interference. The dual loop cancellation system, which generates an auxiliary signal to cancel the interfering signal is shown to be capable of suppressing an interfering signal by 50 dB when the interference signal is greater than an audio bandwidth from the desired signal. The improved performance of passive preselectors that can be obtained through Q multiplication is demonstrated with a Q multiplier device for the UHF region. Effective Q's of approximately 7,000 with relatively small coaxial cavities are realized with this device. Active and passive circuit configurations which incorporate the extremely narrow passbands of quartz crystals are discussed. When used as band stop filters, interference rejection levels greater than 50 dB are possible with these filters.

DD FORM 1 NOV 65 1473

UNCLASSIFIED

Security Classification

UNCLASSIFIED
Security Classification

14. KEY WORDS	LINK A		LINK B		LINK C	
	ROLE	WT	ROLE	WT	ROLE	WT
Q multiplier Crystal Filters Interference rejection						

UNCLASSIFIED
Security Classification